Northumbria University
NEWCASTLE

Southern high-latitude vegetation and climate change across the Eocene and Oligocene and the role of the widening Tasmanian Gateway

MICHAEL AMOO (19007889)

PhD

2022

Southern high-latitude vegetation and climate change across the Eocene and Oligocene and the role of the widening Tasmanian Gateway

by

MICHAEL AMOO (19007889)

Thesis submitted in partial fulfilment of the requirements for the degree of

DOCTOR of PHILOSOPHY

in

Earth Science and Environmental Science

in the

Faculty of Engineering and Environment

at

Northumbria University, Newcastle

November 2022

Dedication

This PhD thesis is dedicated to my family and partner.

Abstract

The shift from a greenhouse to an icehouse climate from the Eocene to the Oligocene is extensively documented by sea surface temperature records from the southwest Pacific and the Antarctic margin, which reveal evidence of significant long-term cooling. However, the identification of a driving mechanism (tectonic deepening of Southern Ocean gateways and/or declining pCO_2 concentration) is contingent upon a greater comprehension of whether this cooling was also present in terrestrial environments. This study provides new records of Eocene to Oligocene vegetation and climate dynamics in the wider Australo-Antarctic region (southeastern Australia/Tasmania and New Zealand) in the context of the widening Tasmanian Gateway based on analyses of sporomorphs from ODP Site 1172, Site 1168, and TNW-1.

Results from Tasmania showed a temperate *Nothofagus*-dominated rainforest with secondary Podocarpaceae (eastern Tasmania; ET) or *Gymnostoma* (western Tasmania; WT) during the late Eocene to Oligocene. Sporomorph-based climate estimates also showed a 2-3 °C terrestrial cooling (in ET) ~3 Myr prior to the EOT, coinciding with the regional Southern Ocean cooling known as the Priabonian Oxygen Maximum (PrOM); fluctuation between cool-and warm-temperate climate phases (ET & WT) coinciding with the initial deepening of the Tasmanian Gateway at ~35.5 Ma; ~2 °C cooling across the EOT, and a remarkable climate rebound in the early Oligocene coinciding with the global decline in pCO_2 in the late Eocene and its recovery in the earliest Oligocene (ET and WT). However, the extended early Oligocene climate recovery seem to have resulted in a mismatch between pCO_2 and sporomorph-based MATs in western Tasmania.

Palynomorph-based biostratigraphic analyses of the TNW-1 drillcore in the Canterbury Basin, Southland, New Zealand, report a Porangan (middle Eocene) to Whaingaroan (late Oligocene) age, and assign a Whaingaroan age (early Oligocene) to the Marshall Paraconformity. The warm-temperate Casuarinaceae-dominated vegetation association of the Porangan is replaced by *Nothofagus*-dominated rainforest with secondary Casuarinaceae by the Bortonian, and into the Whaingaroan. Also, the Kaiatan (latest Eocene) palynoflora bears striking similarity with the Priabonian (PZ 2; ODP Site 1172) palynoflora record. However, further palynoflora comparison is severely constrained by the non-deposition/erosion of the Runangan of TNW-1 which coincides with the initial deepening of the Tasmanian Gateway.

This study shows a strong link between the marine and terrestrial realm across the wider Australo-Antarctic region, a partly decoupling of vegetation and climate for each site used, providing evidence for varying importance of both tectonic (Tasmanian gateway deepening and widening) and pCO_2 forcings.

Table of Contents

List of Figures

List of Tables

List of Abbreviations

AAG – Australo-Antarctic Gulf

ACC – Antarctic Circumpolar Current

AIS – Antarctic Icesheets

brGDGT – Branched Glycerol Dialkyl Glycerol Tetraether

CA – Coexistence Approach

CMMT – Cold Mean Month Temperature

DCA – Detrended Correspondence Analysis

EAIS – East Antarctic Ice Sheet

EECO – Early Eocene Climatic Optimum

EOT – Eocene-Oligocene Transition

EOB – Eocene-Oligocene Boundary

EOGM – Early Oligocene Glacial Maximum

ET – Eastern Tasmania

ETP – East Tasman Plateau

LCNZ – Lord Howe Rise, Campbell Plateau, and New Zealand

MAT – Mean Annual Temperature

MAAT – Mean annual Air Temperature

MAP – Mean Annual Precipitation

MBT'5me – Methylation Index of Branched Tetraethers

m.b.s.f – Metres Below Sea Floor

NLR – Nearest Living Relative

NMDS – Non-Metric Multidimensional Scaling

ODP – Ocean Drilling Programme

PCA – Principal Component Analysis

PLC – Proto-Leeuwin Current

pCO_2 – Atmospheric Carbon Dioxide

PrOM – Priabonian Oxygen Maximum

PZ – Pollen Zone

SST – Sea Surface Temperatures

STR – South Tasman Rise

TC – Tasman Current

TEX_{86} – Tetraether Index consisting of 86 carbon atoms

WMMT – Warm Mean Month Temperature

WT – Western Tasmania

ACKNOWLEDGEMENTS

I am very grateful to my principal supervisor, Professor Ulrich Salzmann for the support, mentoring, training, and scientific advice for the past three years of my PhD. Special thanks also go to my second supervisor Dr. Matthew Pound and external supervisor, Dr. Joe Prebble for their advice, availability to review my work, and their feedback on pieces of research work I send over to them. My supervisors have mentored me to be a better researcher and scientist and this PhD thesis would not have been possible without them. I would also like to thank Lesley Dunlop and Dave Thomas for their help in the laboratory and training in palynology sample preparation.

Many thanks also go to my external collaborators, Dr. Peter K. Bijl for supplying both ODP Site 1172 and Site 1168 samples, and for his helpful comments on manuscripts I have either published and/or are in review.

Special thanks to Northumbria University for awarding me the Research Development Fund (RDF) studentship to undertake this research project. I would also like to thank the Northumbria University Graduate School for awarding me the graduate school bursary that helped me attend the 11th EPPC 2022 conference in Stockholm, Sweden.

I am grateful to my supervision panel, Dr. Emma Hocking (subject expert) and Dr. Vasile Ersek (chair of panel) for their comments, feedback, and encouragement right from my early days as a PhD student, through project approval, and first and second annual progressions.

At the Department of Geography and Environmental Sciences, the encouragement and support from my fellow PhD students, Sefa Sahin, James Linighan, and Christina Gerli is much appreciated. Many thanks to my best friend, Timothy Anane (Massey University, New Zealand) for the many enlightening discussions we had on palynology and for listening to my oral presentations even before I gave them at conferences. Also, to my flatmates, Emmanuel Boamah and Emmanuel Omotosho, many thanks for organising football matches on the console to take my mind off PhD work.

To my family, being on this PhD journey took me away from home and made me miss important family occasions, but you all stood by me and supported me. I say a big thank you for always believing in me.

To my lovely partner, Ethel Naa Bersah Acquah, many thanks for the support, and I am blessed to have you in my corner.

DECLARATION

I declare that this thesis is a result of my own work completed under the supervision of Prof. Ulrich Salzmann, Dr. Matthew Pound, and Dr. Joe Prebble, and where other studies or ideas have been used, these have been properly cited and referenced. I also declare that this thesis has not been submitted, in part or whole, to any university for any degree, diploma or other qualification.

All ethical clearance needed for this research has been duly approved. Approval was sought and granted by the University Ethics Committee on 7th February 2020 with submission reference #18359.

This thesis contains two published peer-reviewed articles (chapters 3 and 4) and six conference and meeting abstracts presented locally and internationally.

I declare that the word count for this PhD thesis is 36,668 words.

Publications by M. Amoo resulting from this PhD Thesis

Amoo, M., Salzmann, U., Pound, M. J., Thompson, N., & Bijl, P. K. (2022). Eocene to Oligocene vegetation and climate in the Tasmanian Gateway region were controlled by changes in ocean currents and *p*CO2. *Climate of the Past*, *18*(3), 525–546. https://doi.org/10.5194/cp-18-525-2022

Amoo, M., Salzmann, U., Pound, M. J., Hoem, F. S., Thompson, N., & Bijl, P. K. (2023). Late Eocene to late Oligocene terrestrial climate and vegetation change in the western Tasmanian region. *Palaeogeography, Palaeoclimatology, Palaeoecology*, 623, 111632. https://doi.org/10.1016/j.palaeo.2023.111632

Conference abstracts

Amoo, M., Salzmann, U., Bijl, P. K., & Thompson, N. (2020). Southern high-latitude vegetation and climate change at the Eocene-Oligocene transition: New Palynological data from ODP Site 1172, East Tasman Plateau. *AASP Palynology Short Talks*.

Amoo, M., Salzmann, U., Bijl, P. K., & Thompson, N. (2020). Southern high-latitude vegetation and climate change at the Eocene-Oligocene transition: New Palynological data from ODP Site 1172, East Tasman Plateau. *UK-IODP 2020 Meeting*.

Amoo, M., Salzmann, U., Bijl, P. K., & Thompson, N. (2021). New palynological data from the East Tasman Plateau (ODP Site 1172) indicate rapid earliest Oligocene warming. *EGU General Assembly Conference Abstracts*, EGU21-9831. https://doi.org/10.5194/egusphere-egu21-9831

Amoo, M., Salzmann, U., Pound, M.J., Hoem, F.S., Thompson, N. & Bijl, P. K., (2022).Terrestrial climate and vegetation in the Tasmanian region controlled by oceanographic and pCO_2 changes from late Eocene to early Oligocene. *11th European Palaeobotany and Palynology Conference, Stockholm, Sweden, Abstract Book, Pp 250.*

Amoo, M., Salzmann, U., Pound, M.J., Hoem, F.S., Thompson, N. & Bijl, P. K., (2022). Terrestrial climate and vegetation in the Tasmanian region controlled by oceanographic and pCO_2 changes from late Eocene to early Oligocene. *6th TMS Silicofossil and Palynology Joint Meeting, Northumbria University, Newcastle.*

Amoo, M., Salzmann, U., Pound, M.J., Hoem, F.S., Thompson, N. & Bijl, P. K., (2022). Evidence of oceanographic and *p*CO2 changes on terrestrial climate and vegetation in the Tasmanian region after the Eocene Oligocene transition. *12th International Conference on Climate and Biotic Events of the Palaeogene, Bremen, Germany.*

Signed by **Michael Amoo**

November 2022

1. Introduction

1.1 **Background of Study**

The past few decades have witnessed an increased interest in studying major climate thresholds of the Cenozoic era (last 65 million years) in the Southern high latitude (Thorn & DeConto, 2006; Francis et al., 2008; Contreras et al., 2014; Pound and salzmann 2017; Holdgate et al., 2017; Korasidis et al., 2019; Hutchinson et al., 2021), with the aim of understanding the potential changes our world may undergo in the not too distant future (Burke et al., 2018). One of the most significant climate transitions of the Cenozoic, the Eocene-Oligocene Transition (EOT; 34.44-33.65 Ma; Katz et al., 2008; Hutchinson et al., 2021) is marked by a change from a largely ice-free greenhouse climate to an icehouse climate, involving the development of the Antarctic cryosphere and global cooling (Liu et al., 2009; Pearson et al., 2009; Pagani et al., 2011; Hutchinson et al., 2021).

As potential causes for this climate transition, tectonic opening of the southern gateways (Kennett, 1977) and a significant and abrupt decrease in atmospheric pCO_2 concentrations (Deconto & Pollard, 2003; Huber et al., 2004; Zachos et al., 2008; Goldner et al., 2014; Ladant et al., 2014) have been put forth. The Antarctic Circumpolar Current (ACC), which thermally isolated Antarctica, was strengthened by the opening of the Australian-Antarctic Seaway (Tasmanian Gateway) and the Drake Passage (Kennett, 1977). Marine geology, micropalaeontology, and model simulation revealed a potential lag between the start of the ACC and palaeogeographic changes, disputing the idea that tectonic movements in the Southern Hemisphere were driving global climate change at the EOT (Huber et al., 2004; Stickley et al., 2004; Goldner et al., 2014).

Despite the fact that southern gateway opening, and deepening have not been able to fully explain Antarctic cooling at the EOT, it has been observed that regional oceanographic changes as a result of gateway opening and deepening have a climatic impact on Southern Ocean surface waters. The extent and impact of the Tasmanian Gateway's opening and deepening, as well as the resulting oceanographic changes, on the contemporaneous terrestrial climate and vegetation, however, are not well understood. This is mainly because, most of the knowledge on palaeoclimate and palaeoenvironment of the EOT

are heavily based on marine proxy records, little is however known about the coeval terrestrial climates. This is because most palaeovegetation reconstruction in the southern high latitude have heavily relied on isolated plant fossils such as leaves, woods and palynomorphs (pollen and spores) with relatively low time resolution and dating control (Lever, 2007; Contreras et al., 2013; Contreras et al., 2014). Likewise, the accurate temporal and geographical reconstruction of vegetation and climate is severely constrained by the lack of continuous and well-dated EOT terrestrial records. This is further exacerbated by the fact that the sparse records of terrestrial palynoflora from the late Eocene and early Oligocene suggest a very variable vegetation response at the EOT (Pound and Salzmann, 2017). For instance, late Eocene to early Oligocene vegetation records in southern Australia show a transition from a warm-temperate to a cool-temperate rainforest, whereas in New Zealand, a warm humid rainforest survived (Pocknall, 1989; Homes et al., 2015; Prebble et al., 2021). Prior to the EOT during the late Eocene, tall woody vegetation in East Antarctica (Prydz Bay) collapsed and was replaced by sparse, taiga-like vegetation with dwarfed trees (Macphail & Truswell, 2004; Truswell & MacPhail, 2009; Tibbett et al., 2021), whereas a significant vegetation change did not occur across the Drake Passage region until the early Oligocene, when gymnosperms and cryptogams expanded, taxon diversity increased rapidly, and terrestrial biomarkers shifted from temperate to cool temperate forests after 33.5 Ma (Thompson et al., 2022). These contradictions in regional vegetation and climate in the southern high-latitude across the mid-Eocene to late Oligocene seek to paint a picture of different potential driver(s) acting in this region, and that is what this PhD study seeks to investigate.

Studies of fossil spores and pollen from high-latitude localities (e.g., Tasmania, New Zealand, Antarctica, Australia, southern South America, and Arctic regions) are not only important for understanding how past ecosystem functioned and adapted in climatically sensitive areas, but increase the understanding of changes most likely to occur due future climate change under global warming. The southern high-latitude plays a crucial role in deciphering past and future changes in climate, due to the potential impact changes/disturbance of thick ice-sheets may have on global sea-level, ocean, and atmospheric circulation changes.

This PhD study/research focuses on the use of fossil pollen and spores across selected sites in southeastern Australia, mainly, Ocean Drilling Programme (ODP) Site 1172 on the East Tasman Plateau and Site 1168 on the western margin of Tasmania, and Southland New Zealand (TNW-1 Well) to reconstruct past vegetation and climate from the Eocene into the Oligocene.

1.1.1 Focus and Experimental setup of study

There are very few well-dated sediment sections for the southern high-latitudes that allow for a thorough reconstruction of Eocene to Oligocene climate (Korasidis et al.,2019; Bijl et al., 2021; Lauretano et al., 2021; Sluiter et al. 2022; Thompson et al., 2022). Most ODP cores are condensed and/or disrupted by hiatuses for the Eocene-Oligocene boundary (EOB), which has been linked to increased ocean circulation intensity and glacioeustatic sea-level drop (Coxall & Pearson 2007). One significant result of ODP Leg 189 was the multi-proxy evidence that the opening of the Tasmanian Gateway significantly predated the Antarctic glaciation by about 2 Myr and was therefore most likely not its primary cause (Huber et al., 2004; Stickley et al., 2004; Wei et al., 2004; Pfuhl & McCave, 2005). The generation of a continuous, well-dated terrestrial climate and vegetation record in marine cores will set the tone for a better understanding of middle to late Palaeogene climate dynamics in the southern high-latitude with an added advantage of proximity to the Tasmanian Gateway. These are ODP Site 1172 (East Tasman Plateau, southwest Pacific; Fig. 1.1) and Site 1168 (western Tasmanian margin, Australo-Antarctic gulf; Fig.1.1).

Uncertainties surrounding the timings of the ocean gateways deepening (Stickley et al., 2004) and the lack of detailed proxy record, especially in the southern high-latitude, places considerable limitation on deciphering the main drivers of this transition (Hutchinson et al., 2021). In several studies (DeConto and Pollard 2003; Huber et al. 2004; Pälike et al., 2006; Pearson et al. 2009; Pagani et al. 2011; Foster & Rohling, 2013; Goldner et al., 2013; Gasson et al., 2014), the importance of pCO_2 concentration has been emphasized as the main cause of the development of Antarctic glaciation and global cooling at the EOT. However, proxy records for declining pCO_2 concentration appear to be heterogenous with cooling

being amplified at higher latitude (Bijl et al., 2009; Liu et al. 2009), and some records reporting short-lived asymmetry between Northern and Southern ocean cooling at the EOT (Liu et al., 2018), making it challenging to reconcile with this proxy alone.

On the other hand, surface oceanographic currents in the Australo-Antarctic region (i.e., Tasmania, East Antarctica, and New Zealand) are reported to have been strongly influenced by the tectonic deepening and widening of the Tasmanian Gateway (Stickley et al, 2004; Huber et al., 2004; Bijl et al., 2013; Holdgate et al., 2017; Sauermilch et al., 2021). Palaeoceanographic modelling described the Pacific sector of the East Tasman Plateau (ETP; Site 1172) to have been under the persistent influence of the relatively cool Tasman Current (TC) in the mid-Eocene as opposed to the western Tasmanian margin (Site 1168) in the Australo-Antarctic Gulf being bathed by the relatively warmer proto-Leeuwin currents (PLC) derived from low-latitude waters from the Indian Ocean (Fig 1.1; Huber et al., 2004). By the late Eocene (~35.50 Ma; Stickley et al., 2004), an accelerated deepening of the Tasmanian Gateway was underway leading to the throughflow of warm waters associated with the PLC into the southwest Pacific (Fig. 1.2; Sijp et al., 2011; Stickley et al., 2004; Huber et al., 2004). The throughflow of warm water from the PLC into the Pacific is reported to have led to the deflection of the Proto-Ross Sea Gyre across New Zealand, further leading to the intensification of shallow water currents across New Zealand aiding in the formation of the Marshall Paraconformity (Fig. 1.2; Lyle et al., 2007). The Marshall Paraconformity, identified as a regional unconformity within the Oligocene sedimentary succession of New Zealand (Carter and Landis, 1972; Carter, 1985; Fulthorpe et al., 1996) and Australia (Abele et al., 1976), has been the subject of extensive debate regarding its timing, mechanism of formation, and regional significance (Findlay, 1980; Lewis & Belliss, 1984; Fulthorpe et al., 1996; Carter et al., 2004). These debates arise mainly due to previous studies in the Canterbury Basin that relied on incomplete stratigraphic information and weathered sections (Findlay, 1980; Lewis, 1992; Fulthorpe et al., 1996). Multiple hypotheses have been put forward to explain the origin of this unconformity, with the main one being erosion resulting from ocean circulation changes linked to the development of throughflow across the Tasmanian Gateway (Carter and Landis, 1972; Lyle et al., 2007; Lever et al., 2007). This late Eocene to Oligocene palaeoceanographic reorganisation resulting from

wind and gateway configuration presumably impacted significantly terrestrial climate in the Australo-Antarctic region (Sites 1168 and 1172) and New Zealand (TNW-1) and form the basis for the selection of these sites, and use of sporomorphs as a proxy for palaeovegetation and palaeoenvironmental reconstruction.

Further to the above, previous preliminary late Eocene to Oligocene palynological studies in southeastern Australia (Holdgate et al., 2017) reveals major palynological differences existing between the Gippsland Basin (facing the cool TC) and the other more westerly located southern Australian coal basins (facing and under the influence of the warm PLC). This have been reported to indicate a post middle Eocene topographical divide existing between the two main areas, and similar or precussor to the present southeastern Australian topographical highs (Greenwood et al., 2017; Holdgate et al., 2017; Korasidis et al., 2023). The southeastern Australian topographic divide is reported to potentially not have been as high as the present East Australian highlands (with an average height ~1000 to 2000 m) but would have extended south through Wilsons Promontory, Flinders Island, eastern Tasmania and connected across the partially emergent South Tasman Rise through into the East Antarctic Mountains (Figs. 1.1 and 1.2; Holdgate et al., 2017). This topographic divide which runs through Tasmania may also have served as the location for higher altitude temperate forest taxa whereas lower regions would have served as sites for lowland forest taxa, thereby establishing an altitudinal gradient on each side of the divide.

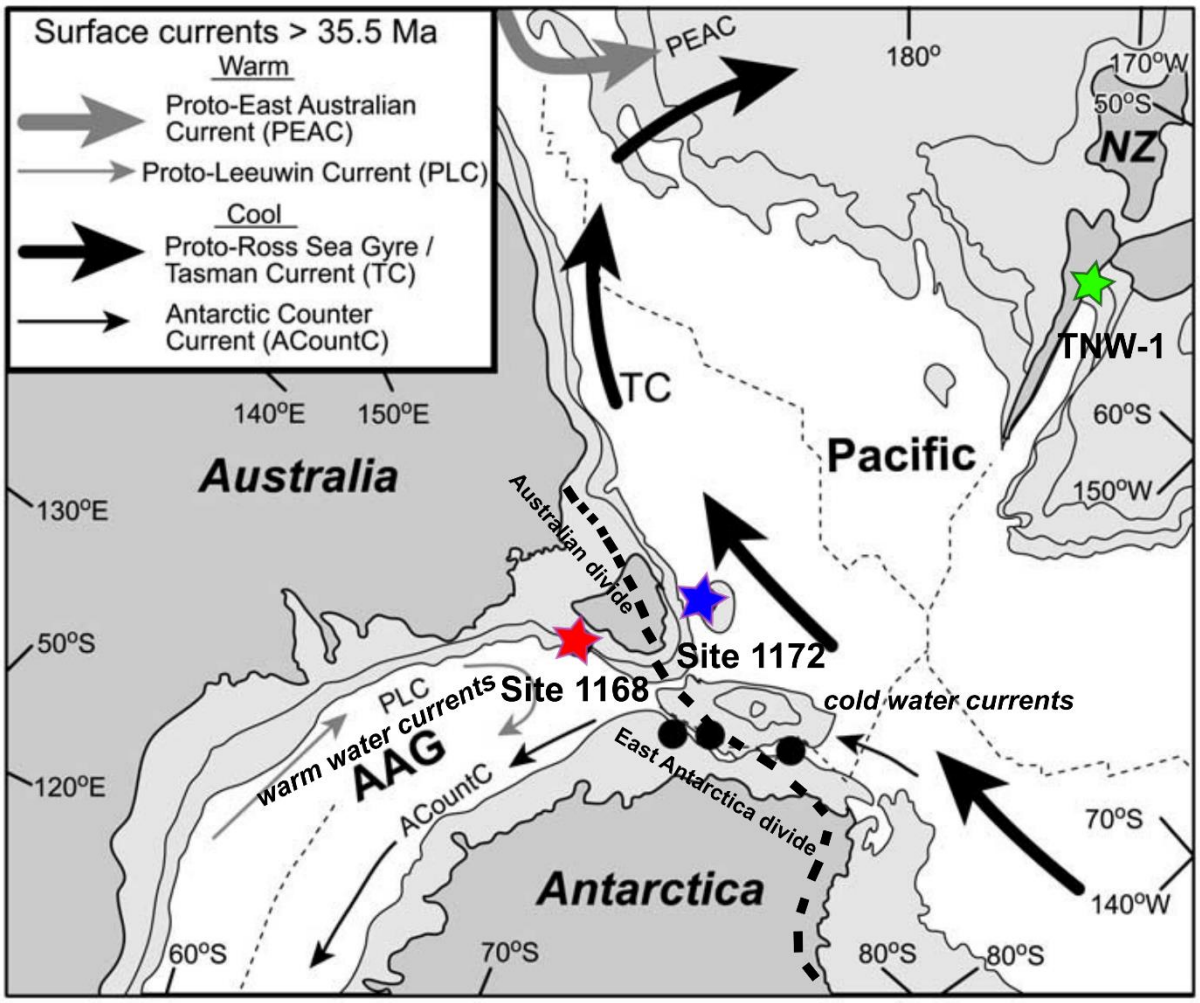

Figure 1.1. Late Eocene (>35.5 Ma) surface circulation map with selected sites for the study before the deepening of the Tasman Gateway (modified after Stickley et al., 2004). ODP Sites 1168, 1172 and TNW-1 are represented by red, blue, and green five-pointed stars, respectively. Short broken black lines from Australian section through to Antarctica represent the East Australian and East Antarctica divides, respectively and modified after Holdgate et al. (2017).

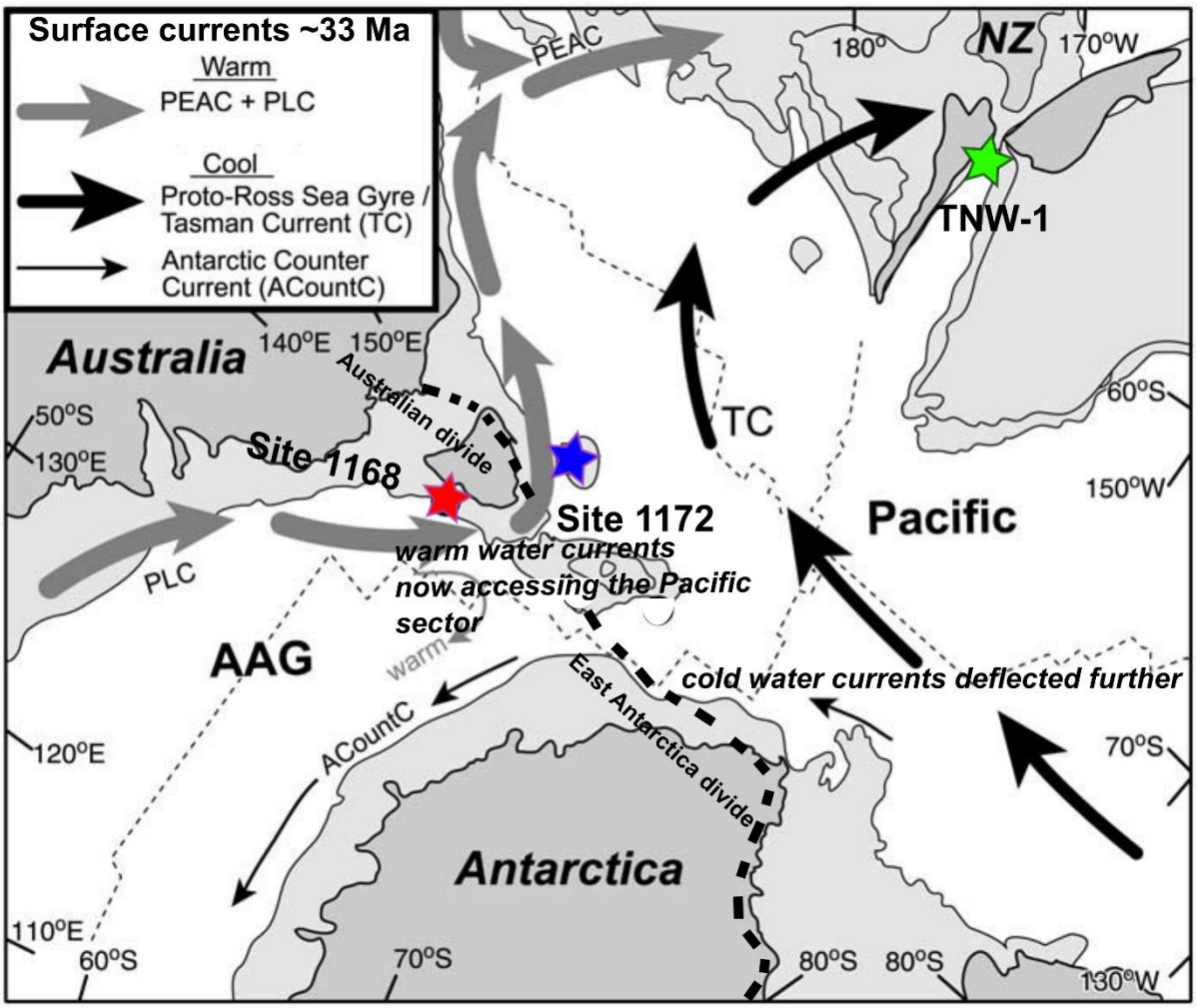

Figure 1.2. Early Oligocene (~33 Ma) surface circulation map with selected sites for the study after the deepening of the Tasman Gateway (modified after Stickley et al., 2004). ODP Sites 1168, 1172 and TNW-1 are represented by red, blue, and green five-pointed stars, respectively. Short broken black lines from Australian section through to Antarctica represent the East Australian and East Antarctica divides, respectively and modified after Holdgate et al. (2017).

In the frame of this research project, pollen analysis will be used to test the following hypotheses:

- Against the backdrop declining global pCO_2 concentrations, the tectonic deepening and/or widening of the Tasman Gateway at the EOT resulted in changes in ocean circulation during which Southeastern Australia (ODP Site 1172) came under the influence of warmer surface waters associated with the PLC, which affected terrestrial climates and vegetation (Chapter 3).

- The continuous deepening of the Tasmanian Gateway during the early Oligocene coincides with considerable reorganisation of climate and vegetation along western Tasmania, thereby establishing a strong linkage between the marine and terrestrial realms (Site 1168; Chapter 4).

- The late Eocene to the early Oligocene throughflow of warm water associated with the PLC from the into the southwest Pacific resulted in the deflection of the proto-Ross Gyre across New Zealand, further leading to the intensification of shallow water currents and the formation of the Marshall Paraconformity and coincides with major reorganisation of climate and vegetation at TNW-1 (Chapter 5).

Based on the hypotheses above, the main expected outcome of this study are:

- The confirmation of the influence of tectonic changes and ocean circulation on terrestrial climates and vegetation in Southeastern Australia during the Eocene-Oligocene transition. The analysis of sporomorphs from ODP Site 1172 (East Tasman Plateau) will reveal a significant shift in vegetation composition and diversity corresponding to the period when Southeastern Australia came under the influence of warmer surface waters associated with the PLC. This outcome will provide robust evidence linking tectonic-driven oceanographic changes to terrestrial climate dynamics and vegetation patterns in the region.
- Identification of the impact of tectonic changes in the Tasmanian Gateway on climate reorganization and vegetation dynamics in western Tasmania post-EOT and during the early Oligocene. Through pollen analysis of Site 1168 (western Tasmanian margin), this outcome will establish a strong linkage between the deepening of the Tasmanian Gateway and changes in climate and vegetation along western Tasmanian. The results will provide insights into the cascading effects of tectonic processes on ocean circulation, local climates, and terrestrial ecosystems during this critical time.
- The assessment of the influence of the late Eocene to early Oligocene throughflow of warm water associated with the proto-Leeuwin Current on climate, vegetation, and the formation of the Marshall Paraconformity in New Zealand. By analysing sporomorphs from the TNW-1 drillcore in the Canterbury Basin, this outcome will shed light on the interactions between ocean currents, paleoclimate dynamics, and vegetation patterns in New Zealand. The findings will reveal the connections between oceanographic changes, the deflection of the proto-Ross Sea Gyre, intensification of shallow water currents, and the formation of the Marshall

Paraconformity. This outcome will contribute to a better understanding of the complex relationships between tectonic processes, ocean circulation, and terrestrial ecosystems in the region.

These expected outcomes will collectively lead to the advancement of knowledge of the interplay between tectonic changes, ocean circulation, and terrestrial climate dynamics during the Eocene-Oligocene transition in the southern high-latitudes. They will provide valuable insights into the long-term consequences of tectonic activity on Earth's surface processes and contribute to a more comprehensive understanding of past climate change in the Australo-Antarctic region and New Zealand.

Considering the above, this study is aimed at reconstructing terrestrial vegetation and climate dynamics using continuous, chronostratigraphically calibrated records from the wider Australo-Antarctic area in the southern high-latitude during the middle to late Paleogene. The main objectives of this project are to:

- Erect a high-resolution palynological record with robust dating control to reconstruct vegetation dynamics across eastern Tasmania (Site 1172) from the Eocene into the Oligocene in the framework of the widening Tasmanian Gateway.
- Compare pollen-based quantitative climate estimates with published TEX_{86}-based sea-surface temperatures (SST) and branched glycerol dialkyl glycerol tetraether-based (brGDGT-based mean annual air temperatures) reconstructions from ODP Site 1172 to establish the relationship between the terrestrial and marine realms.
- Reconstruct the vegetation and climate of western Tasmania (ODP Site 1168) during the late Eocene to the Oligocene and interpret the post-EOT palaeoclimatic and palaeoecological fluctuations by comparing with vegetation and climate records from Site 1172 to highlight the relevance of the potential driver(s) responsible for these changes, if any.

- Erect a high-resolution middle Eocene to Oligocene biostratigraphic record of TNW-1 well while using the sporomorph record to reconstruct climate and vegetation before and after the deepening of the Tasmanian Gateway.

1.2 Vegetation and climate history of the mid to late Palaeogene of Southern-high latitude

This section gives an overview of several studies of the mid to late Palaeogene (Eocene and Oligocene) vegetation and climate history of the southern high-latitude with primary focus on the Australo-Antarctic region (i.e., Southeast Australia, Antarctica, and New Zealand). Though most vegetation and climate records during this timeframe are poorly resolved or documented, the focus on this region is primarily to give a general overview what the vegetation and climate were at the time of regional cooling due to declining pCO_2 concentration and/or tectonic deepening of the Tasmania. This section also reviews the early to middle Eocene acme of Cenozoic warm climates and their transition to cooler climates in the late Eocene into the early Oligocene.

1.2.1 Early to middle Eocene warmth and transition to a cooler climate

The early Eocene was the height of warmer temperatures of the Cenozoic globally (Zachos et al., 2008). This stage was distinguished by deep sea temperatures that are about 10°C higher than modern values (Fig. 1.3; Miller et al., 1987; Lear, 2000; Zachos et al., 2001; Westerhold et al., 2020), higher pCO_2 concentrations with peak values above 2,000 ppm (Pearson & Palmer, 1999; Yapp, 2004; Beerling & Royer, 2011; Huber & Caballero, 2011), and extremely reduced latitudinal temperature gradients that are defined by significantly warm climate conditions just outside the tropics (Barron, 1987; Greenwood & Wing, 1995; Bijl et al., 2009; Huber and Caballero, 2011; Pross et al., 2012). The early Eocene was also a time of substantial modernisation and turnover of the terrestrial biotic community (Greenwood et al., 2000; Carpenter et al., 2012; Contreras et al., 2013, 2014). However, the high-latitudes have been reported to have warmed more rapidly than any other part of the world at the time (Carpenter et al.,

2012), with very warm sea-surface temperatures (~34 °C; Huber et al., 2008; Bijl et al., 2009; Sluijs et al., 2009).

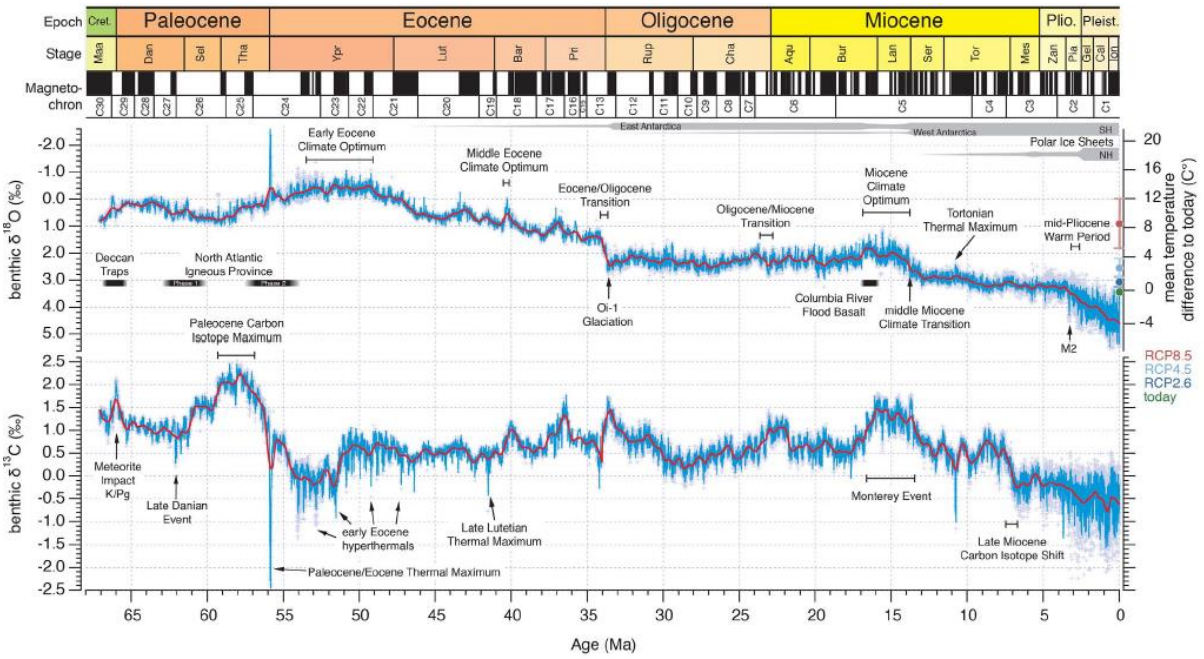

Figure 1.3. Global benthic $\delta^{18}O$ and $\delta^{13}C$ from ocean drilling cores covering the last 66 million years (after Westerhold et al., 2020). Mean temperature difference to the present for the entire Cenozoic indicated on far right of the figure.

The climate of Antarctica during the early Eocene is reported to have been relatively warmer with conditions being warm temperate by the middle Eocene (Francis & Poole, 2002; Florindo et al., 2008; Cantrill and Poole, 2012; Pross et al., 2012; Contreras et al., 2013). Two biomes were described from the Eocene of the Wilkes Land margin (Pross et al., 2012), a highly diverse paratropical rainforest and a more temperate one (Pross et al., 2012). The paratropical rainforests were interpreted to have occupied lowland coastal regions of the Wilkes Land margin and constitute the main forest biome during the early Eocene. Other works also describe the Eocene vegetation on the Wilkes Land margin as a multi-storeyed vegetation community, with a tall, relatively open canopy, a diversified overstorey featuring species like Bombacoideae, *Strasburgeria*, palms, and Proteaceae, and ferns predominating in the understorey (Contreras et al., 2013). The Sporomorph-based temperature estimates for the early Eocene of Wilkes Land were generally warm for the lowland paratropical rainforest with average MATs averaging at 16 ± 5 °C (Pross et al., 2012). Vegetation records from King George Island (South Shetland

Islands) for the early Eocene show rich and diverse flora composed of a *Nothofagus*-conifer-fern assemblage with over 40 angiosperms taxa (Cantrill & Poole, 2012). The MATs for this region are relatively lower than the Wilkes Land margin and range from 10-15 °C (Cantrill & Poole, 2012). By the middle Eocene, the flora of King George Island began to see a change in diversity and taxonomic composition, which are interpreted to reflect changing environmental conditions (Birkenmajer & Zastawniak, 1989). *Nothofagus*, together with Araucariaceae, Cyatheaceae, Gleicheniaceae, Hymenophyllaceae, Slaviniaceae, and several other cryptogams, dominated the mid-Eocene Petrified Forest Creek flora in the Ezcurra Inlet Group (Stuchlik, 1981). The Cytaela flora comprised fossilised leaf impressions of plants of the *Nothofagus*-type and *Blechnum* sp. (Birkenmajer & Zastawniak, 1989). The Mount Wawel flora of the Point Hennequin Group included angiosperms such *Nothofagus, Equisetum* (horsetail), and Podocarpaceae (Birkenmajer & Zastawniak, 1989; Hunt & Poole, 2003). According to Birkenmajer & Zastawniak (1989) and Hunt & Poole (2003), conifers such as Araucariaceae, Cupressaceae, and Podocarpaceae dominated the flora of the Dragon Glacier Moraine. On the Wilkes Land margin, the middle Eocene is characterised by a strong and rapid expansion of *Nothofagus*-dominated rainforest and the near demise of the paratropical rainforest biomes observed in the early Eocene (Pross et al., 2012; Contreras et al. 2013). The cool temperate palaeovegetation of the mid-Eocene on Antarctica is similar to the extant Valdivian rainforest of southern Chile (Poole et al., 2003). It is also worth noting that the transition from a paratropical rainforest biome in the early Eocene to a temperate one by the middle Eocene also translates into overall reduction of taxonomic diversity (Prebble et al., 2006; Contreras et al., 2013).

Across the Bass, Gippsland and Otaio Basins of southeastern Australia, the early Eocene is characterised by relatively warmer conditions with MATs ranging from 13-20 °C (Macphail et al., 1994; Greenwood 2000; Contreras et al., 2014). Terrestrial vegetation and climate show a transition from a relatively cool-temperate rainforest dominated by *Nothofagus* and secondary Araucariaceae in the late Paleocene to a Cyatheaceae dominated paratropical rainforest with an unusual amount of mangrove palm (*Nypa*) in the early Eocene (Contreras et al., 2014). Other studies in southeastern Australia report a similar transition, but from a relatively warm-temperate, conifer-dominated forests in the late

Paleocene and their replacement by meso- to megathermal angiosperm-dominated forest with typical tropical elements such as *Nypa*, Cupanieae, and *Anacolosa* (Macphail et al., 1994; Greenwood et al., 2003; Greenwood and Christophel, 2005).

Early Eocene sporomorph assemblages on New Zealand display a mixed Palaeocene-Eocene character with a consistently high conifer pollen abundance (Crouch and Visscher, 2003; Raine et al., 2009). Although Casuarinaceae pollen abruptly began to predominate the sporomorph assemblages from 54.5 Ma onward, thermophilous taxa like Cupanieae, Casuarinaceae, and Euphorbiaceae (*Austrobuxus*) are prevalent in these records (Pocknall, 1990; Raine et al., 2011). The Early Eocene (Waipawan) to middle Eocene (Bortonian) sporomorph record from Kiwi-1 section in the Taranaki Basin, off the West Coast of New Zealand, shows the common occurrence of *Nypa*, indicating the presence of a localised mangrove vegetation (Pocknall, 1990). Also, the presence of warmth-loving vegetation taxa such as Casuarinaceae, Cupanieae, *Austrobuxus*, and Sapotaceae, support that the early Eocene of New Zealand was warm enough to support the growth of these taxa. Similar vegetation composition is reported by studies from the Hawkes Bay, Canterbury Basin and Otago Basins in New Zealand (Pocknall, 1984; Pocknall, 1990). Pocknall (1990) reported the occurrence of four vegetation associations in the early to middle Eocene in New Zealand. These are the mangrove association with *Nypa* as the dominant element, wetland association with Gleicheniaceae and Liliaceae being the common elements, a coastal lowland shrub and small trees association, and a *Nothofagus*-dominated hinterland rainforest association.

1.2.2 Cooling into the late Eocene and the EOT

Following the relatively warmer conditions in the early-middle Eocene of the wider Australo-Antarctic region, the late Eocene (~37.9-33.9 Ma; Cohen et al., 2015) sees a cooling trend marked by a positive excursion in the $\delta^{18}O$ record (Fig. 1.3; Zachos et al., 2001, Westerhold et al., 2020; Hutchinson et al., 2021). This extensive cooling trend (declining MATs; Table 1.1) in the southern high-latitudes culminated in the development of Antarctic glaciation at the EOT (Fig 1.4; Katz et al., 2008; Liu et al., 2009; Hutchinson et al., 2021).

Table 1.1. Compilation of southern high-latitude mean annual temperatures for the Eocene and Oligocene

Site	Proxy	Eocene MAT (°C)	Oligocene MAT (°C)	Oligocene-Eocene (°C)	Reference
739, 742, 1166	BayMBT	11.0	6.8	-3.2	Tibbett et al., 2021
739, 742, 1166	S-index	10.4	8.1	-2.3	Passchier et al. 2017
WW7	MBTpeat	23.2	20.0	-3.2	Lauretano et al., 2021
WW7	Pollen	16	13	-3.0	Sluiter et al., 2022
696	Pollen	11.9	11.2	-0.7	Thompson et al., 2022
McMurdo	Pollen	13.0			Francis et al., 2009
King George Island	Pollen	13.4			Francis et al., 2009
1166	Pollen	12.0			Truswell and Macphail, 2009
Seymour Island	MBT/CBT	13.8			Douglas et al., 2014

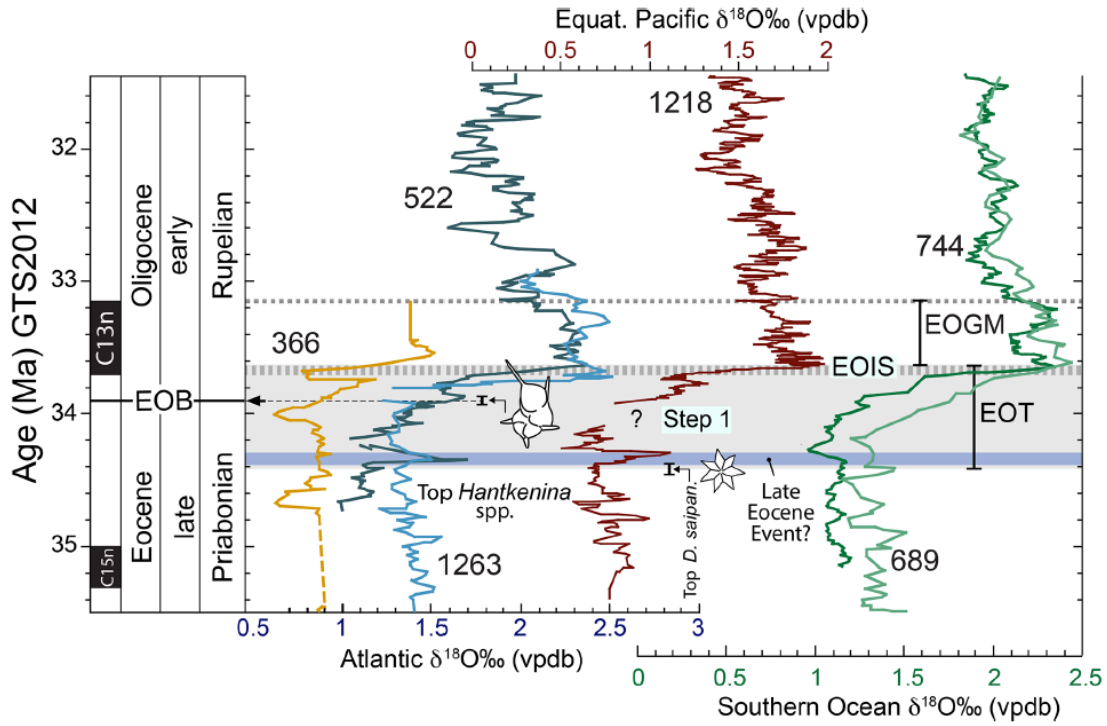

Figure 1.4. Stable Oxygen isotope record of the EOT from deep marine records showing tropical Atlantic, Southern Ocean, and equatorial Pacific sites. EOGM = Earliest Oligocene Glacial Maximum; EOIS = Earliest Oligocene Isotope Step. Figure modified after Hutchinson et al. (2021).

The Eocene-Oligocene transition (EOT; 34.44-33.65 Ma; Katz et al., 2008; Hutchinson et al., 2021) is regarded as a key interval in Cenozoic (last 65 Ma) climate history, marked by a shift from the earth's greenhouse to icehouse climate state (Zachos et al., 2008). This climate transition coincides with the

first major advance of ice sheets on the continent of Antarctica and precedes several million years of declining global temperatures (Zachos et al., 2001; Westerhold et al., 2020). Formally, the Eocene-Oligocene Boundary (EOB; 33.9 Ma; Cohen et al., 2018) is marked by the extinction of members of the planktonic foraminifera belonging to the family Hantkeninidae in the geologic record (Silva & Jenkins, 1993). Changes in ocean circulation and overturning (e.g., Katz et al., 2011; Coxall et al., 2018), ocean biogeochemistry (e.g., Lear et al., 2008; Pälike et al., 2012), global climate (e.g., Liu et al., 2009), and marine ecosystems (e.g., Villa et al., 2013; Houben et al., 2013; Houben et al. 2019) occurred along with Antarctic ice sheets expansion. The relatively rapid expansion of glacial ice over much of Antarctica was the culmination of this cooling, as evidenced by a large excursion in global oxygen isotope records (Zachos et al., 2008) synchronous with other proxies of glaciation such as ice rafted debris in ocean sediments off the coast of Antarctica (Zachos et al., 1992; Scher et al., 2011). Although the Antarctic icesheets (AIS) that formed at the EOT were still highly variable and had not yet reached its full extent during the Oligocene (Pälike et al., 2006; Liebrand et al., 2017), the Northern Hemisphere is thought to have remained largely ice-free until the Pliocene Epoch (5.3-2.6 Ma; Zachos et al., 2008; DeConto et al., 2008).

In as much as evidence for glaciation and ice-sheet expansion is extensive after the EOT, there is evidence for transient/ephemeral polar glaciation and cooling events marked by a sharp increase in $\delta^{18}O$ (similar to the first step of the EOT) in the Southern Ocean ~3 Myr prior to the EOT (Fig. 1.5; Scher et al., 2014). This ~ 140 kyr cooling event in the Kergulean Plateau is named the Priabonian Oxygen Maximum (PrOM) and tentatively placed within the magnetochron C17n.1n (37 Ma; Scher et al., 2014) based on correlation to ODP Site 689 (Maud Rise, Southern Ocean). Similar cooling events are also observed in other sites in the Southern Ocean (e.g., Maud Rise; Villa et al., 2013). On the Kerguelen Plateau, discrepancies in the neodymium isotopic content (Nd) of bottom waters and terrigenous sediments, however, indicate altered sediment provenance rather than altered ocean current rearrangement (Scher et al., 2014) consistent with an increase in deep convection currents in the Southern Ocean.

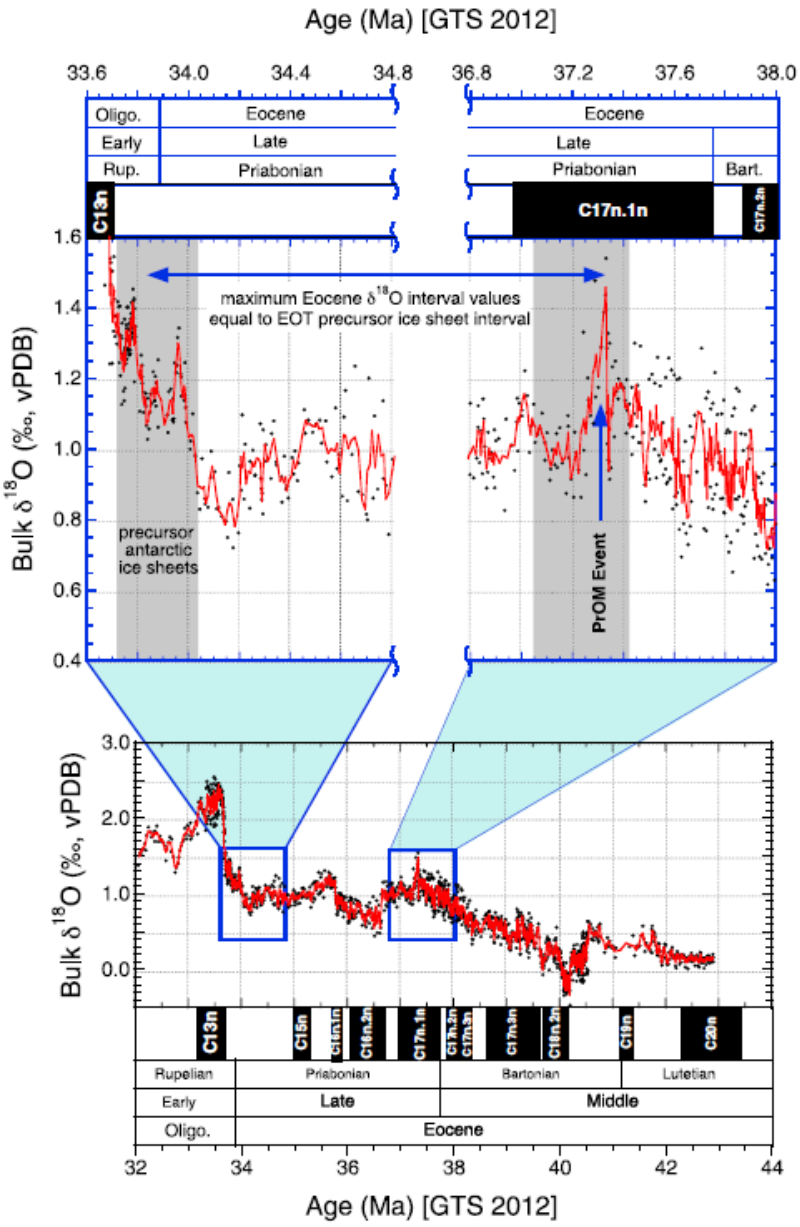

Figure 1.5: Southern Ocean oxygen isotope compilation for ODP site 738 and 748 with focus on the sharp excursion in the Priabonian (magnetochron C17n.1n). Figure is modified after Scher et al. 2014.

The general decline in temperature associated with the late Eocene and EOT leads to a reduction in palynoflora diversity and a shift toward cool temperate vegetation on Antarctica dominated by *Nothofagus* (Askin, 1992; Warny and Askin, 2011; Prebble et al., 2006; Tibbett et al., 2021). In the northern Antarctic Peninsula, this cooling trend sees the overall decline in the diversity of angiosperms (Anderson et al., 2011). In the Prydz Bay region of East Antarctica, the late Eocene vegetation is generally characterised by cool-cold temperate *Nothofagus*-dominated forest association which most

likely saw a reduction in stature to dwarfed trees (Askin, 2000; Askin and Raine, 2000; Truswell and Macphail 2009). Leaf records from the La Meseta Formation of Seymour Island show a general decrease in size during the late Eocene pointing to climate deterioration at end of the Eocene (Francis et al., 2008). Similarly, the late Eocene palynoflora on King George Island show a *Nothofagus*-dominated assemblage with secondary Podocarpaceae and ferns (mostly *Cyathidites* spp. making up ~15% of the total sporomorph taxa) (Troedson & Smellie, 2002). A recently published late Eocene sporomorph-based vegetation and climate reconstruction from Site 696 also shows a cool-temperate *Nothofagus*-dominated rainforest with secondary Podocarpaceae and variable amounts of ferns (Thompson et al, 2022).

Onshore Southeastern Australia, the late Eocene sediments are often thin/condensed with patchy distribution due to sea-level fall coupled with tectonic uplift in the Gippsland Basin resulting in widespread erosion (Macphail et al., 1994). Marine sediments on the other hand do preserve a relatively continuous record for southeastern Australia. However, these sediments are often bioturbated and dominated by wind and water transported pollen types (Macphail et al., 1994). Palynological records along southeastern Australia have shown that the palaeogeography plays an important role in the vegetation composition and climate (Holdgate et al., 2017). In the onshore Gippsland Basin (i.e., basin facing the Tasman currents), the palynoflora record is dominated by *Nothofagus* (*Brassii*-type) with high counts of *Lagarostrobos* (Holdgate et al., 2017, Korasidis et al., 2019; Sluiter et al., 2022). The palynofloral records of the basins facing the Australo-Antarctic Gulf (AAG) are typified by higher counts of Casuarinaceae with common *Nothofagus* (*brassii*-type). The contrast in palynomorph assemblages between the Gippsland Basin and basins facing the AAG are interpreted to have been a result of a topographical divide separating the sites under the influence of the warm AAG to those under the influence of the cool Proto-Ross Gyre (Holdgate et al., 2017).

The late Eocene in New Zealand is characterised by a warm, humid forest with a progressive turnover of palynomorphs (Homes et al., 2015; Pocknall, 1991). Palynofloras recovered from the Kapuni Formation in the Taranaki Basin generally show a vegetation dominated by Casuarinaceae and *Nothofagus* (*fusca*-type), with common Proteaceae (Pocknall, 1989). A similar Casuarinaceae-

dominated vegetation is observed on the west coast of the South Island during the late Eocene in the Brunner Coal Measures (Nathan et al., 1986). By the latest Eocene (Runangan), the sporomorph record from the Upper Waikato Coal Measures shows a transition from a *fusca*-type *Nothofagus* dominated forest to one dominated by the *brassii*-type *Nothofagus* (notably *Nothofagidites mataurаensis* and *N. cranwelliae*), Casuarinaceae, and Myrtaceae. The dominance of the *brassii*-type *Nothofagus* in the latest Eocene of New Zealand is interpreted to represent predominantly cool-temperate climate conditions with MATs ranging from ~ 13-18 °C (Pocknall, 1989).

1.2.3 Oligocene climate and vegetation dynamics

By the early Oligocene, ice sheets in Antarctica had expanded with various studies indicating that the expansion most likely invigorated circulation and bottom water formation in Antarctica with little influence from gateway openings (Miller et al., 2009; Goldner et al., 2014). At Prydz Bay (ODP Site 1166) in East Antarctica, *Nothofagidites* outnumbered gymnosperms, including *Phyllocladidites mawsonii* (Macphail and Truswell, 2004). The drillcore from this site also contained recycled Permian grains (*Protohaploxypinus*) and potentially early Cretaceous spores like *Cicatricosisporites* and *Retitriletes* (Macphail & Truswell, 2004). The species diversity was significantly reduced in glacial erratics from McMurdo Sound that were recognised as probably being Oligocene in age. The taxa from McMurdo Sound included *Nothofagus*, Podocarpaceae, and Proteaceae (Askin, 2000; Levy and Harwood, 2000). *Nothofagidites* from the *N. fusca* and *N. brassii* groups, as well as a large number of recycled Permian grains (e.g., *Protohaploxypinus*), predominate in the pollen assemblages from the CRP cores in the Ross Sea region (Askin & Raine, 2000; Raine & Askin, 2001). *Nothofagidites fusca*-type (*N. flemingii* and *N. lachlaniae*) and *Podocarpidites* sp., together with additional taxa including *Myricipites. harrisii*, *Cyperaceaepollis* sp., and *Tricolpites*, characterise the early Oligocene flora in the CRP2/2A core (Prebble et al., 2006). One *Nothofagus* leaf recovered in the CRP-3 drillhole, which indicates the existence of trees and shrubs in East Antarctica during the early Oligocene, is used to support the discovery of a *Nothofagus* flora in the Ross Sea (Cantrill, 2001). Palynology samples from the CIROS-1 drillhole in McMurdo Sound, Antarctica, revealed assemblages of the *N. brassii* and *fusca*-types with rare *Podocarpidites* (Mildenhall, 1989). In addition, leaf compressions of *Nothofagus*

were also found in the CIROS-1 drillcore (Hill, 1989; 1991). The Oligocene vegetation in Antarctica is interpreted to resemble a tundra vegetation community (Askin & Raine, 2000). In the Ross Sea region, there are woody taxa (e.g., *Nothofagus* and *Podocarpus*) that are suggested to have thrived in protected regions, with minor herbs by the late Oligocene (Prebble et al., 2006). Sporomorphs recovered from Destruction Fan Bay showed that *Nothofagus*-dominated with secondary Podocarpaceae shrub/forest and reduced cryptogams still thriving in Antarctica at the end of the Oligocene (Troedson & Riding, 2002).

Sporomorphs recovered from the Gippsland Basin of southeastern Australia document an earliest Oligocene T0 coal seam with higher abundances of *Lagarostrobos* and *Microcachrys*, coupled with an increased amount of *Nothofagus* (Korasidis et al., 2019; Sluiter et al., 2022). By the early Oligocene, the Gippsland Basin record from the Latrobe Group shows a shift in composition, characterised by high abundances of *Nothofagus*, *Dacrycarpus*, and Elaeocarpaceae. This palynoflora composition is informally referred to as the *Nothofagus-Dacrycarpus* cool-temperate rainforest association (Korasidis et al., 2019). This interpretation is supported by quantitative sporomorph-based MATs that reports a decline in MATs to below 14 °C throughout the Oligocene. However, temperature reconstruction by Sluiter et al. (2022) from the same site in the Gippsland Basin suggests a warm-temperate climate conditions for the Oligocene with MATs between 14-18 °C . Other sites in Australia (e.g., Pioneer, Cethana, and Little Rapid Rivet) further report an increased representation of palynomorphs with affinity to cooler climate conditions (Hill and Macphail, 1983, Macphail et al., 1994). The continuous build-up of ice on Antarctica during the middle Oligocene, leading to relative sea level fall (Haq et al., 1987; Truswell 1993), is suggested to have been responsible for the temporary break in coal seam deposition in Australia (Korasidis et al., 2019).

By the early Oligocene (Whaingaroan) in New Zealand, *Nothofagus* (*brassii*-type) still dominated the palynofloras. However, there is a switch or transition from *N. matauraensis* dominated vegetation to that of *N. cranwelliae* dominated rainforests (Pocknall, 1985; 1989) by the late Oligocene. The rise in abundance of *Nothofagus* has long been interpreted as indicative of a climate cooling regime (Pocknall, 1989; Macphail et al., 1994; Partridge and Dettmann, 2003). Recovered sporomorphs from different

locations in the North Island of New Zealand confirm this interpretation of cooling climate (Pocknall 1985). Samples from the Waikato Coal Measure in the Wharauroa Plateau are dominated by *N. mataurаensis* with secondary *Myricipites harrisii*, Myrtaceae and *Nuphar* (Pocknall, 1985). Though *N. cranwelliae* is reported to have appeared first in the late Oligocene of Southland, New Zealand (Pocknall & Mildenhall, 1984), they are found in over half of the samples from the Wharauroa Plateau, thereby confirming their appearance earlier in the Waikato Basin. In the Te Mata-Kawhia road section, the recovered sporomorphs were also dominated by *N. mataurаensis*, with secondary *Myricipites harrisii*, Myrtaceae, *Rhoipites* and *Sparsipollis acuminatus*. In the Karamu district, *N mataurаensis* still dominated. However, in comparison to the other sites, the secondary taxa here are gymnosperms (*Phyllocladus*, Araucariaceae, *Podocarpus* and *Dacrydium*), with diverse cryptogams (Pocknall et al., 1985). The late Oligocene rainforest of the Karamu district is more diverse than others from the region and has *brassii*-type *Nothofagus* as the main forest component with gymnosperms most likely serving as the emergent cover/canopy. The abundance of gymnosperms here is further interpreted to have resulted from a decline in temperature/climate from a warm temperate early Oligocene to a relatively cool-temperate late Oligocene climate (Pocknall et al., 1985).

1.3 Thesis structure

This PhD thesis consists of six chapters. The first chapter gives a general overview of the study including a general introduction, focus and experimental setup, and review of middle to late Paleogene vegetation and climate in southern Australia (including Tasmania), Antarctica, and New Zealand. The main methods and materials used in this project are described in the second chapter. Chapter 3 takes a closer look at investigating and understanding the timing and nature of southern high-latitude terrestrial environmental (eastern Tasmania) change across the EOT using sporomorphs recovered from ODP Site 1172 in the context of the widening Tasmanian Gateway. Chapter 4 compares the late Eocene to Oligocene changes in terrestrial vegetation and climate from ODP Site 1172 to records from ODP Site 1168 and others in southern Australia to identify the potential driver(s) of vegetation and climate change, especially in the early Oligocene. Chapter 5 uses pollen, spores and dinoflagellate cysts recovered from the TNW-Well, Southland, New Zealand to build a high-resolution biostratigraphic

record. This is then followed by using the recovered sporomorphs to reconstruct vegetation and climate before and after the development of the Marshall Paraconformity and its relationship with the oceanographic changes resulting from the Tasmanian Gateway deepening. Finally, the general conclusions and outlook are highlighted in chapter 6.

2. Methodology

2.1 Summary of palynomorph extraction, processing, and analysis

For this study, a total of 154 palynological samples were analysed for their pollen, spores, and dinoflagellate cysts (though primary focus was on the sporomorphs). 66 samples were analysed for ODP Site 1172 (Chapter 3), 51 for ODP Site 1168 (Chapter 4), and 37 for TNW-1 (Chapter 5). Samples from Sites 1172 and 1168 were prepared and supplied by the GEOLAB of Utrecht University Laboratory of Palaeobotany and Palynology. Rock samples for TNW-1 were supplied by GNS Science, New Zealand and were processed for their sporomorph and dinoflagellate cysts content at the Palynology Laboratory of Northumbria University, Newcastle. A brief description of the palynomorph extraction techniques is provided in the materials and method section of each chapter (from chapter 3 to 5), while the overarching methods are described in this chapter.

Samples for this study/project were analysed using the LEICA DM500 and DM2000 transmitted light microscopes at 400x magnification. The 1000x oil immersion magnification was used in instances where detailed morphological features of the grains are needed. To obtain counts of >100 individual sporomorphs, up to 3 slides were counted for each sample. However, pollen recovery in some samples (33 samples across the three study sites) was poor and almost barren, to the extent that it is nearly impossible to reach counts of about 50 grains. Based on total sum of pollen and spores, sporomorph percentages were calculated for each study site and plotted using Tilia version 2.6.1 (Grimm, 1990). Sporomorph identification and botanical affinities (used for nearest living relative identification of fossil spores and pollen; Appendix 1) were established using Pocknall (1985), Pocknall (1991), Macphail & Cantrill (2006), Macphail (2007), Truswell & MacPhail (2009), Daly et al. (2011), Kumaran et al. (2011), Raine et al. (2011), Bowman et al. (2014), and Macphail & Hill (2018).

2.2 Quantitative Sporomorph Analysis

Six techniques were used to quantitatively analyse the Eocene to Oligocene sporomorph assemblage at Site 1772, Site 1168, and TNW-1.

i. Detrended Correspondence Analysis (DCA) is a multivariate statistical ordination technique used here to evaluate how floral composition changes throughout the sections/samples used in this study. This ordination technique has been applied in numerous palynological studies in the Palaeogene to investigate the overall changes in palynoflora composition through time and space (e.g., Harrington, 2001; Jaramillo, 2002; Wing & Currano, 2013; Contreras et al., 2014). Though this technique is based on the principle of correspondence analysis by reducing the number of dimensions in floral compositions, it works by eliminating the arch effect (Hill & Gauch, 1980; Peet et al., 1988) or "straightening out" points in an arch, in an attempt to prevent clustering of points at the edge, consequently "spreading out" these points (Peet et al., 1988). This analysis was performed using the Vegan package (Oksanen et al., 2019) of R statistical software (R Core Team, 2019)

ii. Principal component analysis (PCA) is an ordination technique that simplifies the complexities in a multi-dimensional data and in the process, retains the trends and patterns that were, hitherto, hidden (Lever et al., 2017). PCA acts as a data reduction technique and transforms the data into fewer dimensions (mainly the first two main axes or principal components), hence summarising the main environmental features. For this study, PCA was applied to the transformed raw species abundance dataset to pick out the correlation between groups of variables (taxa) and the main gradients of variance (environmental parameters; Legendre & Legendre, 2012). The abundance datasets were first normalised using the Vegan Package (Oksanen et al., 2019) of R statistical software (R Core Team, 2019) to reduce the overall symmetry before proceeding to apply the PCA with the same Vegan Package. The motivation for using this ordination technique is explained in detailed in Chapter 4.3.4.

iii. Rarefaction is an interpolation technique used to compare taxonomical diversity in samples of different sizes (Birks & Line, 1992; Birks et al., 2016). For this technique to be used appropriately, individuals are kept at a constant number and sporomorph species obtained accordingly. This analysis was performed in PAST statistical software (Hammer et al., 2001) with samples rarefied at 75 and 100 individuals/grains, respectively. A detailed explanation as

to why samples rarefied at 75 individuals were used for the analysis is given in the methods section of chapter 3.

iv. The Shannon Diversity Index ($H=-sum((n_i/n)ln(n_i/n))$ with n = number of individuals and n_i = number of individuals of taxon i) is a measure of diversity that considers the number of individuals as well as the number of taxa and evenness of the species present. H varies from 0, involving vegetation communities with a single taxon, to higher values where taxa are evenly distributed (Legendre and Legendre, 2012). The Shannon Diversity Index was computed using PAST statistical software (Hammer et al., 2001), and with samples containing counts of ≥ 75 individuals used.

v. Shannon Equitability/Evenness (J = H/Hmax= H/ln S) measures the level of abundance and how they are distributed in an assemblage. J varies from 0 to 1 with 1 signifying complete evenness where the assemblage is represented by the same number of individuals. Low J values indicate the dominance of a few species in the population (Hayek & Buzas, 2010).

vi. Stratigraphically Constrained Cluster Analysis (CONISS) is a multivariate statistical technique used to quantitatively define stratigraphic zones. This technique only considers stratigraphically adjacent clusters for analysis as opposed to the normal, unconstrained cluster analysis (Grimm, 1987). This stratigraphically constrained analysis was carried out in Tilia version 2.6.1 (Grimm, 1990) by the method of total sum of squares with chord distance square root transformation by Cavalli-Sforza & Edwards (1967).

2.3 Sporomorph-based Climate Estimates

The nearest-living relative (NLR) approach was used in this study to estimate and reconstruct mean annual temperature (MAT), warm mean month temperature (WMMT), cold mean month temperature (CMMT) and mean annual precipitation (MAP). The NRL has become a powerful tool in palaeoclimatology and paleoecology, and uses the ecologic or climatic characteristics of modern taxa to estimate or reconstruct conditions under which fossil taxa potentially thrived (Mosbrugger, 2009). The bioclimatic analysis used in this study involved using all pollen and spore taxa that could be related to an NLR and are listed in Appendix 1. The NLR is a uniformitarian approach based on the assumption

that climate tolerance of extant/modern taxa can be extended into the past (Bowman et al., 2014; Utescher et al., 2014; Klages et al., 2020). Uncertainty with this approach increases when analysing plant remains or samples from deep-time geological intervals or records. This stems from the fact that the geologic or stratigraphic age of the fossil taxon determines the accuracy of the palaeonvironmental information extracted, and on the taxonomic level to which the NLR of the fossil taxon is determined (Mosbrugger, 2009; Hollis et al. 2019; Klages et al., 2020). One of the strengths of the NLR is that it reduces the likelihood of taphonomic bias since it is based on the presence or absence of a sporomorph taxa in an assemblage, rather than on relative abundance (Klages et al., 2020). This makes this method particularly suitable for sporomorph-based climate estimates from marine sedimentary deposits, where hydrodynamic sorting of pollen grains may result in variations in the percentage abundance of individual taxa (Thompson et al., 2022). Based on the recommendations of Hollis et al. (2019), and to statistically constrain the most likely climate co-occurrence envelope, the NLR analysis is combined with the probability density functions (PDF; Kühl et al., 2002; Harbert & Nixon, 2015; Greenwood et al., 2017) in this study. The advantage of the PDF method over other NLR approaches, such as the coexistence approach (Mosbrugger & Utescher, 1997) and bioclimatic analysis (Greenwood et al., 2005), is that it statistically limits the range of the most likely climatic co-occurrences. This proffers a solution that potentially mitigates the effects of incorrectly defined climate tolerance on the upper and lower bounds of palaeoclimatic estimates.

Palaeoclimate estimates were generated following the procedures described by Klages et al. (2020); Sluiter et al., (2022), and Thompson et al. (2022). This is performed by first identifying the NLR of each fossil taxa and their bioclimatic envelope by using the dismo package in R (Hijmans et al., 2017) to cross-plot their modern distribution from the Global Biodiversity Information Facility (GBIF) with gridding from the WorldCLIM climate surface (Fick & Hijmans, 2017). These datasets are then filtered to remove multiple entries per climate grid cell, plants whose botanical affinity are vague or doubtful, redundant and occurrences termed exotic such as garden plants. The filter process is performed to avoid bias in the probability function that may likely lead to results to lean towards that location (Reichgelt et al., 2018). To test the robustness of the dataset, bootstrapping was applied to the generated NLR dataset,

which is particularly important for taxa with only a few modern occurrences. This was then followed by calculating the likelihood (*f*) of a taxon (t) that occurs at a value (*x*) for a specific climate variable using the mean (μ) and standard deviation (σ) of the modern distribution range of each taxon (Kühl et al., 2002; Willard et al., 2019) in (***Eq.*1**).

$$f(x)_t = \frac{1}{\sqrt{2\pi\sigma_x^2}} \mathrm{e}^{-\frac{(x-\mu_x)^2}{2\sigma_x^2}} \qquad \textit{Eq.1}$$

Next is calculating the joint likelihood PDFs using the correlation coefficient p(x,y) in (**Eq.2**) for each combination of climate variables MAT, MAP, WMMT, CMMT. This is because intervals where no modern-day occurrence of "t" is observed can be included in the bioclimatic envelopes due to separate reconstruction of climate ranges for each variable (Willard et al., 2019).

$$f(x,y)_t = \frac{1}{2\pi\sigma_x\sigma_y\sqrt{1-p^2}} \mathrm{e}^{-\frac{1}{2(1-p^2)}\left(\frac{(x-\mu_x)^2}{2\sigma_x^2}+\frac{(y-\mu_y)^2}{2\sigma_y^2}-2p\frac{(x-\mu_x)(y-\mu_y)}{\sigma_x\sigma_y}\right)} \qquad \textit{Eq.2}$$

After checking whether the bioclimatic envelopes have a coexistence interval in common, the quantitative climate estimates of the NLR assemblages are then reconstructed by multiplying the individual joint likelihoods of taxa $f(x,y)_{t1}\ldots f(x,y)_{tn}$ with each other (**Eq. 3**)

$$f(x,y)_{\text{Combined}} = f(x,y)_{t1} x f(x,y)_{t2} x \ldots x f(x,y)_{tn} \qquad \textit{Eq. 3}$$

To envelope the main distribution of a group, the range of one ($f(x,y)_{relative}$ = 0.157) and two standard deviations ($f(x,y)_{relative}$ = 0.023) were determined from the occurrence within a group with $f(x,y)_{max}$ representing the most likely climatic conditions in **Eq. 4** (Reichgelt et al., 2018).

$$f(x,y)_{\text{relative}} = \frac{f(x,y)}{f(x,y)_{max}} \qquad \textit{Eq. 4}$$

In this study, climatic ranges are indicated with ±2σ range. However, the ranges of the calculated climate estimate show mathematical error and not the real range, which may have resulted from the uncertainties associated with the NLR approach.

3. Eocene to Oligocene vegetation and climate were controlled by changes in ocean currents and pCO_2 in eastern Tasmania (ODP Site 1172)

3.1 Introduction

The EOT (34.44–33.65 Ma; Katz et al., 2008; Hutchinson et al., 2021) is one of the key climate transitions of the Cenozoic, marked by the development of the Antarctic cryosphere and global cooling (Liu et al., 2009; Pearson et al., 2009; Pagani et al., 2011; Hutchinson et al., 2021). Tectonic opening of the southern gateways (Kennett, 1977), and a substantial and rapid decline in global atmospheric pCO_2 concentration (DeConto and Pollard, 2003; Huber et al., 2004; Zachos et al., 2008; Goldner et al., 2014) have been postulated as the possible driver(s) of this climatic shift.

In as much as the southern gateway opening and deepening have not fully explained Antarctic cooling at the EOT, oceanographic changes following gateway opening and deepening have been reported to climatically impact Southern Ocean surface waters regionally (Stickley et al., 2004; Sijp et al., 2011; Houben et al., 2019; López-Quirós et al., 2021; Thompson et al., 2022). However, the tectonic opening and deepening of the Tasmanian Gateway and concomitant oceanographic impacts on coeval terrestrial climate and vegetation are poorly documented due to the paucity of continuous well-dated EOT terrestrial data, thereby limiting temporal and geographic reconstructions of vegetation and climate.

This chapter presents a new sporomorph record recovered from ODP Site 1172 (Fig. 3.1) on the East Tasman Plateau (ETP) spanning the late Eocene (37.97 Ma) to earliest Oligocene to further the understanding of the timing and potential drivers of southern high-latitude terrestrial environment change at the EOT (33.06 Ma). The study site is in an excellent geographical position to assess potential tectonic or climate effects on the Australo-Antarctic region's terrestrial vegetation because of its proximity to the Tasmanian Gateway. A comparison of pollen-based quantitative climate estimates are made with recently published TEX_{86}-based sea-surface temperature (SST) and mean annual air temperature (MAATsoil) reconstructions from the same location (ODP Site 1172) to investigate any connections between the terrestrial and marine realms (Bijl et al., 2021). In summary, this study/chapter

indicates that eastern Tasmania experienced a significant cooling ~ 3 Ma before the EOT, followed by a warming in the early Oligocene that was most likely controlled by a transient rebound of atmospheric pCO_2 and a sustained deepening of the Tasmanian Gateway.

3.2 Materials and Methods

3.2.1 Tectonic change and depositional environment

The Late Cretaceous (75 Ma; Cande & Stock, 2004) marks the initiation of continental breakup and seafloor spreading between Australia and the continental blocks of Lord Howe Rise, Campbell Plateau, and New Zealand (LCNZ). Through rifting, Australia moved northward, causing the Tasman Sea to form and northeastern Australia to separate in the Paleocene (60 Ma; Gaina et al., 1999). Major ocean currents, the ETP, and the South Tasman Rise (STR) were facilitated by a succession of tectonic events that occurred along the coasts of eastern Australia and Tasmania (Exon et al., 2004a). The AAG and the Pacific Ocean were nevertheless "divided" by the Tasman promontory until the late Eocene (35.5 Ma; Stickley et al., 2004). The study site (ODP Site 1172 on the ETP; Fig. 3.1) is situated on one of the five continental blocks sampled during ODP Leg 189 (Exon et al., 2004b), ~ 170 km southeast of Tasmania (4357.60 S, 14955.70 E; Fig. 3.1a; Shipboard Scientific Party, 2001a), in water depths of ~2620 metres (Exon et al., 2004a), and is enclosed by an 1800-metre-high seamount (Royer & Rollet, 1997). The ETP, which currently forms an oval platform, was previously a portion of Tasmania and the STR before the Tasman Sea broke up in the Late Cretaceous (95 Ma; Royer & Rollet, 1997; Exon et al., 2004b). The East Tasman Saddle, which bathymetric studies show connects the ETP to Tasmania's east coast, gives no evidence of a deep basin between them (Royer & Rollet, 1997; Hill & Exon, 2004). A dredging operation confirmed the plateau's potential continental origin (Exon et al., 1997). The ETP itself, however, is not a likely source of the terrestrial organic debris due to the guyot/seamount's age (36 Ma; Lanyon et al., 1993), which rules it out (Bijl et al., 2021). Additionally, the widespread Permo-Triassic reworked components in the late Eocene–early Oligocene sporomorph assemblage strongly suggest an eastern Tasmanian sporomorph source, in agreement with the Permian–Triassic upper Parmeener Group, which contains terrestrial deposits and currently makes up the surface lithology

across east Tasmania. An early Paleocene–Eocene sporomorph assemblage from the ETP (ODP Site 1172) provides further support for a terrestrial palynomorph source in eastern Tasmania (Contreras et al., 2014).

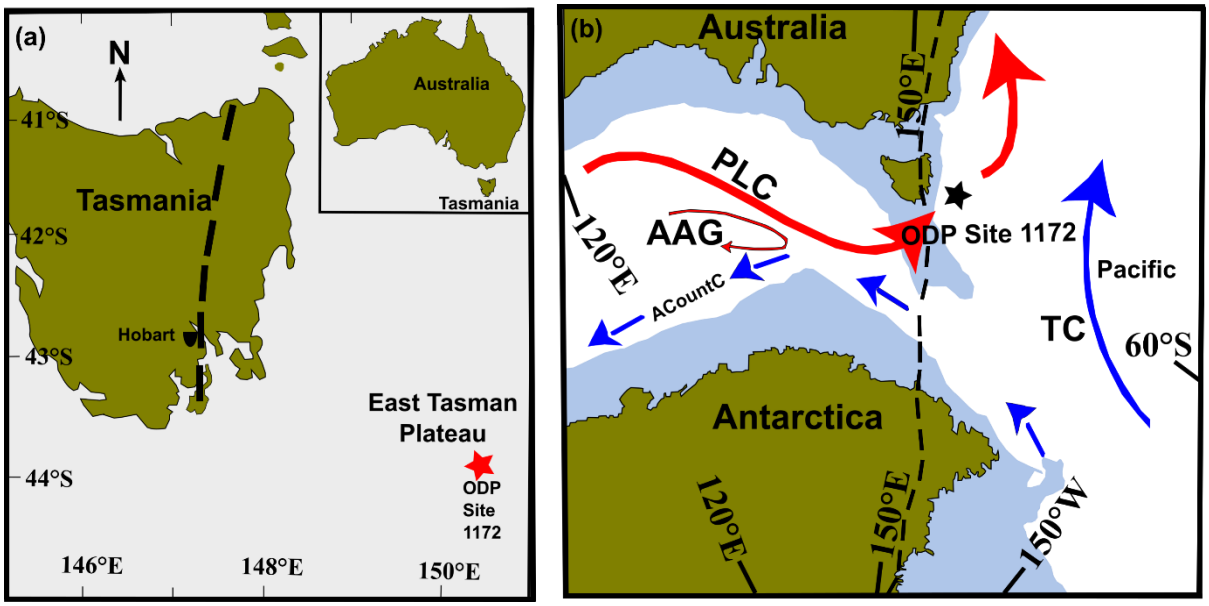

Figure 3.1 (a) Location of the East Tasman Plateau (red star, ODP Site 1172) and present-day Tasmania (Quilty, 2001). The landmass of Tasmania is depicted in green, while the submerged ODP Site 1172 is depicted in grey at a depth of ~2,620 metres. (b) Palaeogeography and palaeoceanography of the Tasmanian Gateway during the Early Oligocene. A black five-pointed star indicates ODP Site 1172. Surface currents are after reconstructions by Stickley et al. (2004). TC stands for the Tasman Current, PLC for the proto-Leeuwin Current, ACountC for the Antarctic Counter Current, and AAG for the Australo-Antarctic Gulf. Red arrows denote ocean currents from the AAG that are warmer, whereas blue arrows denote ocean currents that are colder. The size of the arrow represents the relative strength of the current. Figure is modified after Hoem et al (2021). Short broken black lines from Australian section through to Antarctica represent the East Australian and East Antarctica divides, respectively. Modified after Holdgate et al. (2017).

The marine sedimentary record is divided lithologically into three units: (i) shallow-marine, organic-rich middle Eocene to lower upper Eocene clay; (ii) a highly condensed middle late Eocene to lowermost Oligocene glauconite-rich, shallow-marine silty sandstone; and (iii) a lower Oligocene siliceous-rich carbonate ooze. Both Holes A and D of ODP Site 1172 on the East Tasman Plateau generated EOT records, and their pollen and spore contents were analysed. The age model is based on magnetostratigraphy (which has a particularly strong signal in the late Eocene; Stickley et al., 2004; Fuller & Touchard, 2004) and biostratigraphy (dinoflagellate cysts, nannoplankton, and diatoms; Stickley et al., 2004; Bijl et al., 2013), as described in Houben et al. (2019) and Bijl et al. (2021).

3.2.2 Study samples

To reconstruct past vegetation and climate, 66 samples from the late Eocene to the earliest Oligocene of ODP Site 1172 (37.97–33.06 Ma) were examined for their terrestrial palynomorphs. These samples were prepared at the GEOLAB of Utrecht University Laboratory of Palaeobotany and Palynology using standard palynological processing techniques (Bijl et al., 2013). Treatment of samples with 30% HCl and 38% HF was followed by sifting the residues using a 15 µm nylon sieve (Pross, 2001). As a mounting medium, glycerine gel was used to attach the residue to microscope slides. Sieving is a typical procedure for removing undesirable organic/inorganic debris and increasing pollen concentration when analysing marine sediments like those utilised in this study. To limit the possibility of losing particularly smaller pollen grains, residue were routinely evaluated by sieving through 10- and 15 µm mesh. No indication of a selective loss of smaller pollen grains was discovered, including *Myrtaceidites* and *Sapotaceoidaepollenites cf. latizonatus*. Similar to pollen records recovered from lakes (>200 m in diameter) and estuaries in Australia, Site 1172 marine sporomorph record is likely to be biased toward abundant taxa in the regional vegetation, whereas sporomorphs recovered from coal, lignite, peat, and backswamp deposits are more likely to reflect local flora, with higher diversity and occasional high values of underrepresented taxa (Macphail et al., 1994).

At 400 and/or 1000x magnification, Leica DM 500 and DM 2000 LED microscopes were used to examine at least three slides for each sample. For each sample, between 200-250 fossil spores and pollen grains counts was attempted (excluding reworked sporomorphs), and then the entire microscope slide was scanned to record unusual or rare taxa. Apart from nine samples with counts below 50 grains, pollen preservation and counts were mostly good. The thermal maturity (i.e., colour) of the outer coats (exine) and their existence beyond their known stratigraphic range were used to identify reworked sporomorphs. Non-pollen palynomorphs were documented, but their counts were not included in the overall pollen count. Sporomorph percentages were computed based on the total number of pollen and spores, omitting reworked grains, and plotted with Tilia version 2.6.1. (Fig. 3.2; Grimm, 1990). Using the Edwards and Cavalli Sforza chord distance, a stratigraphically constrained incremental sum-of-squares cluster analysis (CONISS; Grimm, 1987; PZ; Fig. 3.2) was performed. Sporomorph

identification and botanical affinities (used for nearest living relative identification of fossil spores and pollen) were established using Macphail & Cantrill (2006), Macphail (2007), Truswell & MacPhail (2009), Daly et al. (2011), Kumaran et al. (2011), Raine et al. (2011), Bowman et al. (2014), and Macphail & Hill (2018).

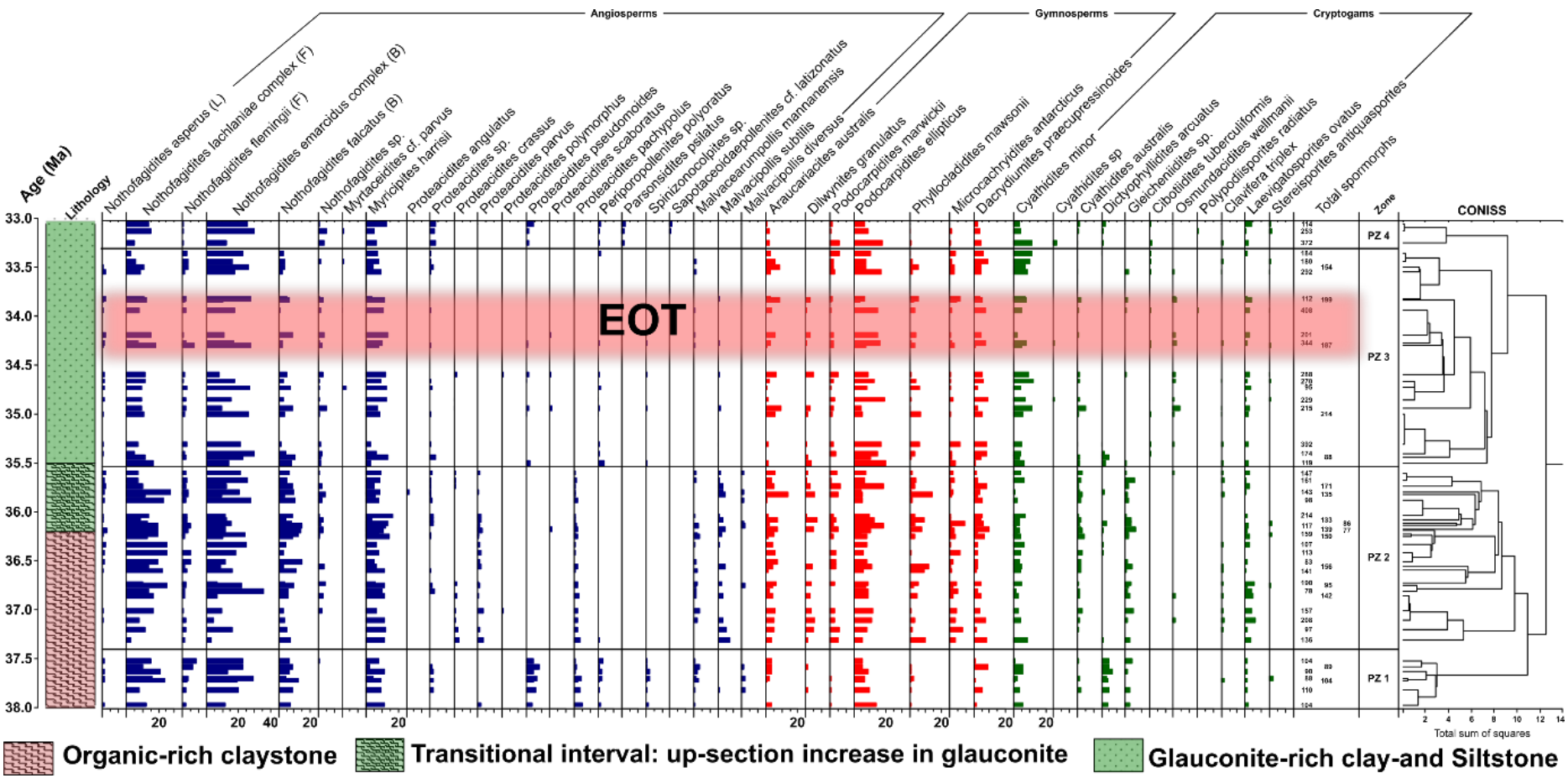

Figure 3.2: Sporomorph assemblages and relative abundances of important sporomorph species (angiosperms, gymnosperms, cryptogams) from the late Eocene to early Oligocene of ODP Site 1172. The relative abundances of angiosperms, gymnosperms, and cryptogams are indicated by blue, red, and green bars, respectively. *Nothofagidites*, a subgroup of angiosperms, is further subdivided into subgenera. These are B, F, and L which represents *Brassospora*, *Fuscospora*, and *Lophozonia*, respectively. CONISS ordination divides the late Eocene to early Oligocene sporomorph assemblages into four discrete pollen zones (PZ 1–PZ 4) or vegetation and climatic stages. The age model is after Houben et al. (2019) and Bijl et al (2021).

3.2.3 Quantitative and statistical analyses

Using the PAST statistical software (Hammer et al., 2001) and sample counts of ≥ 75 individuals, diversity indices (rarefaction, Shannon diversity index, and equitability) were generated.

Rarefaction is an interpolation method used to compare the taxonomic diversity of samples of varying sizes (Birks & Line, 1992; Birks et al., 2016). Using sample counts of ≥75 and ≥100, rarefaction analysis revealed comparable diversity trends. However, counts with ≥75 grains were used for the analysis since they gave the added benefit of filling in the gaps that would have been generated if only samples with counts of ≥100 grains were used, thereby boosting the resolution of the section under study. The Shannon diversity index (H) is a measure of diversity that takes into account the number of individuals, the number of taxa, and the distribution of species present (Shannon, 1948). H ranges from 0 for vegetation communities with a single taxon to higher values for communities with evenly distributed taxa (Legendre & Legendre, 2012). Equitability (J), on the other hand, quantifies the abundance and distribution of species within an assemblage. Low J values represent the dominance of a small number of species in a population (Hayek & Buzas, 2010).

Following stratigraphically constrained analysis (CONISS; Grimm, 1987), pollen zones (PZ) were identified in Tilia (version 2.6.1) utilising the chord distance square-root transformation (Cavalli-Sforza & Edwards, 1967). In addition, the sample-to-sample variance were calculated using detrended correspondence analysis (DCA; Hill & Gauch, 1980) sample scores. Here, the R statistical software vegan package (Oksanen et al., 2019) was used to generate DCA sample scores (R Core Team, 2019).

3.3 Results

3.3.1 Palynological results from ODP Site 1172

The ETP (ODP Site 1172) samples from the late Eocene to early Oligocene yielded moderately to well-preserved sporomorphs. A total of eighty-one (81) distinct sporomorph taxa were identified from the 57 productive samples collected along the examined area. The sporomorph record is dominated by *Nothofagidites* spp., which accounts for between 38% and 48% of all non-reworked sporomorphs over

the examined interval (Fig. 3.2). *Podocarpidites* spp., *Myricipites harrisii*, *Cyathidites* spp., *Phyllocladidites mawsonii*, and *Araucariacites australis* are notable components of the palynoflora and are found with differing frequency (Fig. 3.2).

Based on rarefaction data, the average diversity of the total section analysed was 20.1 ± 1.74 taxa per 75 individual grains. Based on CONISS, the sporomorph record is divided into four pollen zones (PZ; Fig. 3.2): PZ 1 (early late Eocene; 37.97–37.52 Ma), PZ 2 (late Eocene–latest Eocene; 37.30–35.60 Ma), PZ 3 (latest Eocene–earliest Oligocene; 35.50–33.36 Ma), and PZ 4 (earliest Oligocene; 33.25-33.06 Ma). The characteristic palynoflora assemblages of all four zones are detailed below. Taxon names included in brackets refer to NLRs.

3.3.2 Pollen Zone 1 (37.97-37.52 Ma; 7 samples)

Nothofagidites spp. (*Nothofagus*) comprises 48% of all non-reworked palynomorphs in pollen zone 1 (PZ 1). *Brassospora* (28%), followed by *Fuscospora* (19%), and *Lophozonia* (1%) taxa make up the *Nothofagus* assemblage. Other angiosperms (non-*Nothofagus*) account for 24% of all sporomorphs on average. These are mostly represented by *Myricipites harrisii* (*Gymnostoma*), *Proteacidites pseudomoides* (*Carnarvonia*), *Proteacidites* spp., *Spinizonocolpites* spp. (Arecaceae), *Malvacearumpollis mannanensis* (Malvaceae), and *Malvacipollis* spp., in decreasing frequency of occurrence (Euphorbiaceae). Gymnosperms make up ~ 16% of all non-reworked palynomorphs and are generally scarce throughout PZ 1. These are also represented by *Podocarpidites* spp. (Podocarpaceae), *Phyllocladidites mawsonii* (*Lagarostrobos*), *Dacrydiumites praecupressinoides* (*Dacrydium*), and *Araucariacites australis*, in decreasing frequency (Araucariaceae). *Cyathidites* spp. (Cyatheaceae), *Dictyophyllidites* sp. (Gleicheniaceae), *Gleicheniidites* sp. (Gleicheniaceae), *Laevigatosporites* spp. (Blechnaceae), and *Stereisporites* sp. (*Sphagnum*) account for ~ 12% of all sporomorphs.

Based on rarefied data, the quantitative sporomorph diversity for this zone is 19.65 ± 1.32 species per sample of 75 individuals. Regarding diversity indices, Shannon diversity (H) yields range between 2.33 and 2.69, with an average of 2.571.12. The range for Equitability (J) scores is between 0.81 and 0.88, with an average of 0.85 ± 0.02 (Figure 3.3; Table 3.1).

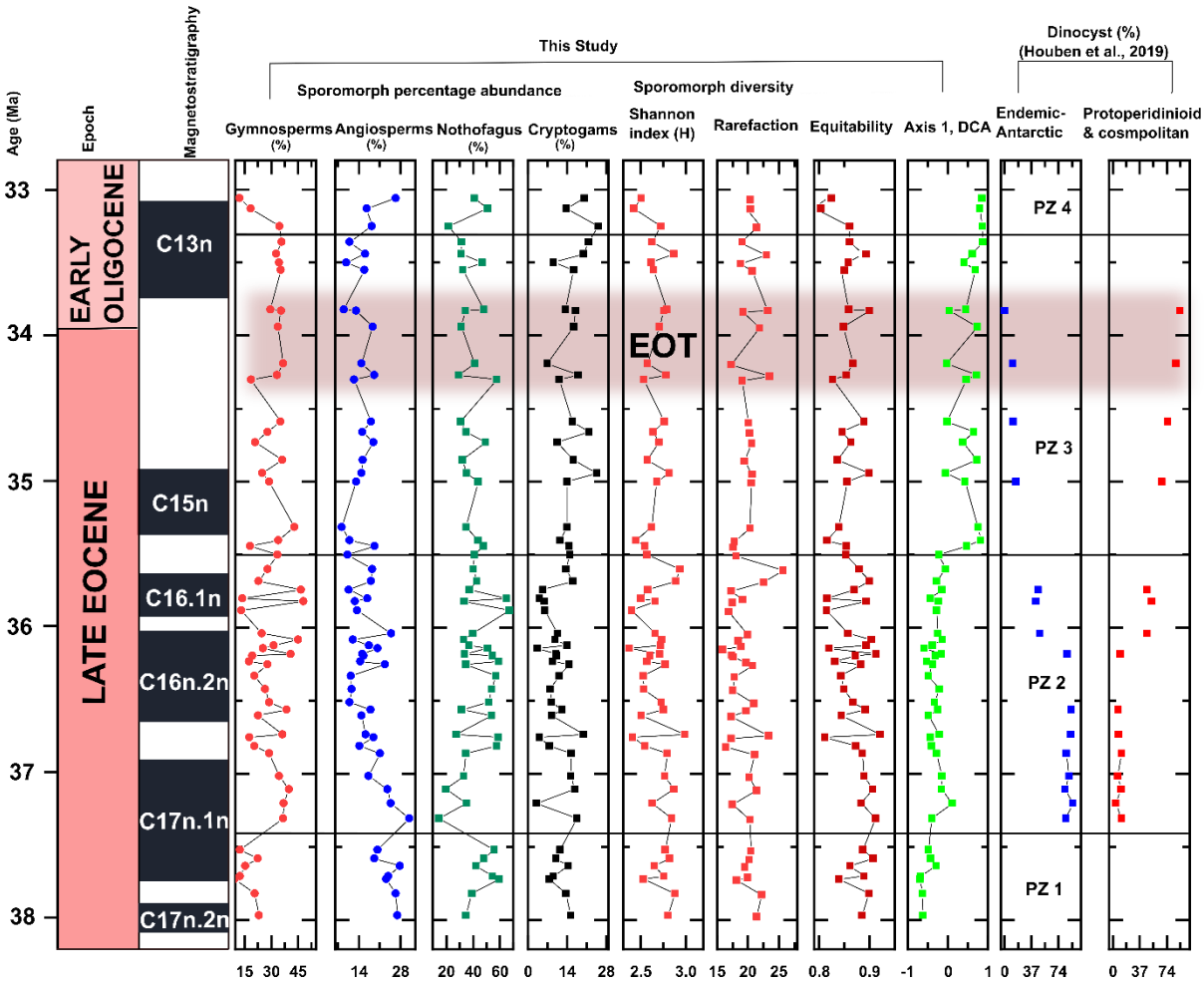

Figure 3.3 Sporomorph percentage abundances, diversity, and detrended correspondence analysis (DCA) data for ODP Site 1172. For all samples with pollen counts of 75 grains, the percentage abundances of the principal groupings (gymnosperms, other angiosperms, *Nothofagus*, and cryptogams) are reported. The DCA results for the late Eocene–early Oligocene Site 1172 samples are generated from the sample scores of axis 1 (which evaluates the sample-to-sample variance) and reveal four distinct compositional groupings, as observed with CONISS. Based on Sander's rarefaction analysis with samples rarefied at 75 grains/individuals, diversity is determined. The relative abundances of Antarctic-endemic and protoperidinioid dinoflagellate cysts, magnetostratigraphy, and age model are based on Houben et al., (2019).

Table 3.1: Summary of quantitative species diversity and Axis 1, DCA sample score between the late Eocene to early Oligocene from ODP Site 1172.

Analysis	Pollen Zone 1		Pollen Zone 2		Pollen Zone 3		Pollen Zone 4	
	Mean	*(SD)*	*Mean*	*(SD)*	*Mean*	*(SD)*	*Mean*	*(SD)*
Rarefaction (75 individuals)	19.65	1.32	19.44	2.49	20.15	1.79	21.16	1.37
Rarefaction (100 individuals)	22.29	1.87	21.78	2.85	22.52	2.31	23.75	1.32
Shannon index (H)	2.57	1.12	2.56	0.22	2.58	0.12	2.54	0.15

Equitability (J)	0.85	0.02	0.86	0.04	0.85	0.02	0.83	0.03
DCA (Axis 1, sample scores)	-0.55	0.15	-0.29	0.15	0.44	0.33	0.83	0.03

3.3.3 Pollen Zone 2 (37.30-35.60 Ma; 27 samples)

In PZ 2, the percentage of *Nothofagidites* spp. decreases to roughly 42%. *Brassospora* remained the leading *Nothofagus* subgenus despite a significant reduction in abundance from around 28% in PZ 1 to 22% in PZ 2. However, the *Fuscospora* and *Lophozonia* subgenera accounted for 19% and 1%, respectively (Fig. 3.2). Other angiosperms (non-*Nothofagus*) see a drop from 24% to 17% relative to PZ 1.

The most significant taxa among non-*Nothofagus* angiosperms include *Myricipites harrisii* (*Gymnostoma*), *Proteacidites* spp. (Proteaceae), *Malvacearumpollis mannanensis* (Malvaceae), and *Malvacipollis* spp. (Euphorbiaceae), in decreasing abundance. A precipitous drop in *Proteacidites pseudomoides* (*Carnarvonia*) coincides with the disappearance of *Spinizonocolpites* spp (Arecaceae). In contrast, the relative abundance of gymnosperms nearly doubles from ~ 16% in PZ 1 to over 29% in PZ 2. In decreasing abundance, *Podocarpus* spp., *Araucariacites australis* (Araucariaceae), *Dacrydiumites praecupressinoides* (*Dacrydium*), and *Phyllocladidites mawsonii* (*Lagarostrobos*) dominate gymnosperm taxa. *Microcachryidites antarcticus* (*Microcachrys*) is a taxon that emerges for the first time in this zone and is a significant component (11%) of the gymnosperm assemblage. In addition to the aforementioned, cryptogams comprise around 10% of the total sporomorphs in this zone. *Cyathidites* spp. (Cyatheaceae), *Gleicheniidites* (Gleicheniaceae), and *Laevigatosporites* spp. (Blechnaceae) are the primary members of this group.

This zone is less diverse than PZ 1. Based on rarefied values, the average species richness in PZ 2 is 19.44 ± 2.49 per 75 individuals. The Shannon diversity index (H) range between 2.15 to 2.97, with an average of 2.56 ± 0.22. The range for equitability is between 0.78 and 0.93, with an average of 0.86 ± 0.04. (Fig. 3.3; Table 3.1).

3.3.4 Pollen Zone 3 (35.50-33.36 Ma; 20 samples)

The percentage of *Nothofagidites* spp. in Zone 3 decreases to 38%. *Brassospora*-type *Nothofagus* displays a modest rise in abundance, whereas *Fuscospora*-type *Nothofagus* plummets from 19% in PZ 2 to 12% in PZ 3. The *Lophozonia*-type is unchanged (1%). Other angiosperms (non-Nothofagus) account for 14% of all non-reworked sporomorphs despite a minor drop. These include *Myricipites harrisii* (*Gymnostoma*), *Proteacidites* spp. (Proteaceae), *Malvacipollis* spp. (Euphorbiaceae), and *Malvacearumpollis mannanensis* (Malvaceae). Another important observation in this interval is reappearance of *Spinizonocolpites* spp. (Arecaceae) and *Proteacidites pseudomoides* (Carnarvonia). In contrast to PZ 1, however, *Spinizonocolpites* spp. are not always present. There is a modest increase of gymnosperms in this zone, which account for 31%. Within the gymnosperms, *Podocarpidites* spp. (Podocarpaceae) continue to dominate. Other significant taxa, such as *Araucariacites australis* (Araucariaceae), *Phyllocladidites mawsonii* (*Lagarostrobos*), and *Microcachryidites antarcticus* (*Microcachrys*), are on the decline. In this zone, *Dacrydiumites praecupressinoides* (*Dacrydium*) reaches its maximum abundance. The abundance of cryptogams greatly increases, and they are represented by *Cyathidites* spp. (Cyatheaceae), *Laevigatosporites* spp. (Blechnaceae), *Osmundacidites* (Osmundaceae), *Polypodiisporites radiatus* (Polypodiaceae), and *Clavifera* spp. (Gleicheniaceae), in that order of abundance.

Based on rarefied results, the average species richness per sample in this PZ is 20.15 ± 1.79. The results for Shannon diversity (H) range from 2.37 to 2.80, with a mean value of 2.58 ± 0.12. Equitability (J) ranges between 0.81 and 0.91, with an average of 0.85 ± 0.02 (Fig. 3.3 ; Table 3.1).

3.3.5 Pollen Zone 4 (33.25-33.06 Ma; 3 samples)

The percentage abundances of *Nothofagidites* spp. (*Nothofagus*), including *Brassospora* (23%), *Fuscospora* (12%), and *Lophozonia*-types, do not alter, however the percentages of other angiosperms increase significantly from 14% in PZ 3 to 20%. These are represented by *Myricipites harrisii* (*Gymnostoma*) and *Proteacidites pseudomoides* (*Carnarvonia*) in decreasing abundance. Additionally, in PZ 4, new angiosperms like *Sapotaceoidaepollenites cf. latizonatus* (Sapotaceae) and *Parsonsidites*

psilatus (*Parsonsia*) emerge. Gymnosperms, on the other hand, see a sharp reduction in this interval, accounting for around 21% of total sporomorph taxa, with *Podocarpidites* spp. (Podocarpaceae) and *Dacrydium praecupressinoides* (*Dacrydium*) as the principal components. The relative abundance of *Microcachryidites antarcticus* (*Microcachrys*), *Araucariacites australis* (Araucariaceae), and *Phyllocladidites mawsonii* (*Lagarostrobos*) all fall significantly, whereas cryptogams grow by up to 20%. *Cyathidites* spp. (Cyatheaceae), *Laevigatosporites* spp. (Blechnaceae), *Dictyophyllidites* sp. (Gleicheniaceae), and *Cibotiidites tuberculiformis* (Schizaeaceae) are the cryptogams, in decreasing order of abundance.

The average diversity is significantly greater than in PZ 3 (21.16 ± 1.37 species per sample), with Shannon diversity (H) ranging between 2.42 and 2.72 and averaging 2.54 ± 0.15. Equitability (J) ranges between 0.80 and 0.87, with an average of 0.83 ± 0.03 (Fig. 3.3; Table 3.1).

3.4 Discussion

3.4.1 Vegetation composition and altitudinal zonation

The presence of dominant *Nothofagidites* spp., and common *Podocarpidites* spp., *Myricipites harrisii*, and *Phyllocladidites mawsonii* throughout the studied section is indicative of the presence of *Nothofagus*-dominated temperate rainforest (Fig. 3.2; Truswell & Macphail, 2009; Bowman et al., 2014). This type of rainforest most likely thrived in lowland and mid-altitude elevations in eastern Tasmania. The presence of sporomorph taxa such as *Araucariacites australis*, *Microcachryidites antarcticus*, and *Proteacidites parvus* indicate that a component of the sporomorph assemblage is reflective of higher altitudes with more open forest conditions (Fig. 3.2; Macphail, 1999; Kershaw & Wagstaff, 2001). In addition, pollen species that belong to families such as Arecaceae, *Gymnostoma*, and *Carnarvonia* show the presence of a paratropical vegetation community that thrived in protected/sheltered lowland and coastal locations (Huurdeman et al., 2021). Comparable to the vegetation communities that predominated on Wilkes Land and Tasmania during the early to middle

Eocene (Pross et al., 2012; Contreras et al., 2013, 2014), the paratropical rainforest most likely occupied lowlands and coastal areas, while the temperate rainforest most likely grew at higher elevations. The presence of different plant groups with NLRs that today grow at different temperatures and elevations shows that vegetation in eastern Tasmania was subject to climatic gradients caused by changes in height and/or distance from the coastline. This is supported by reports of a topographic divide between sites facing the cool Tasman Current (Gippsland basin, eastern Tasmania) and the westerly located south Australian basins (Holdgate et al., 2017). These basins may have served as the locations for higher-altitude temperate forest taxa. The subsequent sub-sections provide a more in-depth description of each of these types of vegetative communities.

3.4.2 Lowland to mid-altitude *Nothofagus*-*Podocarpus* rainforest

A lowland to mid-altitude *Nothofagus–Podocarpus*-dominated rainforest that thrived under high-precipitation regimes (MAP >1300mm/yr) existed in Tasmania during the late Eocene to the earliest Oligocene (Fig. 3.2). This is indicated by abundant *Nothofagidites* spp. and common *Podocarpidites* spp., *Myricipites harrisii*, and *Phyllocladidites mawsonii*. The primary canopy is primarily composed of *Nothofagidites* spp. (southern beech or *Nothofagus*) and *podocarps* (*Dacrydiumites*, *Podocarpidites*, and *Dacrycarpites*), along with a few uncommon Cupressaceae species. Because southern beech forests can either develop as pure stands or as a mixed forest, it is difficult to define and recognise regional or local forest types based on fossil pollen and spores. According to Ogden et al. (1996), pure beech stands in modern-day New Zealand are most commonly found in montane to subalpine environments, whereas lowland mixed beech forests are linked with a variety of broadleaf angiosperms and canopy-emergent gymnosperms. In accordance with Dettmann et al. (1990), the pollen taxa of *Nothofagidites* is grouped into subgenera *Brassospora*, *Fuscospora*, and *Lophozoni*a. Extant types of *Fuscospora* and *Lophozonia* thrive in cool-temperate conditions in Tasmania, southeastern Australia, New Zealand, and southern South America (Hill, 1994, 2017; Veblen et al., 1996; Read et al. (2005), while extant types of *Brassospora* are currently restricted to warm-temperate–subtropical conditions in New Guinea and New Caledonia (Hill & Dettmann, 1996; Veblen et al., 1996). Due to their extensive ecological and climate tolerance (MAT: 10.6 to 23.5 °C; Read et al., 2005), these *Brassospora*-type *Nothofagus* can be seen

growing today in lower to mid-altitudes that receive high and consistent rainfall, as well as in montane and subalpine environments (usually over 500 m).

Myricipites harrisii (Casuarinaceae) possesses two possible NLRs, Casuarina/Allocasuarina and Gymnostoma (Hill, 2017; Lee et al., 2016; Hill et al., 2020). Casuarina and Allocasuarina share xeromorphic properties, which indicate that they have adapted to an arid climate with regular fires. The rainforest clade *Gymnostoma*, is selected as the most likely NLR of the fossil taxon, *Myricipites harrisii*. This was made based on the subtropical affinities of the associated palynoflora. This is also supported by Paleogene vegetation reconstruction for southeastern Australia based on macrofossil remains, which indicates rainforest communities (Christophel et al., 1987; Macphail et al., 1994; Hill, 2017). During this period, *Gymnostoma* was prevalent, but it was eventually replaced by *Casuarina*/*Allocasuarina* (sclerophyll taxa) in the Miocene (Evi et al., 1995; Boland et al., 2006; Holdgate et al., 2017; Hill et al., 2020).

Dacrydium cupressinum is suggested as the most likely NLR of the *Dacrydiumites praecupressinoides* (Rimu; Raine et al., 2011). Today, *Dacrydium cupressinum* can be found as a small component in the kauri forest of Northland, New Zealand. It is also found as an emergent taxon that is usually associated with *Agathis australis* (Araucariaceae) and *Podocarpus totara* (Farjon, 2010). At Site 1172, the NLR of *Phyllocladidites mawsonii*, whose NLR is known as *Lagarostrobos franklinii* (Tasmanian Huon pine; Raine et al., 2011), is found in exceptionally high numbers. *Lagarostrobos* are evergreen trees that thrive in a cool-temperate climate and are seen growing close to riverbanks in Tasmania (Farjon, 2010; Hill, 1994, 2017). Aside from developing in groves that designate stream courses at low elevations (Hill & Macphail, 1983; Farjon, 2010), they are also able to be found in temperate forests away from water courses on damp hillsides (Farjon, 2010; Bowman et al., 2014). The percentage abundance of *Lagarostrobos* at ODP Site 1172 is comparable to that which was recovered from wells located in the Gippsland Basin offshore (the Gropper-1, Mullet-1, and Bluebone-1 wells; Partridge, 2006). In the Middle *Nothofagidites* asperus Zone of the terrestrial record of the Gippsland Basin, where it appears to be overrepresented, *Lagarostrobos* is found to exist at even higher percentages than elsewhere (Holdgate et al., 2017).

Carnarvonia and Lomatia are the two possible NLR relatives for the *Proteacidites pseudomoides*. Large trees can be produced by the *Carnarvonia* plant in regions that are warm-temperate to paratropical in climate, such as the wet northeastern part of Australia (Hyland, 1995; Mabberley, 1997; Cooper & Cooper, 2004). In residual galleries of warm-temperate rainforests, such as those found along creek lines on sandstones in Northern Sydney, *Lomatia* can be found growing both as shrubs and small trees (Bowman et al., 2014; Myerscough et al., 2007). *Carnarvonia* was selected as the likely NLR relative because it considerably rises in intervals where warmth-loving taxa such as Arecaceae, *Brassospora*-type *Nothofagus*, Gleicheniaceae, and Cyatheaceae thrive.

3.4.3 High-altitude temperate rainforest and shrubland

Araucariacites australis, *Proteacidites parvus*, and *Microcachryidites antarcticus* are palynoflora components that indicate higher-altitude and more open vegetation on low-fertility soils (Kershaw & Wagstaff, 2001; Macphail et al., 1999). Araucariaceae trees today occur in cool-temperate forests in Chile and Argentina, reaching the tree line (Veblen et al., 1996; Sanguinetti & Kitzberger, 2008). Araucariaceae trees that are found in the Andes at altitudes of 600-800 m a.s.l., receive significant amounts of yearly rainfall (2000-3000 mm/yr), and undergo hot and dry spells in summer (Farjon, 2010). Araucariaceae form pure stands at higher elevations and mixed Valdivian rainforest at lower elevations (Farjon, 2010). Increases in araucarian sporomorph taxa in Tasmania between 37.30 and 35.60 Ma indicate a dense, emergent cover of Araucariaceae thriving in moderately dry settings (Kershaw and Wagstaff, 2001). Microcachrys is a creeping shrub that grows in alpine/subalpine areas and is today restricted to western Tasmania under conditions ranging from boreal to cool temperate (Truswell and Macphail, 2009; Biffin et al., 2012; Carpenter et al., 2011). It is the closest living relative of *Microcachryidites antarcticus*. Therefore, increases in this Tasmanian endemic alpine shrub (*Microcachrys*) from 37.30 to 35.60 million years ago, along with *Bellendena* (a low-growing protea shrub; NLR of *Proteacidites parvus*), and Araucariaceae (emergent canopy), suggest that the vegetation that thrived at higher altitudes in Tasmania preferred cool-temperate conditions.

3.4.4 Subtropical vegetation and early late Eocene cooling from 37.97 to 35.60

Throughout PZ 1 (37.97–37.52 Ma), the presence of abundant *Nothofagus* (especially the *N. brassii* type), secondary Podocarpaceae and *Gymnostoma*, and minor Arecaceae, *Carnarvonia*, and cryptogams suggests the presence of a temperate *Nothofagus*-dominated rainforest with subtropical elements (Fig 3.2). According to quantitative climate estimates based on sporomorphs, these rainforests thrived at a mean annual temperature of 14.2–15.1 °C and a mean annual precipitation of 1467–1681 mm/yr (Fig. 3.4). The sporomorph-based WMMT reconstructions of ~ 18.5 °C (Fig. 3.4) closely corroborate the brGDGT-biomarker reconstructions from the same site (Bijl et al., 2021), which lends credence to the notion that this palaeothermometer may have a potential summer bias (Contreras et al., 2014; Naafs et al., 2017). The warmth-loving taxa were the primary lowland forest components, and they inhabited sheltered lowland subtropical coastal zones (Dowe, 2010; Carpenter et al., 2012, Tripathi & Srivastava, 2012; Verma et al., 2020) and swamps (Kershaw, 1988). Estimates of temperatures based on sporomorphs produce CMMTs that are significantly above freezing (11.2–12.5 °C; Fig. 3.4). The decline and, to a large extent, the absence of cool-temperate taxa, coupled with persistent warm-temperate (12–17 °C; Emanuel et al., 1985) to subtropical taxa (17–24 °C; Emanuel et al., 1985), further point to the expansion of warm temperate– paratropical rainforest up into the mid-altitudes and uplands.

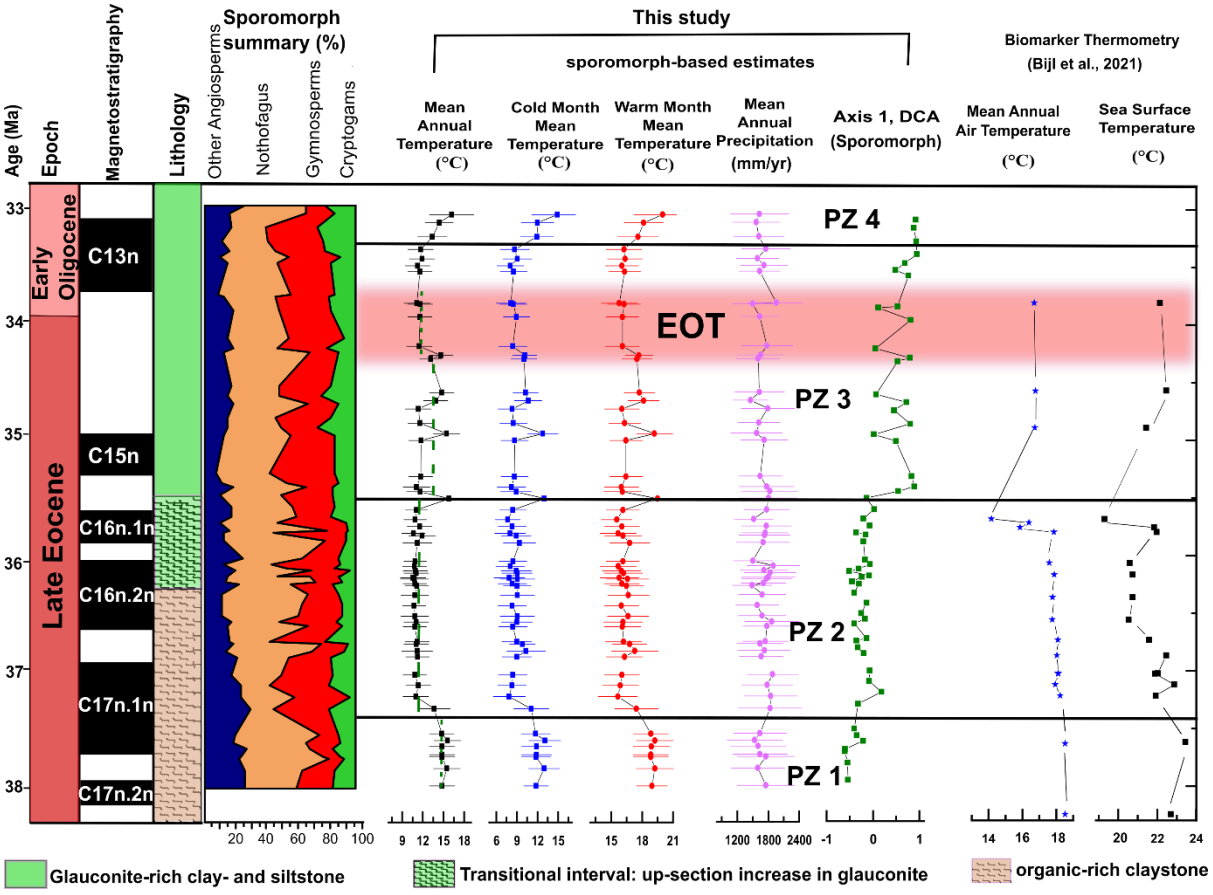

Figure 3.4. Comparison of our sporomorph-based climate estimates, $MAAT_{soil}$ values based on MBT'5me, TEX_{86}-based SST and sample score for DCA Axis 1 from the late Eocene – early Oligocene of ODP Site 1172. Sporomorph-based estimates are based on the use of the NLR and PDF. The ranges of the climate estimates show the mathematical error and not the real range, which may have been a result of uncertainties associated with the use of the NLR approach. Green broken lines indicate average temperatures for sporomorph-based MATs. Biomarker thermometry data are from Bijl et al. (2021). The ~790 kyr interval corresponding to the EOT (34.44-33.65 Ma; Hutchinson et al., 2021) is marked with pink horizontal bar. Age model after Houben et al. (2019).

The rainforest, which was dominated by *Nothofagus*, continued into PZ 2 (37.30–35.60 Ma; Fig. 3.2). However, at ~ 37.30 Ma, a distinct environmental change occurred that resulted in a declicne of warm-temperate and subtropical species (*Nothofagus* subgenus *Brassospora*, *Carnarvonia*, and Arecaceae; Fig. 3.2) and, in certain cases, the extinction of these taxa (Fig. 3.2). This vegetation change continued throughout PZ 2, along with a concurrent increase in the relative abundances of *Lagarostrobos*, *Microcachrys*, and a decline in diversity (Table 3.1) ~3 Ma before the EOT. The increased prevalence of microthermal taxa is indicative of a cool-temperate *Nothofagus*-dominated (southern beech) rainforest with secondary Podocarpaceae extending into lowland zones that were previously occupied

by mesothermal taxa. The cool-temperate *Nothofagus*–Podocarpaceae-dominated rainforest of the late Eocene of eastern Tasmania is comparable to the modern Valdivian rainforest of Chile (Veblen, 1982; Cantrill & Poole, 2012; Bowman et al., 2014), as well as the cool-temperate *Nothofagus*-dominated rainforest with riparian *Lagarostrobos* restricted to river gullies in Victoria, Australia (Read & Hill, 1985) or on fertile soils in lowland Tasmania (Read & Hill, 1985; Macphail, 2007; Francis et al., 2008).

This interpretation is reflected in the sporomorph-based quantitative estimates indicating a 2-3 °C decline in MAT (Fig. 3.4). Previous studies conducted in Australia during the late Eocene indicate an increase in *Nothofagus* subgenus *Fuscospora*, as well as a substantial decline in *Brassospora*-type *Nothofagus*, the extinction of the majority of Proteaceae, Arecaceae, and most Australian angiosperms (Kemp, 1978; Kershaw, 1988; Christophel & Greenwood, 1989; Truswell, 1993; Martin, 1994; Martin, 2006; Macphail et al., 1994; Partridge & Dettmann, 2003; Korasidis et al., 2019). In accordance with palynoflora change, biomarker-based reconstruction from Site 1172 reveals that SSTs dropped by around 2–3 °C beginning around 37.5 Ma (Fig. 3.4). However, the cooling that was indicated by the two independent proxies is not reflected in the estimations of terrestrial MAT that are based on lipid biomarkers, and the cause for this divergent trend is still unknown.

The transition from a warm-temperate rainforest with paratropical elements to cool-temperate forests in the Tasmanian Gateway region matches an early late Eocene (37.3 Ma) cooling in the Southern Ocean (Kerguelen Plateau) ~ 3 Ma before the EOT (Villa et al., 2008; Villa et al., 2014; Scher et al., 2014). The 2-3 °C sporomorph-based MAT (100-200 kyr) cooling at ~ 37.3 Ma correlates with the Priabonian Oxygen Maximum (PrOM; Scher et al., 2014), which is a 140 kyr cooling event first recorded at ODP Site 738 (Kerguelen Plateau). The PrOM event, which occurred during the late Eocene and is located within magnetochron C17n.1n, suggests that there was a transient expansion of ice sheets on East Antarctica due to a positive excursion of benthic $\delta^{18}O$ levels (Scher et al., 2014). However, on the Kerguelen Plateau, discrepancies in the neodymium isotopic composition (Nd) between the bottom waters and the terrigenous sediments point to changes in sediment provenance as opposed to changes in the rearrangement of ocean currents (Scher et al., 2014). After the brief 2–3 °C sporomorph-based MAT cooling phase, a period with a consistently cooler climate occurred from 37.2 to 35.6 Ma (Fig.

3.4). This sustained cooler climate may have caused the climate threshold of the frost-sensitive (subtropical) taxa to be exceeded, hence their continued decline and demise. Dinoflagellate cysts endemic to Antarctica, such as *Deflandrea antarctica*, *Vozzhennikovia* spp., and *Enneadocysta dictyostila*, become predominate in the marine environment at Site 1172 (Fig. 3.3; Stickley et al., 2004; Houben et al., 2019). In addition to general circulation models (Huber et al., 2004), the dominant Antarctic endemic dinocysts suggest that the East Tasman Plateau and east Tasmania are bathed by relatively cool Antarctic-derived surface waters (Houben et al., 2019). This finding is consistent with TEX_{86}-based sea surface temperature records (3–4 °C cooling; Houben et al., 2019; Bijl et al., 2021). This sustained cool-temperate terrestrial MAT matches with oligotrophic conditions associated with low nutrients, stratification of the water mass, and increased efficiency of the ocean's biological pump, all of which favoured cooling due to carbon being sequestered from surface water in the Southern Ocean (Villa et al., 2008, 2014).

The brGDGT MATs and SSTs demonstrate substantial and rapid cooling close to the top of PZ 2 (35.7 Ma; Fig. 3.4), which is not mirrored by the pollen-based climate estimates. However, strong fluctuations in gymnosperms and a rise in cryptogams (Figs. 3.2 and 3.3) and diversity towards the top of PZ 2 imply increased environmental disturbance, which might be linked to their recorded change in lipid biomarker-based MATs. The sudden drop in temperature most likely resulted in voids/gaps within the canopy and/or emergence of extensive wetland/bog or marshes, which in turn stimulated the growth of cryptogams. It is possible that the differences in the proxy signals' sources and the ways in which they are transported may have resulted in the divergence between them. While the lipid biomarkers are heavily affected by the depositional settings, including river run-off, tectonic, and geographic evolution (Bijl et al., 2021), the majority of the terrestrial palynological signal is made up of pollen and spores that are transported by the wind. Due to the large distance that separated the study site (ODP Site 1172) from the mainland of Tasmania during the Eocene (more than 100 km), a significant influence from river or water-transported sporomorphs seems highly unlikely.

3.4.5 Warm and cool-temperate terrestrial climate fluctuation from 35.50 to 34.59 Ma

With a rise in *Podocarpus*, decreases in *Lagarostrobos*, *Microcachrys*, Araucariaceae, and *Fusca*-type *Nothofagus*, and the reappearance of subtropical and warm-temperate taxa, PZ 3 (35.50-33.36 Ma; Fig. 3.2) is characterised by a significant shift in sporomorph assemblages. The peak in tree ferns, especially Cyatheaceae, indicate a period of disturbance (Vajda et al., 2001) within this interval of vegetation shift. However, the environmental disturbance during this period (35.50–34.59 Ma) cannot be attributed to increase in fire frequencies due to the lack of charcoal particles within the Site 1172 record. Reconstructions of temperatures based on sporomorphs reveal significant temperature variations between warm and cool climate phases with mean annual temperatures ranging from 10.6 to 15.3 °C. (Fig. 3.4). In the Australo-Antarctic region, a comparable warming and cooling phase is evident in the late Eocene (35.8–34.7 Ma) climate records of Prydz Bay (Passchier et al., 2017; Tibbett et al., 2021) and southern Australia (Benbow et al., 1995). Again, WMMTs obtained from quantitative sporomorph-based climate reconstructions are remarkably similar to MATs derived from lipid biomarkers at Site 1172 (Fig. 3.4). In comparison, the warm and cool climate fluctuation phase that occurred between 35.50 and 34.59 Ma based on sporomorph-based MAT reconstruction for Site 1172 is documented as a recovery phase in the lipid-biomarker-based MAT reconstruction. The changes in temperature estimates derived from sporomorphs may be at least partially caused by the proxy approach, which depends on presence–absence data. However, the very low resolution of the lipid biomarker in PZ 3 (Fig. 3.4), makes it difficult to conduct a more detailed comparison of proxies.

Expansions and contractions of cool-temperate and warm-temperate forests, indicating cooling and warming phases, are consistent with previous late Eocene geochemical, sedimentological, and palynological studies reporting an increase in sea surface temperature (TEX_{86}-based SST; Houben et al., 2019; Bijl et al., 2021), widespread deposition of glauconite (Stickley et al., 2004), and increases in cosmopolitan and protoperidinioid dinocysts (Fig. 3.3; Stickley et al., 2004; Houben et al., 2019; Bijl et al., 2021). Though the glauconitic unit is interpreted as marking deepening and current inception due to a widening of the Tasmanian Gateway (Stickley et al., 2004), a more recent counterargument links

the deposition of the greensand to atmospherically forced invigorated circulation in the Southern Ocean, which helped to prepare Antarctica for rapid expansion of ice (Houben et al., 2019) and a further circulation change ~ 2 Ma later (at the EOT). Concerning the deposition of greensands along the south Australian margin, however, ocean model studies (Baatsen et al., 2016) indicate a further eastward expansion of the throughflow into the southwest Pacific Ocean. Sporomorph-based MAT demonstrated a 2 °C average temperature increase between 35.50 and 34.59 Ma (Fig. 3.4), consistent with earlier reports of the initial deepening of the Tasmanian Gateway (Stickley et al., 2004). This is further confirmed by the prevalence of low-latitude cosmopolitan dinoflagellate cyst species that, rather than being supplied by the East Australian Current, are reported to have originated from the PLC's eastward throughflow (Huber et al., 2004; Stickley et al., 2004; Houben et al., 2019). These events, coupled with a 2 °C recovery in SSTs (TEX_{86}-based; Houben et al., 2019; Bijl et al., 2021) between 35.7 and 34.59 Ma, most likely indicate the influence of warm surface waters associated with the AAG at ODP Site 1172 (Houben et al., 2019), which is reported to have been close to land (eastern Tasmania; Stickley et al., 2004) at that time, thereby affecting the terrestrial climate and vegetation.

3.4.6 EOT cooling and climate rebound in the earliest Oligocene from 34.30 to 33.06 Ma

Site 1172 sporomorph data shows that Tasmania saw a rebound to a colder phase lasting from 34.30 to 33.82 Ma at the start of the EOT (Figs. 3.4 and 3.5). The loss of *Spinizonocolpites* sp. (Arecaceae), a decline in Cyatheaceae and Gleicheniaceae, and marginal increases in *Microcachrys* and *Lagarostrobos* all occur during this EOT cool phase. Gymnosperms and *Nothofagus* (*Brassospora*-type) are prevalent and co-dominant, and the variety of angiosperms (non-*Nothofagus*) as a whole decreased during the EOT, further defining the palynoflora assemblage (Fig. 3.2). Previous studies in southeast Australia (e.g., Macphail et al., 1994; Benbow et al., 1995; Holdgate et al., 2017; Lauretano et al., 2021) record a drop in angiosperm diversity and the final demise of Arecaceae (thermophilous elements) at the end of the Eocene (Pole & Macphail, 1996; Martin, 2006). Quantitatively, the sporomorph-based MAT reconstruction records a 2 °C decrease across the EOT (Fig. 3.4). This decrease in temperature coincides with ~ 2.4 and 5 °C cooling steps in southeastern Australia (MBT'5me-based MAATsoil; Lauretano et

al., 2021) and East Antarctica (Prydz Bay; MBT'5me-based MAATsoil; Tibbett; et al., 2021), respectively. This cooling in the terrestrial record further matches the principal geochemical signature of EOT in the marine realm, which is the ~ +1.5 excursion of the oxygen isotope ratio of deep-sea benthic foraminifera (Zachos et al., 1996; Coxall et al., 2005; Pälike et al., 2006; De Vleeschouwer et al., 2017; Figure 3.5). This excursion is associated with global cooling (Zanazzi et al., 2007; Pearson et al., 2009; Pagani et al., 2011; Hutchinson et al., 2021; Tibbett et al., 2021). This cooling at the EOT has been linked to a global decline in atmospheric pCO_2 (Pearson et al., 2009; Lauretano et al., 2021). Although the estimated cooling at the PrOM (37.3 Ma) and EOT appear to be only minor (2-3 °C) and with overlapping error ranges, a shift in the abundance of several taxa at the onset and during these events provide substantial backing for a major change in vegetation cover in response to cooling. Also, because the bioclimate analysis uses presence/absence of taxa only, these changes in pollen percentages are not captured in the quantitative climate estimates. Hence, the use of qualitative vegetation and climate description to buttress the quantitative climate estimates.

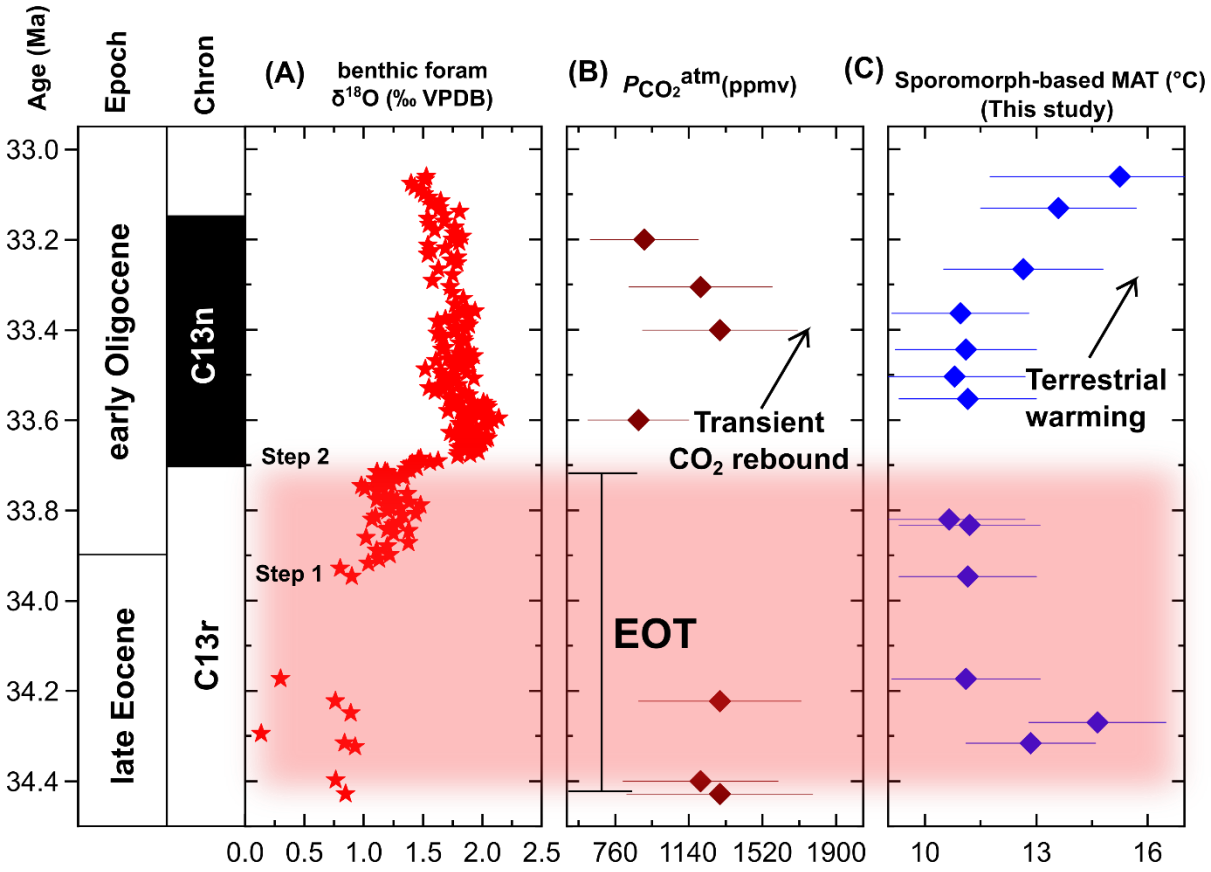

Figure 3.5. Comparison of the sporomorph-based MAT in the Tasmanian Gateway region across the EOT and earliest Oligocene to regional and global marine EOT and earliest Oligocene records. (A) Marine benthic foraminiferal calcite $\delta^{18}O$ record from ODP Site 1218 (Pälike et al., 2006). (B) Marine δ^{11} B-derived atmospheric pCO_2 record (Anagnostou et al., 2016). (C) Terrestrial temperature change across the EOT and earliest Oligocene based on our sporomorph-based MATs from ODP Site 1172.

The sporomorph-based climatic estimations show a warming between 33.25 and 33.06 Ma (PZ 4) with MATs between 12.7 and 15.2 °C. (Fig. 3.4). In addition, the existence of warmth-loving taxa, like the Sapotaceae, *Parsonsia* (Silkpod), and Polypodiaceae (subtropical epiphytes), indicates a warming phase. Pollen flora mimics Oligocene warm-temperate brassii southern-beech-dominated forests of Karamu in New Zealand's Waikato Coal Measures (Pocknall, 1985). The increase in *brassii*-type *Nothofagus* and the advent of Sapotaceae and subtropical epiphytes show that, at least locally on lowlands, eastern Tasmania was warm enough in the earliest Oligocene to support warm-temperate flora (Fig. 3.2). Previous studies from the early Oligocene in southeast Australia (Korasidis et al., 2019) demonstrate the presence of a cool-temperate rainforest community. The palynoflora in northeast Tasmania (Hill & Macphail, 1983) and east Antarctica (Askin, 2000; Askin & Raine, 2000; Prebble et

al., 2006; Tibbett et al., 2021) point to an early Oligocene cold-temperate *Nothofagus* (subgenus *Lophozonia* or *Fuscospora*)-Podocarpaceae vegetation. It has been suggested that the palynoflora in northern Tasmania and east Antarctica likely consisted of small-stature confined southern beech/podocarp refugia or prostrate deciduous dwarf trees, with a vegetation community that probably struggled to thrive (Askin, 2000; Askin and Raine, 2000; Prebble et al., 2006; Francis et al., 2008; Tibbett et al., 2021). However, rather than a widespread scrub (such as in Antarctica), the minor increase in angiosperms (other than *Nothofagus*) and cryptogams indicate a limited warm-temperate forest along eastern Tasmania during the earliest Oligocene. Today, temperate forests in New Zealand and Tasmania are home to a variety of cryptogams, in contrast to scrub ecosystems, which do not support the growth of other species due to their low, closed canopies (Prebble et al., 2006).

A partial return to warmer temperatures was seen in previously reported terrestrial (Colwyn & Hren, 2019; Lauretano et al., 2021) and marine studies (Katz et al., 2008; Lear et al., 2008; Liu et al., 2009; Houben et al., 2012), which matches the terrestrial cooling that was observed across the EOT, followed by a rapid recovery in the earliest Oligocene. The synchronicity between terrestrial and marine records shows that the EOT and earliest Oligocene ETP record may also be responding to a much larger regional or global event in addition to responding to localised events (sustained Tasmanian Gateway deepening and widening; Stickley et al., 2004). The decrease in atmospheric pCO_2 concentration and its recovery or rebound in the earliest Oligocene, respectively, are the most frequently cited causes of both the global cooling across the EOT (Zanazzi et al., 2007; Pagani et al., 2011; Hutchinson et al., 2021; Tibbett et al., 2021) and the transient warming post-EOT (Pearson et al., 2009; Heureux & Rickaby, 2015; Anagnostou et al., 2016; Fig. 3.5). Findings from ODP Site 1172 imply that the warming, or at least the lack of sustained cooling after the EOT in eastern Tasmania, may be related to a combination of the pCO_2 recovery (Pearson et al., 2009) and sustained Tasmanian Gateway deepening and widening (Stickley et al., 2004; Houben et al., 2019). This would have most likely resulted in the influx of more warm surface waters from the AAG into the southwest Pacific, affecting the terrestrial climate and vegetation along eastern Tasmania.

3.5 Conclusions

The late Eocene to early Oligocene flora reconstructed from terrestrial palynomorphs recovered from ODP Site 1172 (East Tasman Plateau) is distinguished by three main climate changes.

The early late Eocene sporomorph record suggests a distinct 2–3 °C terrestrial cooling at 37.30 Ma accompanied by a transition from a warm-temperate *Nothofagus*–Podocarpaceae–dominated rainforest with paratropical elements to a cool-temperate Nothofagus–Podocarpaceae–dominated rainforest with secondary Podocarpaceae. This terrestrial cooling at 37.30 Ma and sustained cool climate from 37.2–35.60 Ma coincides with a long-term SST decline from 23 to 19 °C at ODP Site 1172, a regional transient cooling event (PrOM) at ODP Site 738 (Kerguelen Plateau; Scher et al., 2014), and a relatively long-term regional Southern Ocean cooling due to carbon being sequestered at the surface of the water (Villa et al. 2008, 2014).

The expansion and contraction of cool- and warm-temperate forests between 35.5 and 34.49 Ma were followed by a period of cooling across the EOT (34.30–33.3 million years ago). The terrestrial climate fluctuation in this interval is consistent with latest-Eocene geochemical, sedimentological, and palynological studies indicating an increase in SST, a recovery in MBT'5me-based MAATsoil (biomarker thermometry), widespread deposition of glauconite, and the common occurrence of low-latitude cosmopolitan and protoperidinioid dinocysts. These are attributed to the early deepening of the Tasmanian Gateway, paving the way for the warm water associated with the PLC to influence both the terrestrial and marine climate in this region.

From 33.55 to 33.06 Ma, the post-EOT (earliest Oligocene) recovery was characterised by a warm-temperate forest association. This earliest Oligocene recovery in Tasmanian terrestrial temperatures coincides with a rebound in atmospheric pCO_2 at the earliest Oligocene glacial maximum (EOGM; Pearson et al., 2009), coupled with ice sheet expansion in Antarctica (Galeotti et al., 2016) and sustained deepening of the Tasmanian Gateway (Stickley et al., 2004).

This chapter demonstrates that, against the backdrop of global cooling in the late Eocene (a sustained decline in *p*CO2), a series of regional events in the marine realm, including a change in the stratification

of water masses, sequestration of carbon from surface water, and changes in the ocean circulation due to Tasmanian-Gateway-accelerated deepening, may have contributed to terrestrial climate and vegetation change in the Tasmanian Gateway region.

4. Evidence of oceanographic and pCO_2 changes on terrestrial climate and vegetation in western Tasmania (ODP Site 1168) after the Eocene Oligocene transition

4.1 Introduction

The Earth's climate is reported to have changed dramatically from the late Eocene to the early Oligocene, resulting in a shift from a greenhouse to an icehouse environment (Pearson et al., 2009; Villa et al., 2014; Galeotti et al., 2016; Hutchinson et al., 2021). The long-term late Eocene cooling trend peaked at the EOT (34.44-33.65 Ma; Katz et al., 2008; Hutchinson et al., 2021), which was highlighted by a positive excursion in benthic foraminiferal $\delta^{18}O$ (Zachos et al., 2001; Westerhold et al., 2020). As potential drivers for this transition from a greenhouse to an icehouse planet, two major mechanisms have been postulated (Lauretano et al., 2021; Hutchinson et al., 2021). Earlier research ascribed the EOT cooling to the opening of Southern Ocean gateways (Tasmanian gateway and Drake Passage; Kennett, 1977), but subsequent studies attribute this cooling to declining pCO_2 concentration (DeConto & Pollard, 2003; Anagnostou et al., 2016; Cramwinckel et al., 2018; Lauretano et al., 2021). Other mechanisms, including deep-water formation and CO_2 sequestration due to the strengthening of the Atlantic Meridional Overturning Circulation (Elsworth et al., 2017; Hutchinson et al., 2021), are also considered to have provided the required preconditions for global cooling.

A late Eocene-early Oligocene marine pollen record from ODP Site 1172 on the ETP suggests that surface oceanographic changes caused by accelerated deepening of the Tasmanian Gateway and atmospheric pCO_2 most likely influenced terrestrial climate and vegetation change in eastern Tasmania (Amoo et al., 2022). The fluctuation between cool and warm-temperate climate conditions with MATs between 11-15 °C (35.5-34.59 Ma), cooling across the EOT, and climate rebound post-EOT are evidence of this (Amoo et al., 2022). However, a gap in the palynomorph record of ODP Site 1172 between ca. 33 and 30 Ma, caused by a series of hiatuses and barrenness, impedes a detailed reconstruction of Tasmanian vegetation and climate after the EOT, as well as the identification of potential drivers of the terrestrial post-EOT climate recovery. Furthermore, two previously published Eocene and Oligocene vegetation and climate reconstructions from southeastern Australia (Gippsland

Basin) report disparate Oligocene climates, with one implying unidirectional microthermic conditions throughout the Oligocene (Korasidis et al., 2019) and the other implying predominant mesothermic conditions (Sluiter et al., 2022). Differences in dating and palaeoclimate estimate approach between the two studies could explain the different climate trends, particularly in the Oligocene (Sluiter et al., 2022). Additional southern Australian (regional) vegetation and terrestrial climate records from the Eocene, particularly the Oligocene, are scarce and frequently poorly dated (Macphail et al., 1994; Macphail, 2007; Bijl et al., 2021; Lauretano et al., 2021).

This chapter focuses on a new, well-dated, high-resolution marine pollen record and sporomorph-derived climate estimates recovered from ODP Site 1168 (Fig.4.1a) on Tasmania's western margin spanning the late Eocene (35.5 Ma) to the early-late Oligocene (27.46 Ma) to reconstruct vegetation and climate dynamics on Tasmania. According to high-resolution model simulation, seismic, and geochemical data (Stickley et al., 2004; Sijp et al., 2011, 2014; Sauermilch et al., 2019; Sauermilch et al., 2021), the accelerated deepening and widening of the Tasmanian Gateway between 35.50 and ~ 30.20 Ma controlled and strengthened ocean current circulation and PLC throughflow into the southwest Pacific (Fig. 4.1b). However, by the early Oligocene, the elimination of Antarctic-derived peridinioid cysts and increase in cosmopolitan dinocyst species on the eastern side of the Tasmania Gateway (ODP Site 1172) has been attributed to PLC throughflow (Sluijs et al., 2003). Throughout the Eocene and Oligocene, Site 1168 was influenced by warm waters associated with the PLC (Exon et al., 2001; Stickley et al., 2004; Holdgate et al., 2017; Hoem et al., 2021), whereas ODP Site 1172 and Gippsland Basin sites were influenced by the cool proto-Ross gyre of the Pacific Ocean (latest Eocene; Stickley et al., 2004; Houben et al., 2019; Holdgate et al., 2017). Their palaeogeographic locations are thought to have resulted in divergent temperature regimes, with a cooler and wetter eastern Tasmania (corresponding to the cooler Proto-Ross Sea Gyre) and a warm-wet western Tasmania (Site 1168) linked to warm water currents associated with the PLC (Holdgate et al., 2017). The late Eocene to early Oligocene sporomorph data from the western Tasmanian margin (ODP Site 1168) are crucial for furthering the understanding of Tasmanian and southern Australian terrestrial climate and vegetation.

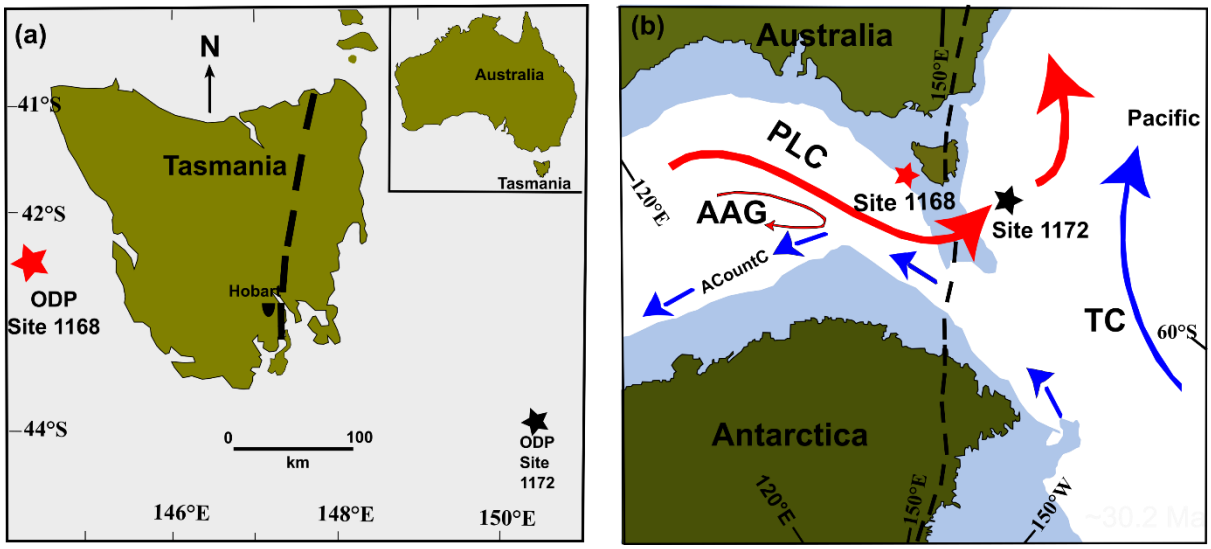

Figure 4.1. (a) Present-day Tasmania and locations of the western margin of Tasmania (ODP Site 1168; red star) and East Tasman Plateau (ODP Site 1172; black star) after Quilty (2001). ODP Site 1168 is submerged at a water depth of ~2463 m and ODP Site 1172 at a water depth of ~2620 m. (b) Tasmanian Gateway palaeoceanography and palaeogeography during the early Oligocene. Surface ocean currents are modified after reconstructions by Stickley et al. (2004). TC: Tasman current, PLC: proto-Leeuwin current, ACountC: Antarctic Counter Current, AAG: Australo-Antarctic Gulf. Red arrows indicate warmer surface currents associated with the PLC, and blue arrows show cooler surface currents associated with the Proto-Ross Gyre. Short broken black lines from Australian section through to Antarctica represent the East Australian and East Antarctica divide, respectively. Modified after Holdgate et al. (2017).

This chapter will evaluate whether the continuous deepening and expansion of the Tasmanian Gateway during the early Oligocene coincides with considerable reorganisation of climate and vegetation at Site 1168 by comparing the new sporomorph record (western Tasmania; ODP Site 1168). with Site 1172 (Amoo et al.,2022; Chapter 3). Sporomorph-based climate and vegetation reconstruction of Site 1168 record demonstrate a partial decoupling of vegetation and climate, indicating that the relevance of tectonic and *p*CO2 forcing varies in Tasmania.

4.2 Materials and Methods

4.2.1 Tectonic evolution and study site

The Cretaceous to middle Eocene separation of Australia and Antarctica led to the development of the Australo-Antarctic Gulf (Shipboard Scientific Party, 2001) and the shift of western Tasmania to the

northwest. Following the northwest-southeast strike-slip faulting in western Tasmania, the resulting epicontinental basin between Antarctica and Tasmania is subdivided into a succession of narrow basins. This led to the subsequent creation of a buffer surrounding western Tasmania (WT; Shipboard Scientific Party, 2001). The ODP Site 1168 is one of the five sites drilled during the Ocean Drilling Program (ODP) Leg 189 expedition around Tasmania to investigate and provide with precision the timing and climatic consequences of the opening of the Tasmanian Gateway, resulting in the deepwater connection between the Indian and southwest Pacific oceans and the development of the Tasman Seaway (Fig. 4.1a; Exon et al., 2001). Site 1168 is situated in the Sorell Basin, ~ 70 kilometres off the western coast of Tasmania (42°38'S, 144°25' E; Fig.4.1a), at a depth of 2440 metres (Exon et al., 2001). During the late Eocene and early Oligocene, however, the western margin of Tasmania was located between 63 and 57 °S (van Hinsbergen et al., 2015), as opposed to its present-day location at 42 °S (Cande & Stock, 2004) near the eastern end of the 2500 km-long AAG. In contrast to other ODP sites examined during Leg 189, there are more spores and pollen than dinoflagellate cysts at Site 1168, indicating a stronger runoff and a closer proximity to a river outlet (Exon et al., 2004a; Hill & Exon, 2004)

The marine sedimentary unit is divided lithologically into: (1) organic-rich, shallow-marine brown and grey mid-Eocene to late Eocene silty mudstones (Unit V; until 788.76 m b.s.f.); (2) a condensed late Eocene to earliest Oligocene transitional unit with high glauconite (greensand) content (upper unit IV to III; 749.4-666.6 m.b.s.f); (3) a calcareous succession mainly composed of nannofossil ooze deposited during the Oligocene (Unit II; 340-660 m b.s.f.; Exon et al., 2001). A detailed description of the depositional and oceanographic setting is given in Hoem et al. (2021). ODP Hole 1168A on the western margin of Tasmania yielded EOT records that have been analysed for their sporomorph content in this study. The age model relies on a clear palaeomagnetic signal in the late Eocene-early late Oligocene sedimentary record, which are defined by matching the palaeomagnetic reversals to biostratigraphic events from dinocyst, foraminifera, and calcareous nannofossils (Pfuhl and McCave, 2003; Sluijs et al., 2003; Stickley et al., 2004; Pross et al., 2012; Houben et al., 2019) as updated in Hoem et al. (2021).

4.2.2 Sample preparation and pollen analysis

To reconstruct the flora and past climate, the sporomorph content of a total of 51 samples spanning from the late Eocene to the early late Oligocene at ODP Site 1168 (35.50-27.46 Ma) was investigated. At the GeoLab at Utrecht University, the standard preparation procedures were followed for the processing of samples for palynological analysis (Brinkhuis et al., 2003; Bijl et al., 2018). To process the samples, they were first dried, then crushed and weighed (on average 10 g), and then treated with 30% cold hydrochloric acid (HCl) and 38% hydrofluoric acid (HF) to remove carbonate and silicate minerals, respectively. After that, the palynological residue was passed through a nylon mesh of 10 and 15 µm to remove any unwanted organic or inorganic debris. The residue were transferred onto microscope slides using glycerine gel as the mounting medium, and the slides were afterwards sealed with nail polish.

Under the Leica DM 500 and DM 2000 LED transmitted light microscopes, two to three slides were counted for each sample at 400x and 1000x magnification, respectively. When logging each sample, an attempt was made to count between 200-250 fossil spores and pollen specimens (excluding those that had been reworked). After that, the entire microscope slide was scanned for rare taxa. Samples that do not contain enough pollen grains (< 75 individuals) were discarded and not used in further analysis. The overall sporomorph preservation and counts were good, with the exception of twelve samples that did not contain enough sporomorph grains (< 75 specimen each). Reworked sporomorphs were identified and documented based on the colour of their exine and the fact that they occurred outside of their known stratigraphic range; however, they were not added to the overall number of pollen and spores counted. Calculations of pollen percentages were made using the total number of sporomorphs, and the results were shown using Tilia version 2.6.1. (Fig. 4.2; Grimm, 1990). In order to distinguish between different palynological zones, the stratigraphically constrained incremental sum-of-squares cluster analysis (CONISS; Grimm, 1987) was applied. Identification of sporomorphs, taxonomic categorization, and botanical affinities were determined using Macphail and Cantrill (2006), Macphail (2007), Raine et al., (2011), Bowman et al., (2014), and Macphail and Hill (2018).

With a sample size of ≥75 individual grains, PAST statistical software (Hammer et al., 2001) was used to generate diversity indices such as rarefaction, Shannon diversity, and equitability/evenness. The rarefaction approach is used to eliminate the effect that varying sample sizes have on the estimation of sporomorph species and to make this estimation possible while maintaining a fixed sample size (Birks & Line, 1992; Birks et al., 2016). The Shannon index (H) is the next step in the sporomorph diversity measurement process. The H index considers the number of individuals in addition to the number of taxa and the evenness of the species that are present (Shannon, 1948). H ranges from 0 in cases when vegetative communities only contain a single taxon to larger values in situations where taxa are spread in an equitable manner (Legendre & Legendre, 2012). On the other hand, equitability (J) is a measurement that assesses the amount of abundance in addition to how it is distributed in an assemblage. The dominance of only a few species in the population is indicated by J values that are low (Hayek & Buzas, 2010). Following stratigraphically constrained analysis (CONISS; Grimm, 1987), Pollen Zones (PZ) have been defined in Tilia (version 2.6.1; Fig. 4.2) by utilising total sum of squares with chord distance square root transformation (Cavalli-Sforza & Edwards, 1967).

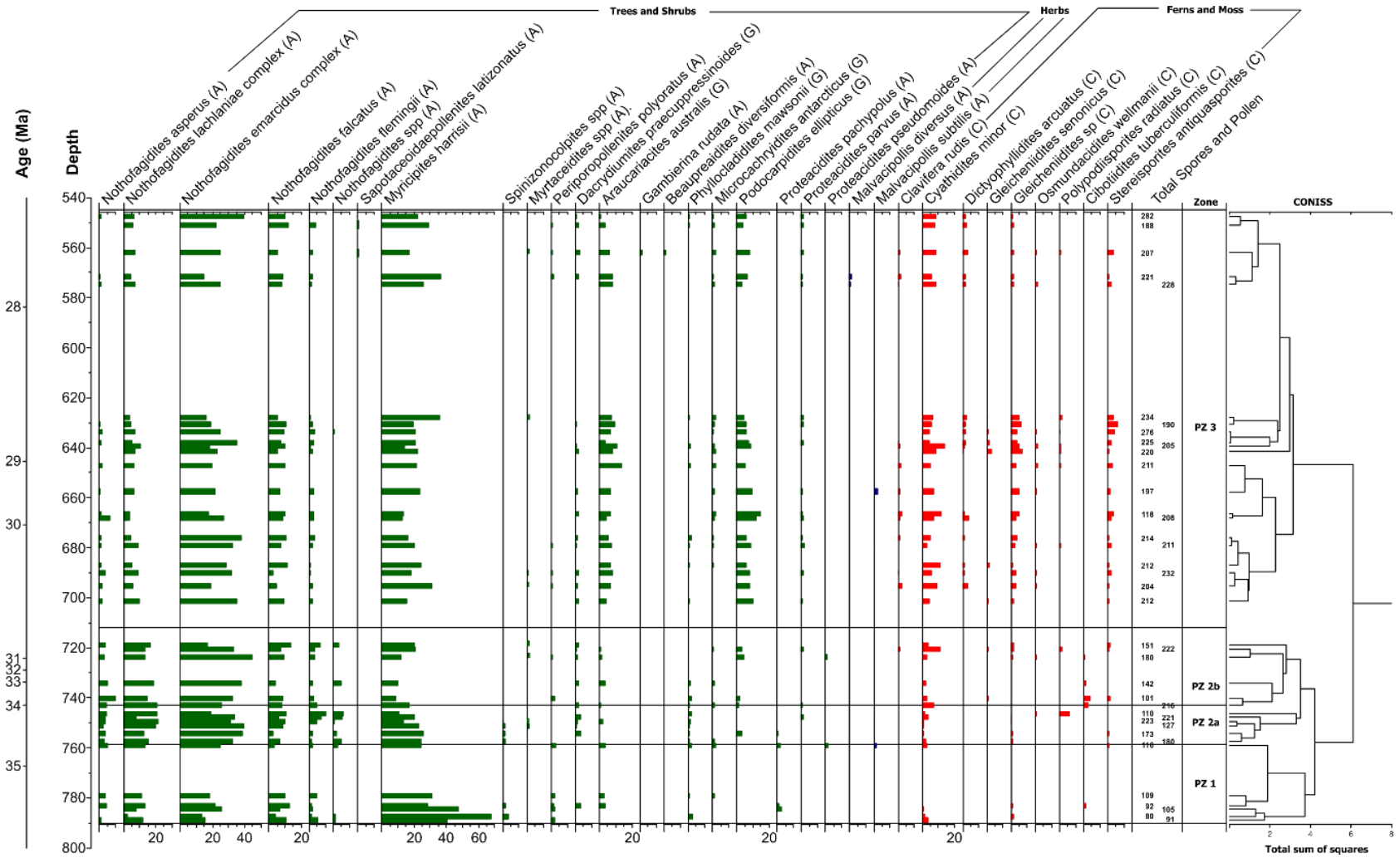

Figure 4.2. Sporomorph assemblages and relative percentage abundances of major taxa (i.e., Trees and shrubs, Herbs, Mosses, and Ferns) recovered from the latest Eocene (35.50 Ma) to early-late Oligocene (27.46 Ma). A, G, and C are angiosperms, gymnosperms, and cryptogams, respectively. CONISS ordination constrains the latest Eocene to early-late Oligocene sporomorph assemblages into three main pollen zones (PZ 1-PZ 3), with PZ 2 divided into PZ 2a and PZ 2b. For components of the lowland and upland taxa, see Fig. 4.5.

4.2.3 Multivariate statistical ordination techniques

The sporomorph percentage data were originally downweighted by removing pollen taxa < 5%, then normalised and analysed using Detrended Correspondence Analysis (DCA) and Principal Component Analysis (PCA). Across the analysed section, these multivariate ordination techniques were used to assess how species and sample composition alter and overlap over time. DCA is a metric ordination technique that use "reciprocal averaging" and permits the determination of species distribution in a two-dimensional space (Gauch, 1982). Species turnover across sample gradients, primarily four standard deviation (4-SD) units, may not contain identical species (Gauch, 1982). However, when the length of the first axis of the DCA is less than two standard deviations, it shows that the distribution of the species is linear rather than unimodal (ter Braak & Šmilauer, 2002). Consequently, ordination approaches based on linear response models, such as principal component analysis (PCA; Goodall, 1954), are appropriate for "homogeneous" data sets. PCA and DCA were conducted using the statistical computer software R (R Core Team, 2019) and the vegan package (Oksanen et al., 2019).

4.3 Results

The late Eocene-late Oligocene samples from the western margin of Tasmania (ODP Site 1168) analysed for pollen generally show good pollen recovery. 12 of the 51 samples analysed do not show enough sporomorph counts and were therefore excluded from further examination. Across the examined interval, 60 pollen taxa (including 11 gymnosperms and 34 angiosperms) and 15 spores were detected. The relative number and distribution of pollen taxa are depicted in the pollen diagram (Fig. 4.2). *Nothofagidites* spp. (23-73%) and *Haloragacidites harrisii*/*Myricipites harrisii* (9%-68%) dominate the sporomorph record. These also include *Podocarpidites* spp., *Cyathidites* spp., *Araucariacites australis*, and *Gleicheniidites* spp., which appear rarely to moderately during the Eocene but commonly across the Oligocene.

According to rarefaction data, the average diversity of the entire section is 14.0 ± 2.3 taxa/sample at 75 individuals. The section is divided into three major pollen zones (PZ; Fig.4.2) based on the results of

CONISS analysis: PZ 1 (late Eocene; 35.50-34.81 Ma), PZ 2 (2a and 2b; later Eocene-early Oligocene; 34.78-30.81 Ma), and PZ 3 (early Oligocene-late Oligocene; 30.55-27.46 Ma).

4.3.1 Pollen Zone 1 (35.50-34.81 Ma; 788.76-759.0 m b.s.f.; 6 samples)

Pollen Zone 1 (PZ 1) is distinguished by an abundance of *Nothofagidites* spp. (*Nothofagus*; 44%; Figure 4.2) and *Myricipites harrisii* (*Gymnostoma*; 40%). Within the genus *Nothofagus*, *brassii*-type taxa (28%) predominate, followed by *fusca*-type taxa (~13%) and *menzii*-type taxa (~3%). This zone is dominated by *Myricipites harrisii* (40%), with *Proteacidites* spp., *Periporopollenites polyoratus*, and *Spinizonocolpites* spp. (Arecaceae) occurring often. In order of decreasing relative abundance, *Podocarpidites* spp., *Araucariacites australis* (Araucariaceae), *Phyllocladidites mawsonii* (*Lagarostrobos*), *Dacrydiumites praecupressoides* (*Dacrydium*), and *Microcachryidites antarcticus* (Microcachrys) are the most abundant gymnosperms. Cryptogams, on the other hand are the smallest group, comprising less than 5% of all non-reworked sporomorphs. These include *Cyathidites* spp., *Gleicheniidites* sp. (Gleicheniaceae), and *Cibotiidites tuberculiformis* (Schizaeaceae), in order of decreasing abundance.

Quantitatively, PZ 1 is characterised by a low diversity of sporomorph species. At 75 individuals, the average number of sporomorph taxa based on rarefaction is 12.97 ± 2.73 (mean ± SD) (Table 4.1). Shannon diversity (H) and equitability (J) are 1.84 ± 0.37 and 0.50 ± 0.11 on average (Fig.4.3)

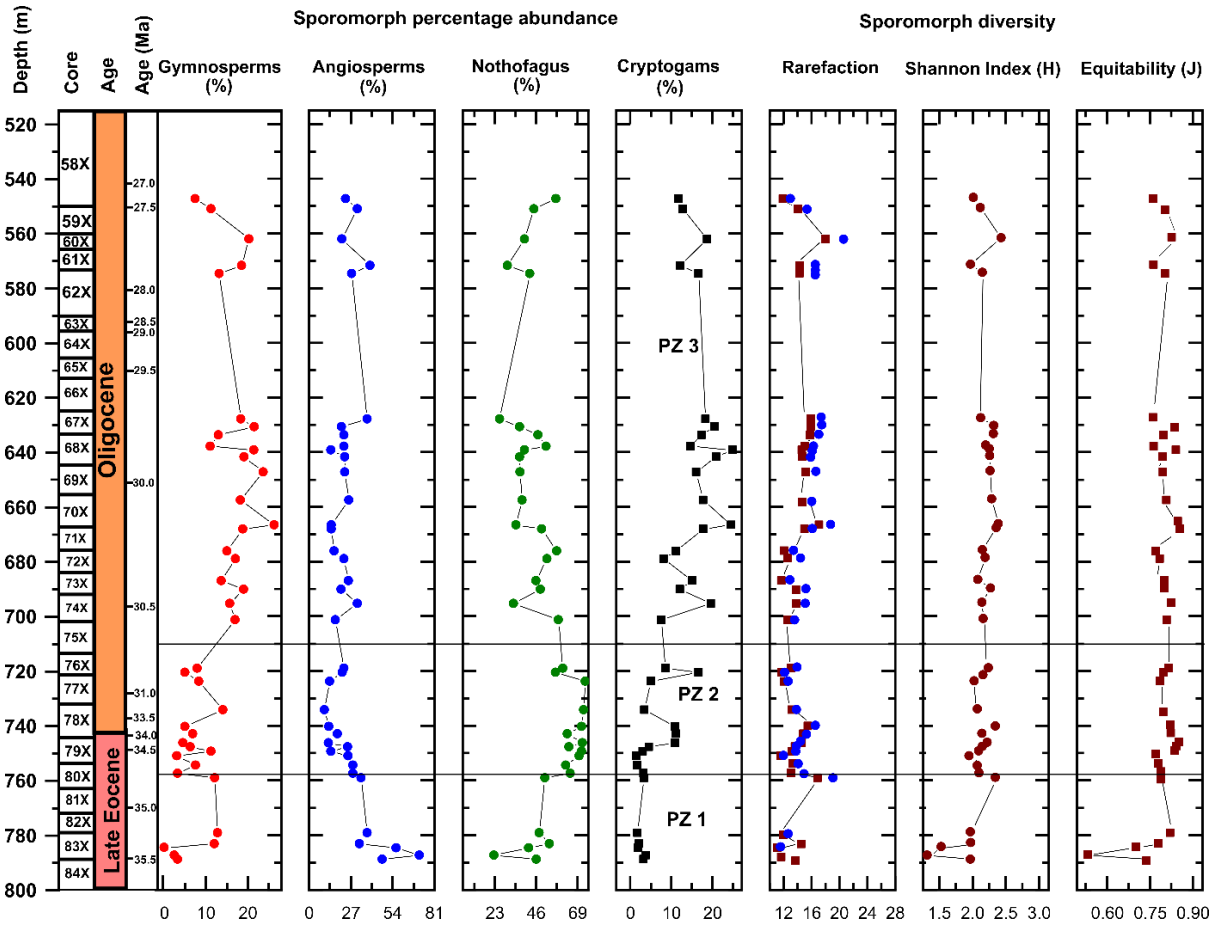

Figure 4.3: Percent abundances and diversity indices of sporomorphs at ODP Site 1168. Only samples with pollen counts 75 grains are provided, and these samples are categorised into the principal groupings (angiosperms, gymnosperms, Nothofagus and cryptogams). Even though samples are rarefied at 75 and 100 individual grains, they exhibit similar trends, only samples ≥75 grains were utilised for the calculation of diversity indices.

Table 4.1: Summary of quantitative species diversity from the late Eocene to early Oligocene of ODP Site 1168.

Analysis	Pollen Zone 1		Pollen Zone 2		Pollen Zone 3	
	Mean	*(SD)*	*Mean*	*(SD)*	*Mean*	*(SD)*
Rarefaction (75 individuals)	12.97	2.73	12.78	1.56	14.46	1.41
Rarefaction (100 individuals)	13.95	4.72	13.92	2.12	16.28	2.62
Shannon index (H)	1.84	0.37	1.98	0.19	2.16	0.15
Equitability (J)	0.72	0.11	0.78	0.04	0.81	0.03

4.3.2 Pollen Zone 2 (34.78-30.81 Ma; 757.46-719.0 m b.s.f.; 12 samples)

In this zone, the relative abundance of *Nothofagidites* spp. increases substantially and, on average, comprises ~ 67% (Figs. 4.2 and 4.3) of all non-reworked sporomorph taxa . The *brassii*-type *Nothofagus* (40%) is still the most common, followed by the *fusca*-type (20%) and the menzii-type (4%). Other angiosperms (non-*Nothofagus*) are still dominated by *Myricipites harrisii* (*Gymnostoma*), but their abundance decreases significantly from PZ 1 (40%) to PZ 2 (17%). Though *Proteacidites* spp., *Periporopollenites polyoratus*, and *Assamiapollenites inanis* represent components of non-*Nothofagus* angiosperms, they are rare and occur sporadically across PZ 2. Importantly, *Spinizonocolpites* spp. (Arecaceae) are gradually disappearing from this zone. Gymnosperms represent the second most abundant group and accounts for ~12% of all non-reworked sporomorphs. These gymnosperms are represented by taxa (in order of decreasing abundance) *Podocarpidites* spp. (Podocarpaceae)., *Araucariacites australis* (Araucariaceae), *Phyllocladidites mawsonii* (*Lagarostrobos*), and *Microcachryidites antarcticus* (*Microcachrys*). Cryptogams, which make up roughly 10% of all non-reworked sporomorphs, are generally more prevalent in PZ 2. Among these, *Cyathidites* spp. (Cyatheaceae), *Gleicheniidites* spp. (Gleicheniaceae), and *Cibotiidites tuberculiformis* (Schizaeaceae) are the most prevalent species.

Even though PZ 2a and 2b generally have comparable sporomorph contents, subzone 2a (34.78-34.31 Ma) is distinct from 2b (34.00-30.81 Ma) due to the declining numbers of *Myricipites harrisii* (*Gymnostoma*), *Nothofagidites asperus* (*menzii*-type *Nothofagus*), and *Cyathidites* spp. Despite being small components of subzone 2a, angiosperms including *Malvacipollis subtilis*, *Spinizonocolpites* spp., and *Proteacidites* sp. are strikingly absent from subzone 2b. However, *Cibotiidites tuberculiformis* (Schizaeaceae) are only found in subzone 2b and not subzone 2a.

Based on rarefaction statistics, the average number of sporomorph species per 75 individual grains in this zone is 12.78 ± 1.56, which is slightly lower than in PZ 1. Shannon diversity (H) and equitability (J) are 1.98 ± 0.19 and 0.78 ± 0.04 on average (Table 4.1; Figure 4.3), respectively.

4.3.3 Pollen Zone 3 (30.55-27.46 Ma; 701.30-547.30 m b.s.f.; 21 samples)

Between 30.55 and 27.19 Ma (Oligocene), PZ 3 displays an increase in gymnosperms and cryptogams alongside an increase in sporomorph species diversity. According to rarefaction analysis results, the average number of sporomorph taxa per sample of 75 individuals is 14.46 ± 1.41 species, which is substantially greater than PZ 1 and 2. (Table 4.1). Shannon diversity (H) and equitability (J) are, on average, 2.16 ± 0.15 and 0.81 ± 0.03, respectively (Table 4.1; Figure 4.3).

PZ 3 palynoflora records indicate a dramatic drop in *Nothofagidites* spp., from a peak of 67% in PZ 2 to 43% in PZ 3. Pollen taxa belonging to the *brassii*-type *Nothofagus* continue to dominate, accounting for 33% of all non-reworked palynomorphs, followed by the *fusca*- and *menzii*-types, which account for 8% and 2% of all non-reworked palynomorphs, respectively. Other angiosperms (non-*Nothofagus*) continue to be dominated by *Myricipites harrisii* (*Gymnostoma*), but their relative abundance has increased from a record low of 17% in PZ 2 to 22% in PZ 3. In this zone, additional non-*Nothofagus* angiosperms are uncommon and typically represented by one to three occurrences. These are *Proteacidites* spp. (Proteaceae), *Tricolpites* spp., *Gambierina rudata*, *Malvacipollis* spp. (Euphorbiaceae), *Microalatidites paleogenicus* (Phyllocladus), *Myrtaceidites* spp. (Myrtaceae), and *Sapotaceoidaepollenites latizonatus* (Sapotaceae). The relative abundance of gymnosperms in this zone increases from ~12% in PZ 2 to ~18 in PZ 3. In this zone, *Podocarpidites* spp. (Podocarpaceae) and *Araucariacites* australis (Araucariaceae) produce ~8% and ~7% of all non-reworked sporomorphs, respectively. These are followed by modest but consistent number of taxa like *Microcachryidites antarcticus* (*Microcachrys*), *Dacrydiumites praecupressinoides* (*Dacrydium*), *Dilwynites granulatus* (Araucariaceae), and *Phyllocladidites mawsonii* (*Lagarostrobos*). Cryptogams, on the other hand, experience a substantial increase in relative abundance and account for ~18% of all non-reworked sporomorphs. In this zone, *Cyathidites* spp. (Cyatheaceae) and *Gleicheniidites* spp. (Gleicheniaceae) account for an average of ~8% and ~7%, respectively, of all non-reworked sporomorphs. *Osmundacidites* spp. (Osmundaceae), *Stereisporites antiquasporites* (*Sphagnum*/Sphagnaceae), *Polypodiisporites radiatus* (Polypodiaceae), *Clavifera* spp. (Gleicheniaceae), and *Baculatisporites*

comaumensis (Hymenophyllaceae/*Hymenophyllum*) are additional minor but important and consistent members of this group.

4.3.4 Principal component analysis

The length of the first DCA axis (1.25 SD; Table 4.2) indicates that species turnover varies linearly across the examined interval (time), making the application of principal component analysis (PCA) appropriate for this data analysis.

Table 4.2: Total variance (eigenvalue) and axis lengths for the first four DCA components of the pollen data set from ODP Site 1168.

	DCA1	DCA2	DCA3	DCA4
Eigenvalues	0.132	0.080	0.023	0.022
Axis lengths	1.248	1.272	0.644	0.600

The two main axes (PC axis) of the principal component analysis account for 40.9% of the overall variance. The first principal component analysis axis explains 27.8% of the variance, distinguishing *Araucariacites–Gleicheniidites* from *Spinizonocolpites* spp.–*Proteacidites* sp., and providing evidence that these taxa survive under different ecological and environmental conditions (Fig. 4.4). Based on the ecology of the NLRs represented by the encountered sporomorphs, the first PCA axis (Dimension 1; Fig. 4.4) most likely represents a shift in climate (temperature) from relatively warm-temperate rainforests with paratropical (thermophilic) elements through to cool-temperate forests expanding and taking over lowland areas previously occupied by the warm-temperate forests. This is demonstrated by the distinction between taxa with negative sample scores, such as *Spinizonocolpites* spp., *Proteacidites* sp., *Periporopollenites polyoratus*, and *Proteacidites pachypolus*, which most likely indicate warm-temperate lowland habitats, and those with positive sample scores, such as *Araucariacites australis*, *Podocarpidites* sp., *Microcachryidites antarcticus* and *Gleicheniidites* possibly suggesting cool temperate climate conditions with MATs between 6 and 12 °C.

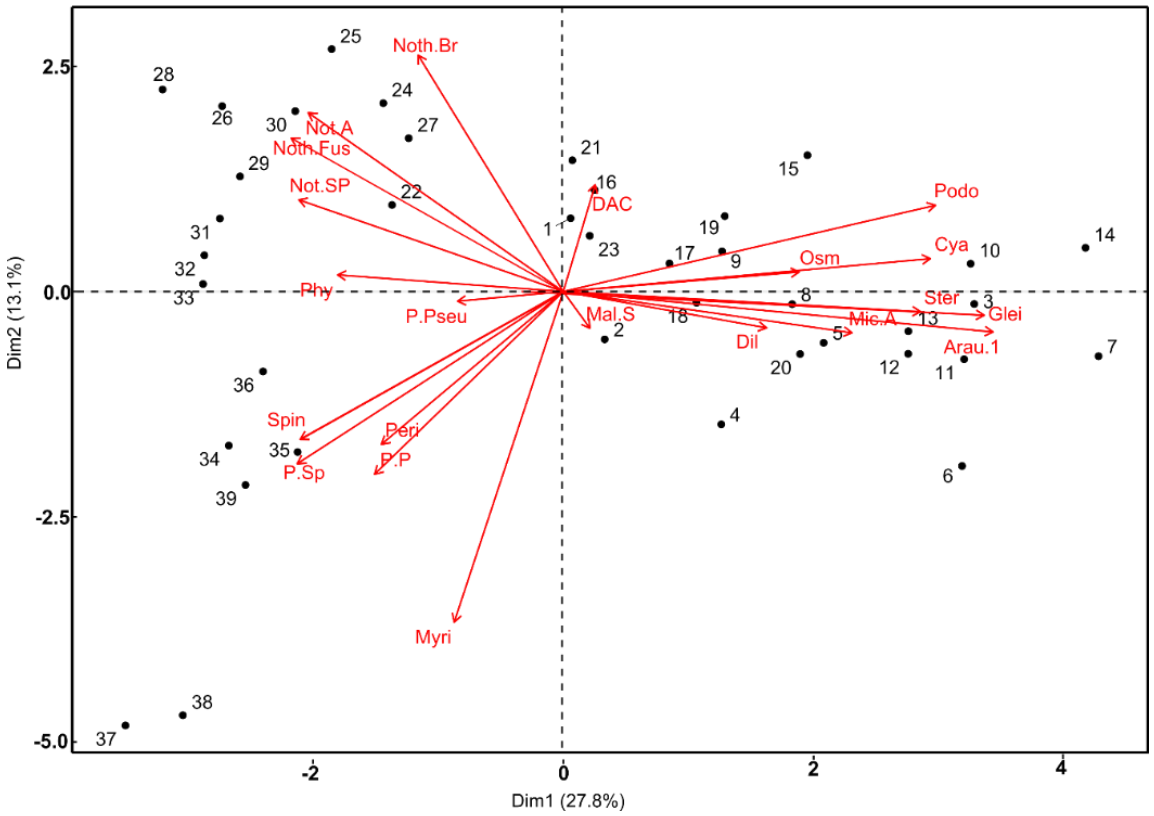

Figure.4.4. PCA biplot of western Tasmania pollen data showing the scores for the main pollen types. The main PCA axis (Dim 1) coupled with knowledge of the ecological preference of these taxa show a shift in latitudinal gradient from a lowland habitat through to upland conditions. Numbers from 1 to 39 represent sample IDs, with 39 being the oldest (35.50 Ma) and 1 being the youngest (27.46 Ma). Taxa are explained as follows; Myri = *Myricipites harrisii*, P.P = *Proteacidites pachypolus*, Peri = *Periporopollenites*, Spini = *Spinizonocolpites* spp., P. pseu = *Proteacidites pseudomoides*, Phy = *Phyllocladidites mawsonii*, Not. Sp = *Nothofagidites* spp, Noth. Fus = *Nothofagidites fuscospora*, Not. A = *Nothofagidites asperus*, Noth.Br = *Nothofagidites brassospora*, DAC = *Dacrydiumites*, Podo = *Podocarpidites*, Osm = *Osmundacidites*, Cya = *Cyathidites*, Ster = *Stereisporites*, Glei = *Gleicheniidites*, Mic.A = *Microcachryidites antarcticus*, Mal.S = *Malvacipollis subtilis*, Dil = *Dilwynites*, Arau = *Araucariacites australis*.

4.4 Discussion

4.4.1 Warm temperate lowland forest versus cold temperate mid-high-altitude forest taxa

The varying percentages of cool-temperate and thermophilic taxa (Fig. 4.4), suggest that the vegetation across the studied time interval in western Tasmania was subject to temporal changes in temperature. However, the co-occurrence of different vegetation communities with different climate envelopes also suggest that vegetation across Tasmania were subject to a spatial climatic gradient related to differences in elevation and/or distance to the coastline. This is supported by reports of a topographic divide

between sites facing the cool Tasman current (Gippsland basin, eastern Tasmania) and the westerly located south Australian basins (Holdgate et al., 2017) that may have served as the location for higher altitude temperate forest taxa. Abundant *Nothofagidites* spp. (especially *brassii*-type *Nothofagus*), with *Myricipites harrisii*, and common *Phyllocladidites mawsonii* give an indication of *Nothofagus-Gymnostoma* dominated warm-temperate temperate rainforest (Figs. 4.2 and 4.5) thriving under high precipitation regimes (MAP >1400 mm/yr) in western Tasmania during the late Eocene. In addition, pollen taxa belonging to Arecaceae and *Proteacidites pseudomoides*, indicate the existence of thermophilic elements between 35.50 and 34.81 Ma that most likely occupied the warmer sheltered lowlands and coastal areas (Huurdeman et al., 2021; Amoo et al., 2022). The two possible NLR relatives for *Proteacidites pseudomoides* are *Carnarvonia* and *Lomatia*. *Carnarvonia* thrives in warm temperate to tropical areas such as wet northeastern Australia (Cooper and Cooper, 2004) whereas *Lomatia* grows as shrubs and small trees in remnant gallery warm temperate rainforests (Bowman et al., 2014; Myerscough et al., 2007). *Carnarvonia* is selected as the likely NLR based of the PCA grouping with other thermophilic taxa (Fig. 4.4). This is also in agreement with comparable studies in the southern high latitude (e.g., Bowman et al., 2014; Amoo et al., 2022; Sluiter et al., 2022).

During the early to late Oligocene (~ 30.4 to 27.46 Ma; PZ 3), there was a transition from a primarily warm-temperate rainforest with paratropical components to a mostly cold-temperate rainforest. Increases in common occurrence taxa such as Araucariaceae, *Microcachrys*, *Sphagnum* (peat moss), and proteaceous shrubs are the basis for this interpretation. These taxa are a part of the palynoflora record that thrived at high latitudes with cool, temperate climates and vegetation that is more open. They thrive in soils that are low in nutrients but have good drainage (Macphail et al., 1999; Kershaw & Wagstaff, 2001; Bowman et al., 2014). This PZ 3 phase may very well be the establishment of a prominent cool-temperate upland vegetation community, with araucarian trees marking the margins of this forests/shrubland with proteaceous shrubs, *Microcachrys*, and shrubs of *Nothofagus* subgenera *Fuscospora*, *Lophozonia* (e.g., Anker et al., 2001), as well as scrubs of *Gymnostoma* and *Dacrydium* (e.g., in New Caledonia; Hope, 1996) and *Sphagnum* (e.g., in Tasmania and Australia; Seppelt, 2006) which were expanding and taking over areas that were previously occupied by lowland vegetation. The

widespread appearance of fern spores and mosses such as Cyatheaceae, Gleicheniaceae, Osmundaceae, and *Sphagnum* (Fig. 4.4 and Fig. 4.5) is most likely indicative of climate disruption (rapid cooling), which created gaps in the canopy and triggered the proliferation of cryptogams in the early Oligocene.

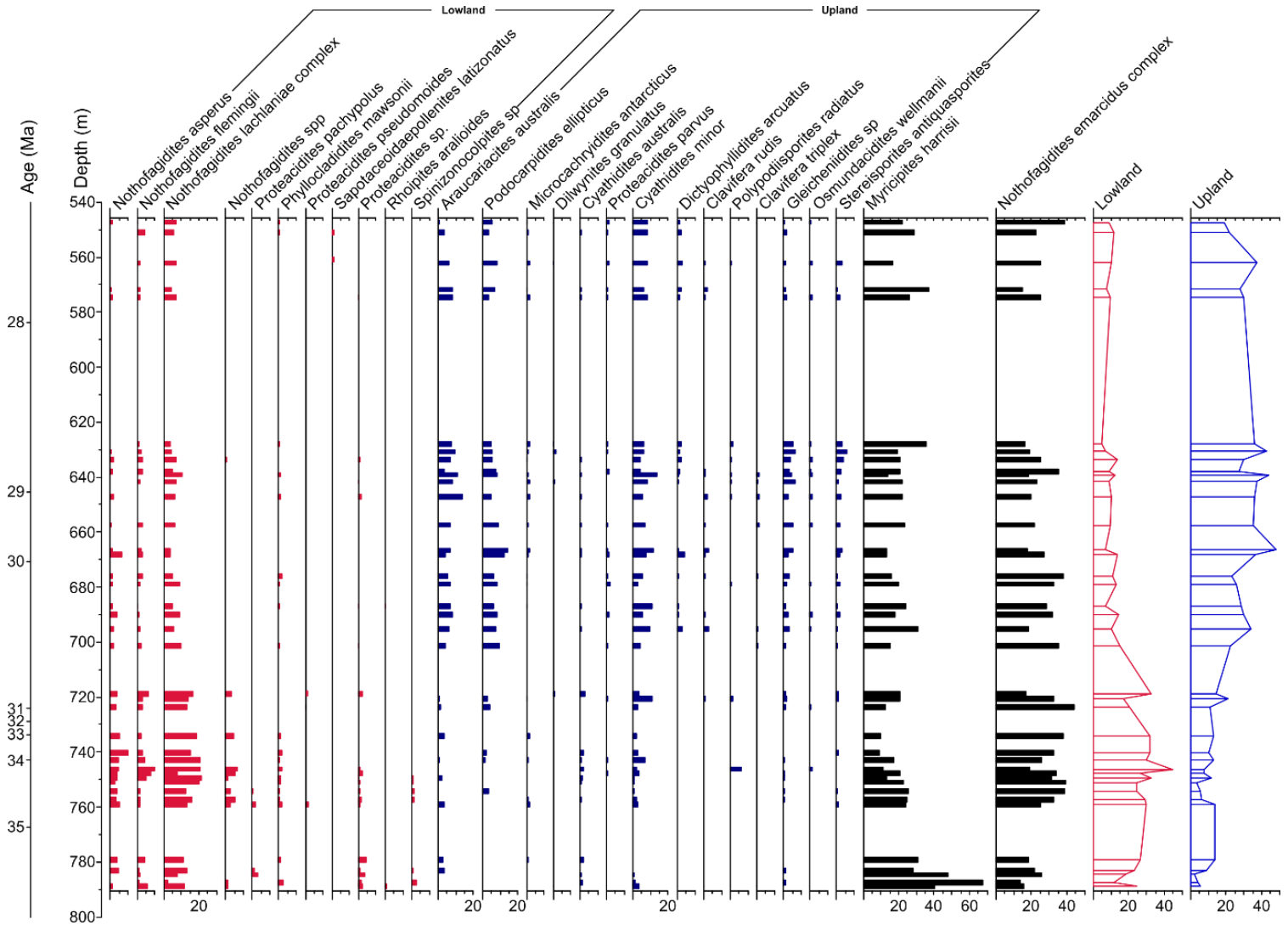

Figure 4.5 Relative abundance of the different categories of sporomorphs. The taxa represented by red bars are those whose NLRs are today mostly found thriving in warm-temperate to subtropical lowland regions; the taxa represented by blue bars are those whose NLRs are found thriving in cool-temperate uplands areas; and the taxa represented by black bars are those that dominate the entire section and could thrive in both warm and cool-temperate environments.

Nothofagus subgenus *Brassospora* and *Gymnostoma* were not only present throughout the studied interval, but also formed the dominant taxa and could not be grouped under the typical lowland warm temperate or cool temperate upland taxa (Fig. 4.5). In New Guinea and New Caledonia, where the climate range from temperate to subtropical, there are populations of *Brassopora*-type Nothofagus that dominate (Read et al., 2005). Because of their extensive ecological and climatic tolerance (MAT: 10.6 to 23.5 °C; Read et al., 2005), these *Brassospora*-type *Nothofagus* can be seen growing today in lower to mid-altitudes that receive high and consistent rainfall, as well as in montane and subalpine environments (usually above 500m a.s.l). *Gymnostoma*, on the other hand, are tropical to subtropical rainforest trees that can grow up to 12 metres in open, sunny gaps ranging from riparian (along riverbanks) niches to mountain top situations (altitudes between 200 and 1000 m above sea level). They are mostly found in the Malesian-Australian Melanesian region and New Caledonia today (Hope, 1996; Prider & Christophel, 2000; Steane et al., 2003; Korasidis et al., 2019). Although *Myricipites harrisii* (Casuarinaceae) has two possible NLRs, *Casuarina*/*Allocasuarina* and *Gymnostoma*, the rainforest clade *Gymnostoma* has been chosen as the most plausible NLR. This can be inferred from the associated taxa that existed in the study sample during the late Eocene of Tasmania (southern Australia) and was primarily dominated by rainforest taxa. This interpretation is supported by previous southern Australian Paleogene studies, which suggest that the rainforest clade, *Gymnostoma*, dominated throughout the Eocene and Oligocene (Hill, 2017; Lee et al. 2016). However, in the Miocene, the sclerophyllous/xeromorphic clade *Casuarina*/*Allocasuarina* took over as the dominant vegetation type in southern Australia (Hill & Scriven, 1995; Boland et al., 2006; Holdgate et al., 2017).

4.4.2 Latest Eocene warm-temperate climate and vegetation from 35.50 to 34.81 Ma

Across the entire PZ 1 assemblage (35.50-34.81 Ma), abundant *Nothofagus* spp., with secondary *Gymnostoma*, and minor angiosperm (*Carnarvonia*, Arecaceae, Proteaceae) suggest the presence of a temperate *Nothofagus*-dominated rainforest with subtropical elements, growing in western Tasmania under MATs of ~13 °C and MAPs between 1483-1892 mm/yr (Fig.4.6). It is also possible that input or transfer from high-altitude cold temperate woods was responsible for the existence of minor

components of cold-temperate taxa, such as *Microcachrys*, Podocarpaceae, and Araucariaceae. The presence of warmth-loving (mesothermal) species in this zone, such as the Arecaceae, *Carnarvonia*, Myrtaceae, *Gymnostoma*, and Proteaceae families, supports the presence of a temperate-paratropical vegetative community. There is also a unique cluster of taxa along the second principal component axis (Dim 2; Fig.4.4), with all groupings of *Nothofagus* clustered in one region/areas (positive scores), and taxa such as *Carnarvonia*, Arecaceae, Proteaceae, Trimeniaceae, and *Gymnostoma* on the other end (negative scores). Therefore, across the lowland rainforest groups, there is a possible distinction between a more coastal forest that is more diverse and an inland forest that is composed entirely of *Nothofagus*. The paratropical elements such as Arecaceae, based on the habitat of their NLRs are considered to have occupied sheltered lowland and coastal areas requiring relatively milder/non-freezing winter temperatures, due to the sensitive nature of palms to frost (Larcher & Winter, 1981; Tomlinson, 2006; Reichgelt et al., 2018). In addition, CMMTs yield winter temperatures above freezing conditions (7.8-13.1 °C; Fig. 6). All the samples in this zone produce sporomorph-based MATs higher 12 °C, except for one sample at 35.27 Ma, which records a MAT of 11 °C (Fig. 4.6). This predominantly warm-temperate climate deduced from our sporomorph-based climate estimate is comparable to an observed warmth based on brGDGT between 37.7 and 34.7 Ma on Prydz Bay (Tibbett et al., 2021), coincidentally marking the last flickers of Antarctic warmth before the EOT. In eastern Tasmania, there is a fluctuation between warm-and-cold temperate climate between 35.50-34.59 Ma (Amoo et al., 2022) which have been linked to the initial deepening and widening of the Tasmanian gateway causing eastern Tasmania to come under the influence of the warm PLC (Stickley et al., 2004; Hoem et al., 2021). A general mesothermic condition is reported with sporomorph-based MATs between (14-22 °C; Korasidis et al., 2019) and (15-20 °C; Sluiter et al., 2022; Fig. 4.7) for the late Eocene of southeastern Australia (Gippsland Basin). These mesothermal conditions are further in agreement with late Eocene terrestrial biomarker records from southeastern Australia (Lauretano et al., 2021).

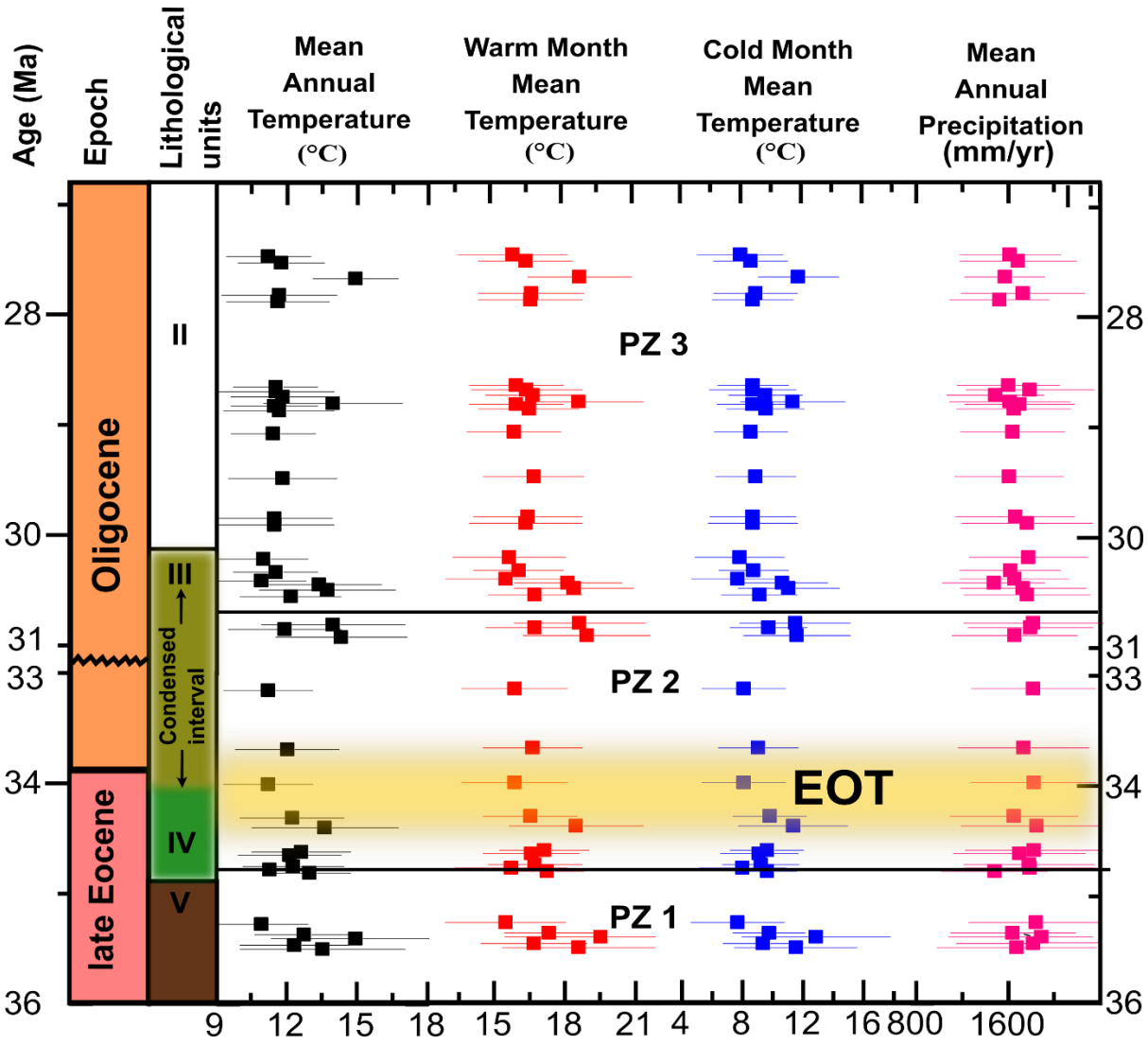

Figure 4.6: Climate estimations based on sporomorphs utilising probability density functions (PDFs). Mean annual temperature (MAT), warm month mean temperature (WMMT), cold month mean temperature (CMMT), and mean annual precipitation (MAP) are arranged from left to right (MAP). The quantitative temperature estimations are given in degrees Celsius, while MAP is given in millimetres per year. The wiggle line between 33 and 31 Ma indicates the age gap.

4.4.3 Progression towards cooler climate conditions across the EOT (~34.46-33.69 Ma) and rebound in the earliest Oligocene (33.15-30.81 Ma)

PZ 2 eventually captures both the EOT and the post-EOT (earliest Oligocene). Sporomorph-based MATs at the EOT show an overall cooling spanning 34.46 to 33.69 Ma on western Tasmania, with ~ 2 °C temperature drop (Fig. 4.6). Although this estimated cooling appears to be only minor and with overlapping error ranges, a shift in the abundance of several taxa at the onset of the EOT provide additional evidence for a major change in vegetation cover in response to this cooling. Also, as the

bioclimatic analysis uses presence/absence of taxa only, these changes in pollen percentages are not captured in the quantitative estimated temperatures. Though *Nothofagus* dominated the whole studied section, this taxon increased dramatically in the EOT (accounting for around 69% of all non-reworked sporomorphs). Distinct alterations, such as a steep reduction in the warmth-loving rainforest clade *Gymnostoma* and a minor increase in the *Nothofagus* subgenera *Lophozonia* and *Fuscospora*, corroborate the idea of a brief cold spell across the EOT. The decline of Arecaceae (NLR of *Spinizonocolpites* spp.), a drop in angiosperms (non-*Nothofagus*), and a modest increase in cryptogams all contribute to the evidence for the EOT cool phase (Fig. 4.3). Previously in southern Australia (e.g., Macphail et al., 1994; Benbow et al., 1995; Macphail 2007; Holdgate et al., 2017; Korasidis et al., 2019; Lauretano et al., 2021) and eastern Tasmania (Amoo et al., 2022), the concurrent demise of diverse angiosperm flora including Proteaceae, sharp rise in *Nothofagus* and decline and demise of megathermal taxa was attributed to increasingly cooler climate conditions (Martin, 1994; Partridge & Dettmann, 2003). The increase in relative abundance of *Nothofagus* in New Zealand in the late Eocene and across the EOT is similarly attributed to the advent of cooling (Pocknall, 1989), which is consistent with the palaeoclimatological reconstruction for western Tasmania. This terrestrial cooling across the EOT corresponds to regional and worldwide temperature records (Colwyn & Hren, 2019; Korasidis et al., 2019; Lauretano et al., 2021; Tibbett et al., 2021) and is generally associated with global pCO_2 reduction. The equatorward shift of the Australian continent, similar to other sites in southeastern Australia (Lauretano et al., 2021), may have mitigated the cooling caused by lowering pCO_2 over the EOT. The development, and in certain cases, increase, of fern spores (Cyatheaceae, Gleicheniaceae, and Schizaeaceae) throughout this zone indicates the presence of a wetland or marshes and could be linked to cooling around this time. The cooling and subsequent decrease of warmth-adapted taxa may have also led to the creation of gaps in the canopy that these ferns have occupied.

The interval between 33.69 and 33.15 Ma corresponds to the early Oligocene glacial maximum (EOGM; Liu et al., 2009; Hutchinson et al., 2021). This interval is generally correlated with the early Oligocene's normal magnetic polarity C13n (33.705-33.157 Ma; Gradstein et al., 2012). Four samples fell within this zone of interest, however due to very low pollen counts (75 individual grains per sample)

in two of the samples (e.g., 33.29 and 33.43 Ma), they were eliminated from further study. The sporomorph-based temperature estimates show cool-temperate climate conditions with MATs ranging from 11.2 to 12 °C (Fig. 4.6). Furthermore, the dominance of *Nothofagus* (*Brassospora* and *Fuscospora*) and the persistent occurrence of *Lagarostrobos* and *Microcachrys* suggest a period of sustained cool-temperate temperatures. Today, *Nothofagus* (*fusca*-type) normally dominates cool-temperate vegetation in New Zealand, Tasmania, and southern Australia (Kershaw, 1988), and its co-dominance with *Brassospora*-type, which can also be found in temperate montane and high precipitation regions of New Guinea and New Caledonia, may represent a refugium and/or change in stature (Pocknall, 1989; Read et al., 2005). This interval of continuous cool-temperate conditions is akin to the earliest Oligocene uppermost T0 climatic estimations from southeastern Australia's Gippsland Basin (Korasidis et al., 2019) and the earliest Oligocene of eastern Tasmania (Amoo et al., 2022). The extended post-EOT (early Oligocene) record available for this study compensates for the relatively low resolution of Site 1168's EOGM record in comparison to Site 1172. Whereas climatic estimations for Site 1172 show a post-EOT warming phase lasting from 33.25 to 33.06 Ma, our data from Site 1168 shows that the post-EOT warming phase lasted until 30.44 Ma (base of PZ 3) with an average quantitative sporomorph-based estimate of 13 °C (Fig. 4.6). Other studies from southern Australia (Korasidis et al., 2019; Sluiter et al., 2022) demonstrate a similar cooling across the EOT but with divergent post-EOT climate trajectories (early Oligocene). Korasidis et al. (2019) reported a monotypic cooling trend from late Eocene mesothermic/warm-temperate climatic conditions to early Oligocene microthermic/cool-temperate climate conditions across the EOT and early Oligocene. Sluiter et al. (2022) used a comparable sedimentary record from the Gippsland Basin to create a similar climatic reconstruction, which did not totally corroborate. Sluiter et al. (2022) presented evidence for a cooling trend across the EOT, followed by a return to mesothermal conditions (warming) in the early Oligocene (post-EOT; Fig. 4.7). Though the EOT and early Oligocene (30.4 Ma) MAT records for Site 1168 indicate overall concordance in trends, the Gippsland Basin MATs (Sluiter et al., 2022) are generally 2-4 °C warmer than western Tasmania. This could be attributed to latitudinal differences between these sites (the Gippsland Basin was 5 °N of western Tasmania during the late Eocene and early Oligocene). The drop in atmospheric carbon dioxide (pCO_2) concentration and its recovery were linked to the EOT

terrestrial cooling and transient warming in the early Oligocene of Site 1172. (Amoo et al., 2022). However, the sporomorph-based MAT records from Site 1168 show that the composite post-EOT warm-temperate phase lasted long into the early Oligocene at 30.44 Ma, which is consistent with the general sporomorph-based MAT trend in southeastern Australia (Sluiter et al., 2022). The Site 1172 MATs and pCO_2 post-EOT have a general match. However, the temperature change at Site 1168 from 33.0 to 30.4 Ma during the warm-temperate post-EOT period appears to be decoupled from the global pCO_2 trend (Fig. 4.7).

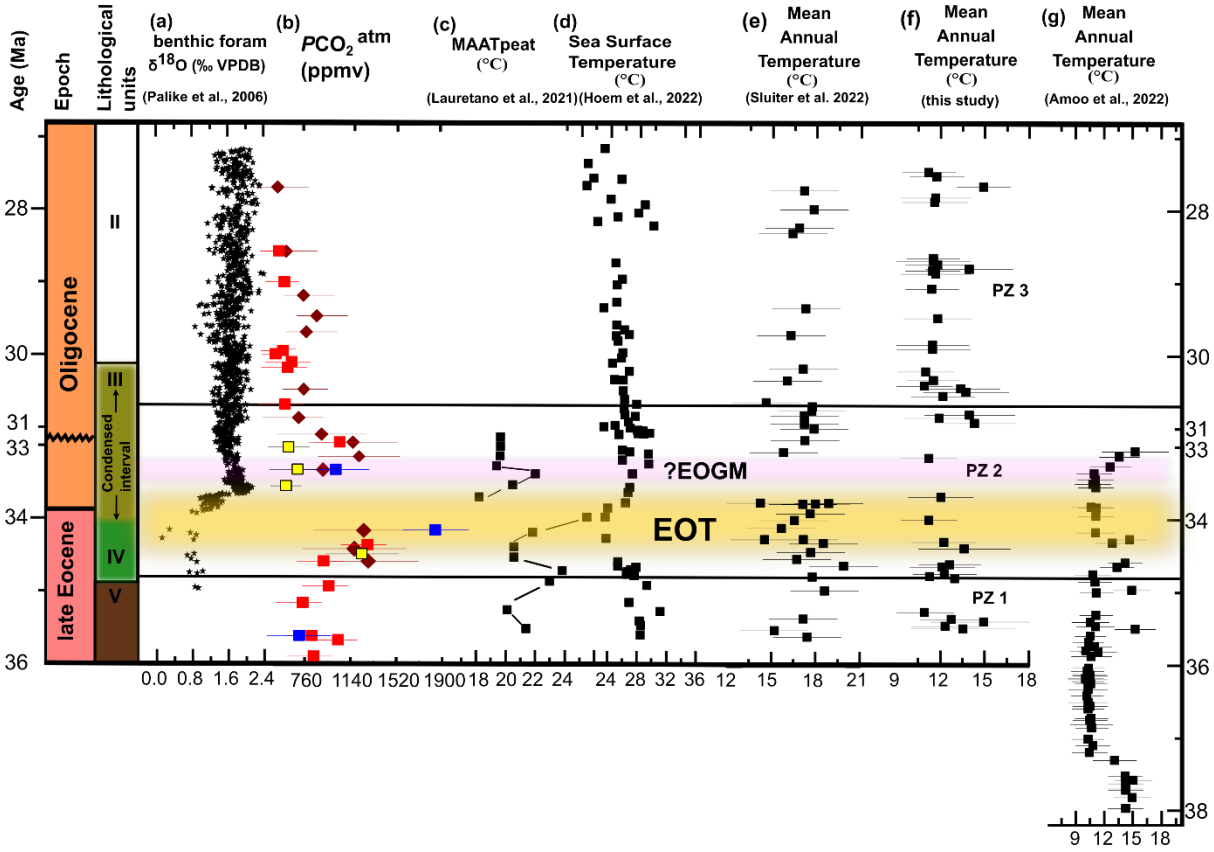

Figure 4.7. Comparison of the sporomorph-based MATs in the Tasmanian Gateway region across the EOT and post-EOT global marine EOT and early Oligocene records. (a) benthic foraminiferal $\delta^{18}O$ record from ODP 1218 (Pälike et al., 2006). (b) Marine δ11 B-derived atmospheric pCO_2 record (brown kite-like symbol with error bars; Anagnostou et al., 2016); Alkenone-based pCO_2 estimates derived from haptophyte algae for Site 516 and 612 (Pagani et al., 2005; data points are red boxes with error bars); Refined Alkenone-based pCO_2 estimates for ODP Sites 277 and 511 (blue and yellow boxes, respectively; Zhang et al., 2020). (c) MBT'5me-based MAATsoil (Lauretano et al., 2021). (d)TEX_{86}-derived Sea surface temperature from ODP site 1168 (SST; Hoem et al., 2022). (e) Sporomorph-based quantitative MATs of the Gippsland Basin (Sluiter et al., 2022). (f) Sporomorph-based quantitative from ODP Site 1168 (this study). (g) sporomorph-based MATs from ODP site 1172 (Amoo et al., 2022). Wiggle line between ~ 33 and 31 Ma shows age hiatus.

A detailed examination of the SST trend shows a 4 °C cooling (from 27 to 23 °C) across the EOT, followed by a return to relatively high temperatures equivalent to pre-EOT values until 30 Ma (Fig. 4.7; Hoem et al. 2022). Although absolute temperatures are substantially lower, the marine-based temperature trends correspond with Site 1168 terrestrial sporomorph-based MATs (10-15 °C) (Fig. 4.7). This is most likely due to the TEX_{86} temperature proxy's warm bias (Naafs et al., 2017; Hartman et al., 2018). According to model simulations (Sauermilch et al., 2021) and palaeoceanographic reconstructions (Stickley et al., 2004; Hoem et al., 2021), the interval across the EOT and until 30.2 Ma is characterised by a condensed section and series of hiatuses, indicating the most significant increases in deepening and currents associated with bottom-water activity in the Tasmanian Gateway region. The data show no evidence of a decline in SST, but by 30.2 Ma, a stable, deep-marine setting consistently affected by very warm waters had been established (Stickley et al., 2004; Hoem et al., 2021). As a result, alternative forcing(s) may have been responsible for the comparatively continuous warm terrestrial climate phase until 30.4 Ma, in addition to the drop of pCO_2 across the EOT and its temporary recovery in the early Oligocene. The most likely source(s) of this phenomenon is a somewhat local forcing (e.g., the sustained deepening of the Tasmanian Gateway) working in tandem with a more global driver such as atmospheric pCO_2.

4.4.4 Establishment of a relatively cool-temperate vegetation and climate in the early (30.4 Ma) Oligocene to early-late Oligocene (27.46 Ma)

Despite evidence for a warm-temperate post-EOT climate continuing into the lower parts of PZ 3 (30.4 Ma), the vegetation composition of the terrestrial palynomorph assemblage from western Tasmania (Site 1168) did not alter dramatically until after ~30.4 Ma. The terrestrial palynomorph assemblage, although suggesting a minor drop in relative diversity, continues to point to a *Nothofagus*-dominated temperate forest, with secondary *Gymnostoma* (Fig. 4.2 and Fig.4. 3). This period (30.4-27.46 Ma) displays an increase in the diversity of conifer trees and cryptogams (Fig. 4.3), as well as an increase in taxonomic diversity (Table.4.1). The PCA backs up this distinct variation in the early Oligocene flora of western Tasmania (Fig.4.4). The presence of coniferous taxa and boreal shrubs (gymnosperms) such as Araucariaceae, *Podocarpus*, *Dacrydium*, and *Microcachrys* on the right side of the PC 1 (Dim 1; Fig.

4.4) in conjunction with samples suggests that cool-temperate vegetation that previously thrived at high altitudes/elevation in the hinterland begins to displace and occupy lowland regions of western Tasmania. According to the Shannon diversity index, the early Oligocene cool-temperate forest was more diverse than the latter Eocene vegetation (Table 4.1). This interpretation is consistent with the early Oligocene *Nothofagus*-dominated rainforest in the Drake Passage region (Thompson et al., 2022). Conversely, previous early Oligocene investigations in Antarctica (Cantrill, 2001; Raine & Askin, 2001; Prebble et al., 2006; Griener & Warny, 2015) show a loss in taxonomic diversity due to considerable cooling and drying, resulting in low-stature and shrubby *Nothofagus*-Podocarpus vegetation. However, given the greater diversity of taxa in this interval, as well as increases in relative abundance of non-*Nothofagus* angiosperms (particularly *Gymnostoma*) and cryptogams, the *Nothofagus*-dominated rainforest with secondary *Gymnostoma* is most likely to have been intermediate in stature, with openings or gaps occupied by ferns, mosses, and shrubs (Macphail et al., 1994). This interpretation is bolstered by an increase in *Sphagnum* moss (*Stereisporites*) during this period. *Sphagnum* moss has been identified as low-diversity tundra vegetation in several Oligocene records from Antarctica, Tasmania, and southern Australia (Askin & Raine, 2000; Prebble et al., 2006; Amoo et al., 2022; Sluiter et al., 2022; Thompson et al., 2022). They mainly grow in carpet-like fashion in nutrient-poor acidic wetlands/swamps in cold temperate alpine-subalpine ecosystems in Australia and Tasmania today (Seppelt, 2006). Within the same early Oligocene epoch, sporomorph-based quantitative estimations show mainly cold-temperate climates with average MATs of 11 °C, which validates the qualitative vegetation reconstruction. However, because the PDF method is based on the presence or absence of taxa, two samples within this interval (e.g., at 27.68 and 28.80 Ma) yield MATs of 14 °C, indicating warm temperate conditions due to the presence of warmth-loving taxa (e.g., *Beauprea*, Myrtaceae, and Sapotaceae), indicating that even in an interval characterised by cool temperate conditions, minor pockets of warm temperate vegetation may exist.

Palaeoceanographic reconstructions indicate that the formation of a stable deep-marine setting, consistently impacted by the very warm surface waters associated with the PLC, lasted until the early Oligocene (Stickley et al., 2004). Apart from the time around 28 Ma, SST records after 31 Ma generally

show a cooling trend (Hoem et al., 2022). This general cooling trend is consistent with the long-term cool-temperate climate conditions in our terrestrial records, and it also corresponds to the general decline in pCO_2 concentrations in the early Oligocene (Fig. 4.7). Temperature correspondence or synchroneity (SST gradual decline; Hoem et al., 2022) with atmospheric pCO_2 most likely indicate the coupling of the ocean-atmosphere system in southern Australia, as well as the role of pCO_2 in driving terrestrial climate and vegetation change in the Tasmanian Gateway region.

4.5 Conclusions

This Chapter presents a new late Eocene (35.50 Ma) to Oligocene (27.46 Ma) marine pollen record from ODP Site 1168 to reconstruct vegetation and provide insight into the evolution and dynamics of Tasmania's terrestrial climate. Three major vegetation zones/phases characterise the sporomorph record across the examined interval (PZ 1, PZ 2, and PZ 3). The latest Eocene PZ 1 (35.50-34.81 Ma) is distinguished by a warm-temperate *Nothofagus* rainforest with paratropical elements and sporomorph-derived MATs 14 °C. The sporomorph assemblage in this interval is comparable to the latest Eocene PZ 3 of Site 1172, which is thought to mark the stage of the Tasmanian Gateway's initial deepening. PZ 2 (34.4-30.5 Ma) is distinguished by a 2 °C decrease in terrestrial MAT over the EOT (34.40-33.65 Ma) and an extended period of warm-temperate temperatures after the EOT. However, the relatively long post-EOT warming results in a mismatch between pCO_2 and terrestrial temperatures after 33 Ma, suggesting that factors other than greenhouse forcing (such as the sustained deepening of the Tasmanian Gateway and the resulting equatorward movement of the Australian landmass) may have contributed to this phenomenon. Modelling and palaeoceanographic studies confirm the early Oligocene (30.2 Ma) establishment of a stable deep-marine setting consistently influenced by warm surface water associated with the PLC. The *Nothofagus*-dominated temperate forest did not undergo a notable change in composition until 30.5 Ma (PZ 3), when a rapid increase in gymnosperms (particularly Araucariaceae), cryptogams, and angiosperms was noted, along with a minor increase in taxonomic diversity. The spread of cool-temperate forest (long-term cool-temperate climate conditions in our terrestrial records) corresponds to the general decline in pCO_2 values in the early Oligocene. The early Oligocene synchrony between temperature (gradual decline in SST and MATs) and atmospheric pCO_2 most likely

indicates the coupling of the ocean-atmosphere system in the southern Australia region, as well as the role of pCO_2 in driving terrestrial climate and vegetation change onshore Tasmania. This chapter emphasises a partial decoupling of vegetation and climate in the Tasmanian region from the late Eocene to the early-late Oligocene, providing evidence for variable relevance of both tectonic and pCO_2 forcing.

5. Middle Eocene to Oligocene vegetation and climate in Southland, New Zealand before and after the development of the Marshall Paraconformity

5.1 Introduction

The sedimentary basin-fill of the Canterbury Basin, Southland, New Zealand is made up of a characteristic condensed late Eocene to early Miocene sequence with hiatus known as the Marshall paraconformity (Carter & Landis, 1972; Lewis, 1992; Fulthorpe et al., 1996). The Marshall Paraconformity is described as a regional unconformity in the Oligocene sedimentary succession of New Zealand (Carter and Landis, 1972; Carter, 1985; Fulthorpe et al., 1996), and Australia (Abele et al., 1976), and its development (timing and mechanism of formation) and regional significance have been debated extensively (Findlay, 1980; Lewis & Belliss, 1984; Fulthorpe et al., 1996; Carter et al., 2004). This is mostly because, earlier works on the Marshall Paraconformity in the Canterbury Basin have relied on stratigraphically incomplete and weathered sections/outcrops (Findlay, 1980; Lewis, 1992; Fulthorpe et al., 1996). Several theories have been proposed as likely drivers of the formation of this unconformity, including (1) erosion due to ocean circulation changes associated with the development of throughflow across the Tasmanian Gateway (Carter and Landis, 1972; Lyle et al., 2007; Lever et al., 2007); (2) sub-aerial exposure (Lewis and Belliss, 1984); (3) glacio-eustatic sea-level change (Fulthorpe et al., 1996); (4) cut in sediment supply due to major transgression and system highstand (Carter, 1985).

This chapter presents a new sporomorph record recovered from TNW-1 well (Fig. 5.1) ~ 4 km northeast of the village of Cave to better understand the chronostratigraphy and terrestrial vegetation response to the changes in global and/or regional climate and ocean circulation from the mid-Eocene to the Oligocene. The TNW-1 drillcore provides a long and almost continuous record making it possible to use the extracted palynomorphs (sporomorphs and dinoflagellate cysts) to erect a biostratigraphic record for the Eocene-Oligocene of Southland, New Zealand. This has become necessary because preliminary age determination approach based on magnetostratigraphy (Fig. 5.2; Tinto, 2010) yielded ages with poor resolution, especially prior to the development of the Marshall paraconformity. The palynomorph

record will further the understanding of the events leading to the formation of the Marshall Paraconformity in the TNW-1 drillcore.

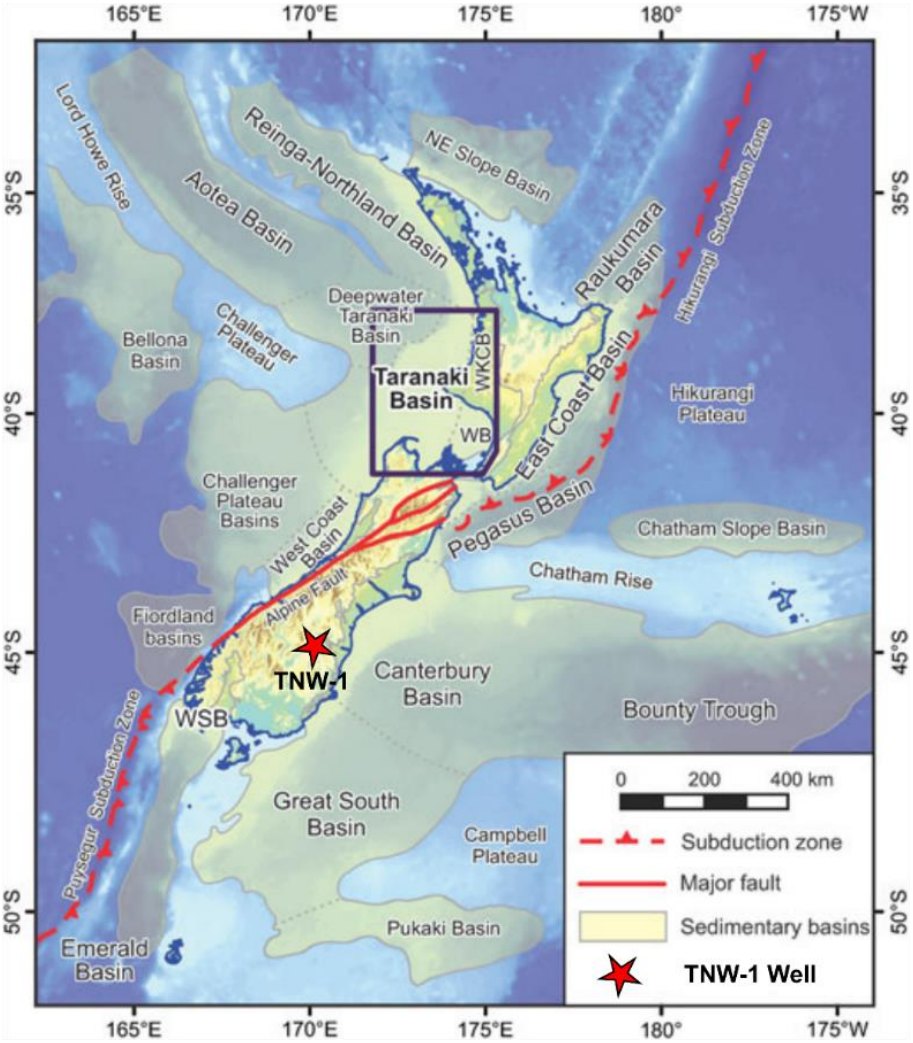

Figure 5.1 Location map of the New Zealand area showing the major sedimentary basins (Taranaki, Canterbury, Chatham Slope, Great South, Pukaki, Fiordland, Bellona, Aotea, Raukumara, NE Slope and Reinga-Northland Basins) and structural features. The main study site (TNW-1) is marked as the red 5-pointed star. Modified after Strogen et al. (2019).

The Eocene to the Oligocene of the southern-high latitude is regarded as an interval of remarkable climatic transitions (Contreras et al., 2014; Holdgate and Sluiter, 2017; Korasidis et al., 2019; Thompson et al., 2022) of the Cenozoic. Marine pollen record from southern Australia (Tasmania; Chapters 3 and 4) show a distinct climate cooling across the EOT and a recovery in the early Oligocene, while the first major advance of ice onto the continent of Antarctica occurred (Tibbett et al., 2021). The (micro-) continent of New Zealand (Zealandia), showed the persistence of warm humid climate

conditions from the late Eocene into the early Oligocene (Pocknall, 1989; Homes et al., 2015; Prebble et al., 2021) until the extensive submergence of New Zealand landmass during the Oligocene (McGlone et al., 1996).

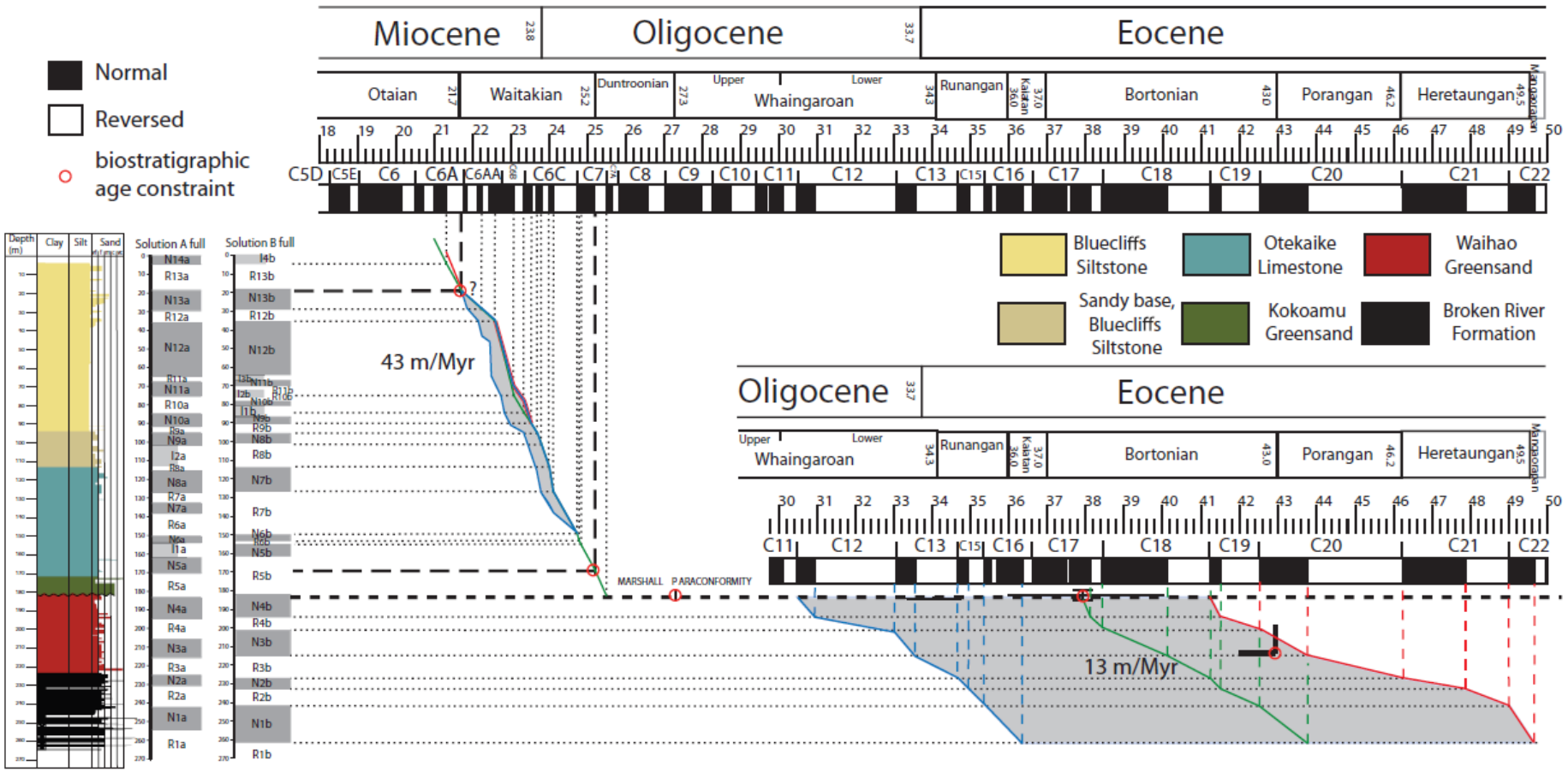

Figure 5.2: Age model for the TNW-1 drillcore from magnetostratigraphy. Green lines are preferred age model, with possible oldest (red line) and youngest (blue line) ages also shown. Red hollow circle represents biostratigraphic age constraints based on benthic forams. Figure is adapted from Tinto (2010).

Deepening of the Tasmanian Gateway (between 35.5 to 30.2 Ma) resulted in the throughflow of warm water from the PLC into the Pacific (Huber et al., 2004; Stickley et al., 2004; Fig. 5.3) thereby deflecting the Proto-Ross Sea Gyre across New Zealand and resulting in an intensification of shallow water currents across New Zealand, potentially aiding in the formation of the Marshall Paraconformity (Lyle et al, 2007). In the frame of the above model, this study will test whether the deflection of cold water associated with the Tasman current across New Zealand resulting from the throughflow of warm water associated with the PLC coincides with major reorganisation of climate and vegetation at TNW-1 (Southland, New Zealand).

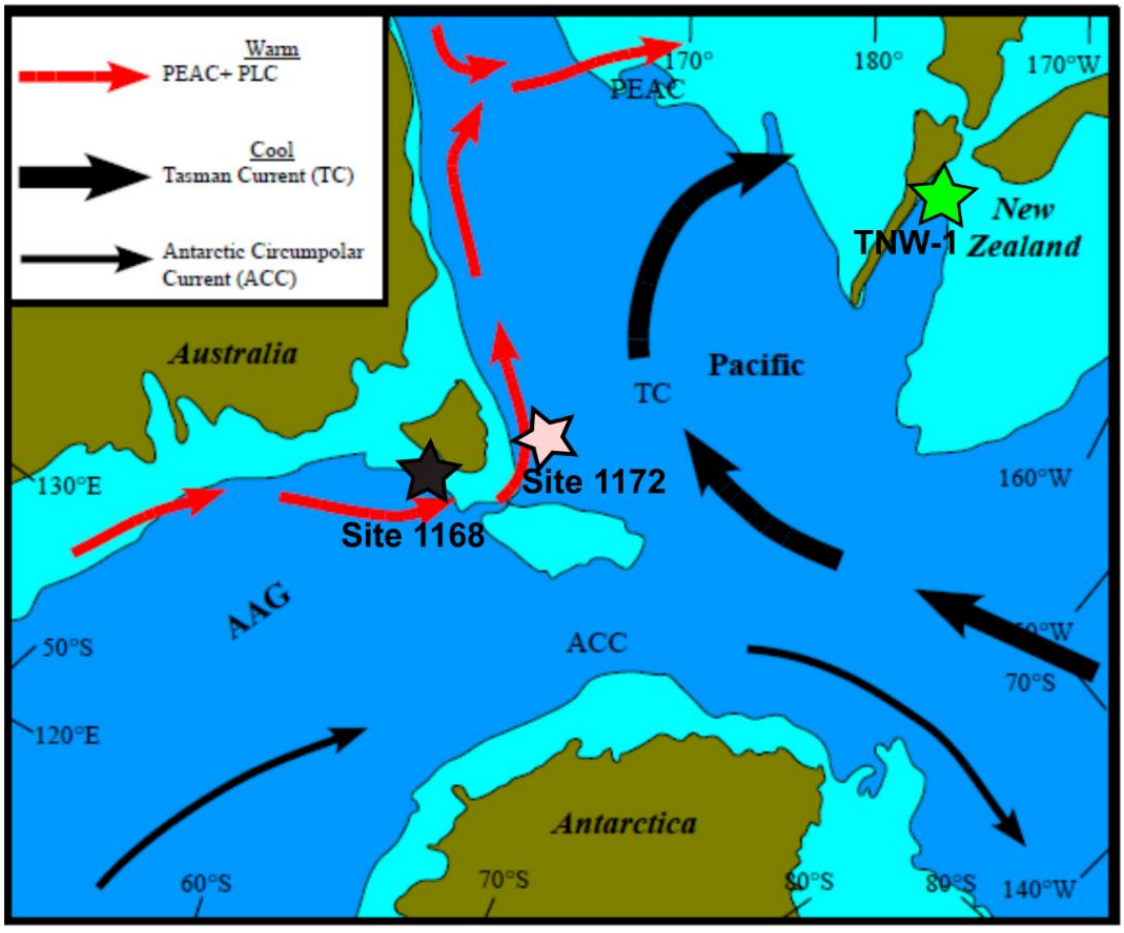

Figure 5.3: Surface water circulation around the Tasmanian Gateway region showing post gateway deepening (~30.2 Ma; early Oligocene). TNW-1 site is indicated by green five-pointed star, with Site 1172 and 1168 indicated by pink and black five-pointed stars, respectively. Surface oceanographic circulation modified after Stickley et al., 2004.

5.2 Materials and Methods

5.2.1 Geological setting of the Canterbury Basin, TNW-1 drillcore site, acquisition, and lithology

The Canterbury Basin is located along the eastern coast of Southland, New Zealand, with most part of this basin lying offshore (Mortimer et al., 2017). The lateral extent and boundaries of basin are defined by the Chatham Rise, Southern Alps, Bounty Trough and Great South Basin (Fig. 5.1; Barrier, 2019). The tectonic evolution of the Canterbury Basin started in the Cretaceous (145.5-65.5 Ma) during the eastern Gondwana continental breakup (Field & Browne, 1989), and contains strata up to a total thickness of about 8 km ranging in age from ~110 Ma to the present (Wood & Herzer, 1993; Laird & Bradshaw, 2004; Davy, 2014; Sahoo et al., 2014). The Cretaceous rift sequence was then followed by a post-breakup quiescence (~85-23 Ma), marking a period of widespread transgression of shoreline facies resulting in an almost complete inundation during the Oligocene (Field and Browne, 1989; Lever, 2007). By this time, Zealandia had drifted northwards to reach a latitude between 45-60°S from the Cretaceous to the Eocene. The northward drift of Zealand further resulted in a shift from a temperate climate regime in the Cretaceous to a sub-tropical climate during the Eocene (Pocknall, 1989; Kennedy, 2003; Vajda & Raine, 2003; Browne et al., 2008; Kennedy et al., 2014; Hollis et al., 2015, 2014). Overall deepening of the basin is associated with the progressive transgression of the facies from east to west (Field and Browne, 1989). However, increases in plate convergence rates, coupled with initiation of the Alpine Fault during the Oligocene and early Miocene led to tectonic uplift, erosion, and marine regression across New Zealand, including the Canterbury Basin (Mortimer & Campbell, 2014).

The study site (TNW-1 drillcore) is located in the Canterbury Basin on a farmland to the immediate east of Clelland's bridge and to the north of the Tengawai River. The TNW-1 well reached a total depth of 275.26 metres (Tinto, 2010). The entire core recovery was around 98%, with the first 62 metres of the core having a diameter of 85 mm and the remaining 210 metres having a diameter of 63.5 mm (Tinto, 2010). The 2% loss occurred at the bottom of the hole and drilling came to a halt when flowing sand that made drilling through it difficult was discovered. Based on preliminary data from

magnetostratigraphy (Tinto, 2010; Fig. 5.2) samples between ~93 to 272 m representing the middle Eocene to late Oligocene were used for this study.

In terms of lithology, the recovered sedimentary strata are divided into (1) Broken River Formation which is a mid-Eocene (late Porangan-Bortonian) coarse sandstone with many plant fragments and coal between 272 to ~215 metres; (2) Waihao Greensands described as a mid-Eocene (early to late Bortonian) sandstone (total thickness of ~40 m) with an increasing but variable amount of glauconite upsection, and occasional concretions of calcite; (3) Marshall Paraconformity (~183 m) defined by glaucony-filled burrows on the top 5 cm of the Waihao and formed in the early Oligocene (Whaingaroan) (4) Kokoamu Greensands thought to have been deposited in the early Oligocene and made up of bioturbated dark green coarse sand sized glauconitic formation; (5) Otekaike limestone is represented by a mottled, cream-coloured limestone with glaucony content decreasing upsection, deposited in the late Oligocene; (6) Bluecliffs Siltstone, deposited in the latest Oligocene to earliest Miocene and made up grey siltstone with some sand-sized glaucony either distributed or concentrated in patches (Figure 5.4; Tinto, 2010).

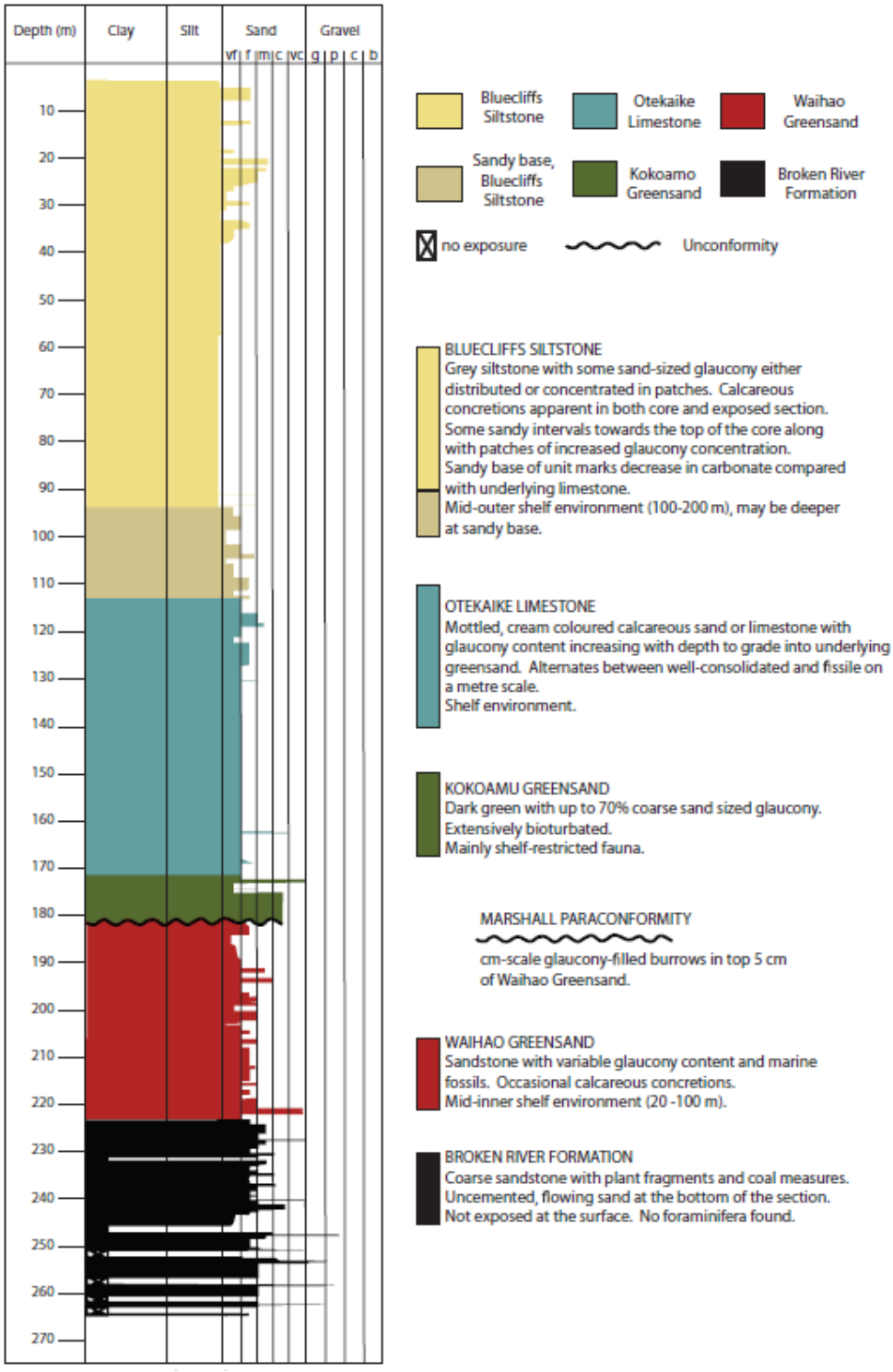

Figure 5.4 A lithostratigraphic log showing the various rock formations from the ~272 m drillcore. Marshall Paraconformity is located ~183 m. Figure is modified after Tinto (2010).

5.2.2 Palynomorph extraction and analysis

37 samples from TNW-1 well, Southland, New Zealand (~272-93 m) were investigated for their sporomorph content to reconstruct past flora and climate. Standard procedures at Northumbria University Palynology Laboratory were used to process these samples (Brinkhuis et al., 2003; Bijl et al., 2018; Riding, 2021). Crushing and weighing (~10 g) dried samples was followed by treatment with 20% cold hydrochloric acid (HCl) and 38% hydrofluoric acid (HF) to remove carbonate and silicate minerals. Palynological residue is sieved through 10 µm nylon mesh to eliminate organic/inorganic materials. The remnants were mounted with glycerine gel and sealed with nail polish.

Under 400x and 1000x magnifications, Leica DM 500 and DM 2000 LED transmitted light microscopes were used to count two slides per sample. An attempt was made to count between 200-250 fossil spores and pollen specimens (excluding reworking) for each sample. The slide was then searched for rare taxa, with slides/samples containing less than 75 grains discarded and not used for further analysis. Except for 12 samples (with < 75 specimens), sporomorph preservation and counts were good. Reworked sporomorphs were identified and recorded based on the colour of their exine and occurrence beyond their known stratigraphic range. Calculated pollen percentages were plotted using Tilia version 2.6.1. (Fig. 5.3; Grimm, 1990). Palynological zones were delineated using CONISS (Grimm, 1987). Pocknall (1985), Pocknall (1991), Macphail & Cantrill (2006), Macphail (2007), Raine et al. (2011), Bowman et al. (2014), and Macphail & Hill (2018) were consulted for sporomorph identification, taxonomic classification, and botanical affinities.

PAST statistical programme (Hammer et al., 2001) was used to create diversity indices with samples containing ≥75 individual grains. Rarefaction approach removes sampling size disparities to estimate sporomorph species at a constant sample size (Birks & Line, 1992; Birks et al., 2016). The Shannon diversity index (H) is a measure of diversity that considers the number of individuals, the number of taxa, and the distribution of species present (Shannon, 1948). H ranges from 0 for vegetation communities with a single taxon to higher values for communities with evenly distributed taxa (Legendre and Legendre, 2012). Equitability (J), on the other hand, quantifies the abundance and

distribution of species within an assemblage. Low J values represent the dominance of a small number of species in a population (Hayek and Buzas, 2010). Following stratigraphically constrained analysis (CONISS; Grimm, 1987), pollen zones (PZ; Fig. 5.5) were identified in Tilia (version 2.6.1) utilising the chord distance square-root transformation (Cavalli-Sforza and Edwards, 1967). Refer to chapter 3.3 for climate reconstruction method.

5.3 Results

The analysed mid-Eocene (Porangan) to Oligocene (Whaingaroan) samples from the TNW-1 generally show good palynomorph recovery, especially pollen and spores with minor amounts of dinoflagellate cysts. A total of 66 pollen and spore taxa were identified across the studied interval. The relative abundance and distribution of these miospores are shown in the pollen diagram (Fig. 5.3) and are grouped into angiosperms, gymnosperms, and cryptogams. The sporomorph record is dominated by *Myricipites harrisii* (4-63%) and *Cyathidites* spp. (5-51%). *Podocarpidites* spp., *Araucariacites australis, Nothofagidites* spp., *Polypodiisporites* spp., *Gleicheniidites senonicus, Laevigatosporites* spp., and *Dacrydiumites praecupressinoides* form common elements of the mid-Eocene to Oligocene TNW-1 sporomorph record.

Average diversity for the entire section based on results from rarefaction is 17 ± 3.8 taxa/sample at 75 individuals. Based on results from CONISS analysis, the section is grouped into four main pollen zones (PZ; Fig.5.3); PZ 1 (Porangan; 272.27-257.43 m), PZ 2 (PZ 2a and PZ 2b; early Bortonian to ?Kaiatan; 251.93-186.37 m); PZ 3 (earliest Whaingaroan; 183.40-147.37 m); PZ 4 (Whaingaroan; 138.75-93.49 m). Age assignment is discussed in section 5.4 below. Dinoflagellate cysts formed minor components of the palynomorph assemblage and are shown in Fig. 5.6. This is based on their utility as important palynomorphs for biostratigraphic purposes.

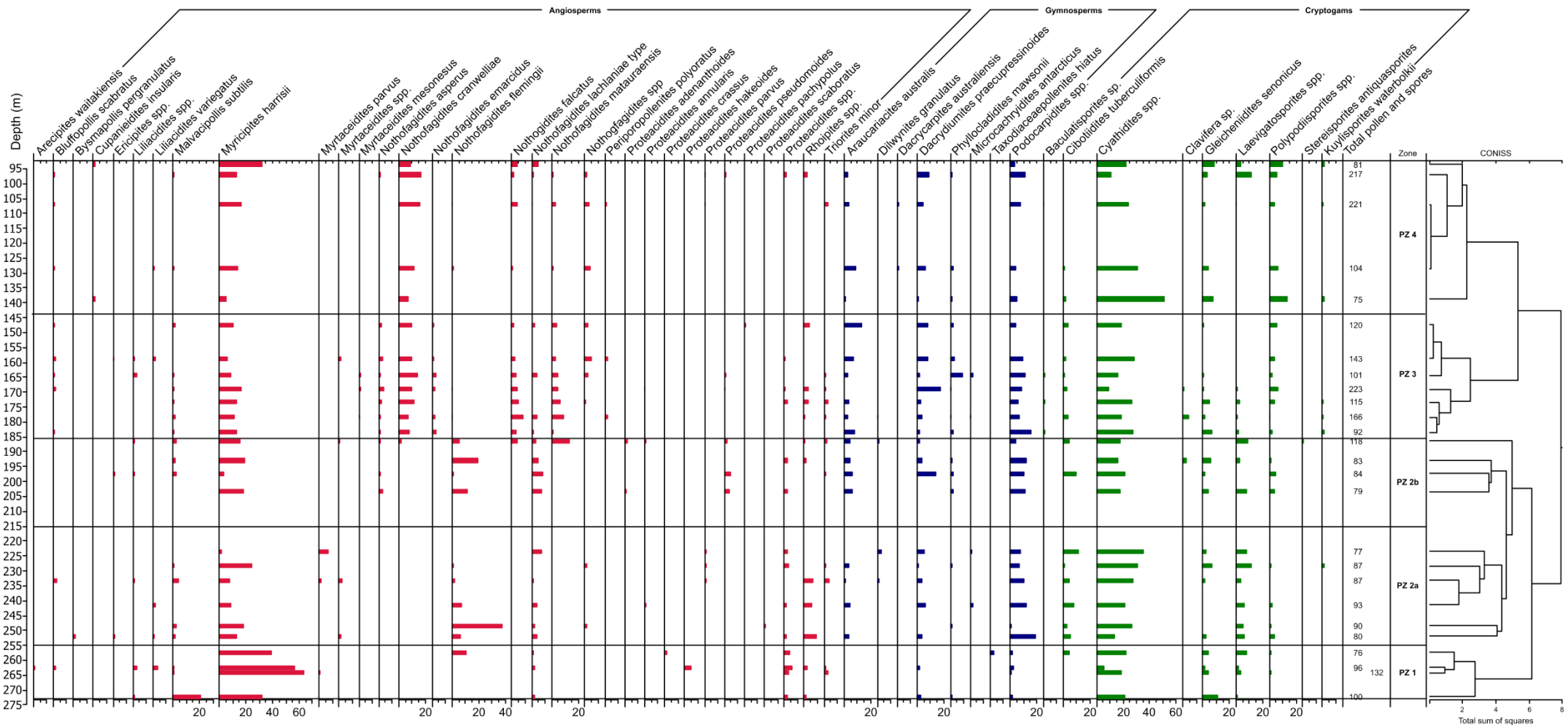

Figure 5.5 Sporomorph assemblages and relative percentages abundances of major taxa (angiosperms, gymnosperms, cryptogams) recovered from the middle Eocene to Oligocene**.** The relative abundances of angiosperms, gymnosperms, and cryptogams are indicated by red, blue, and green bars, respectively. CONISS ordination divides the Eocene to Oligocene sporomorph assemblages into four discrete pollen zones (PZ 1–PZ 4) or vegetation and climatic stages. The TNW-1 core depths is reported in metres.

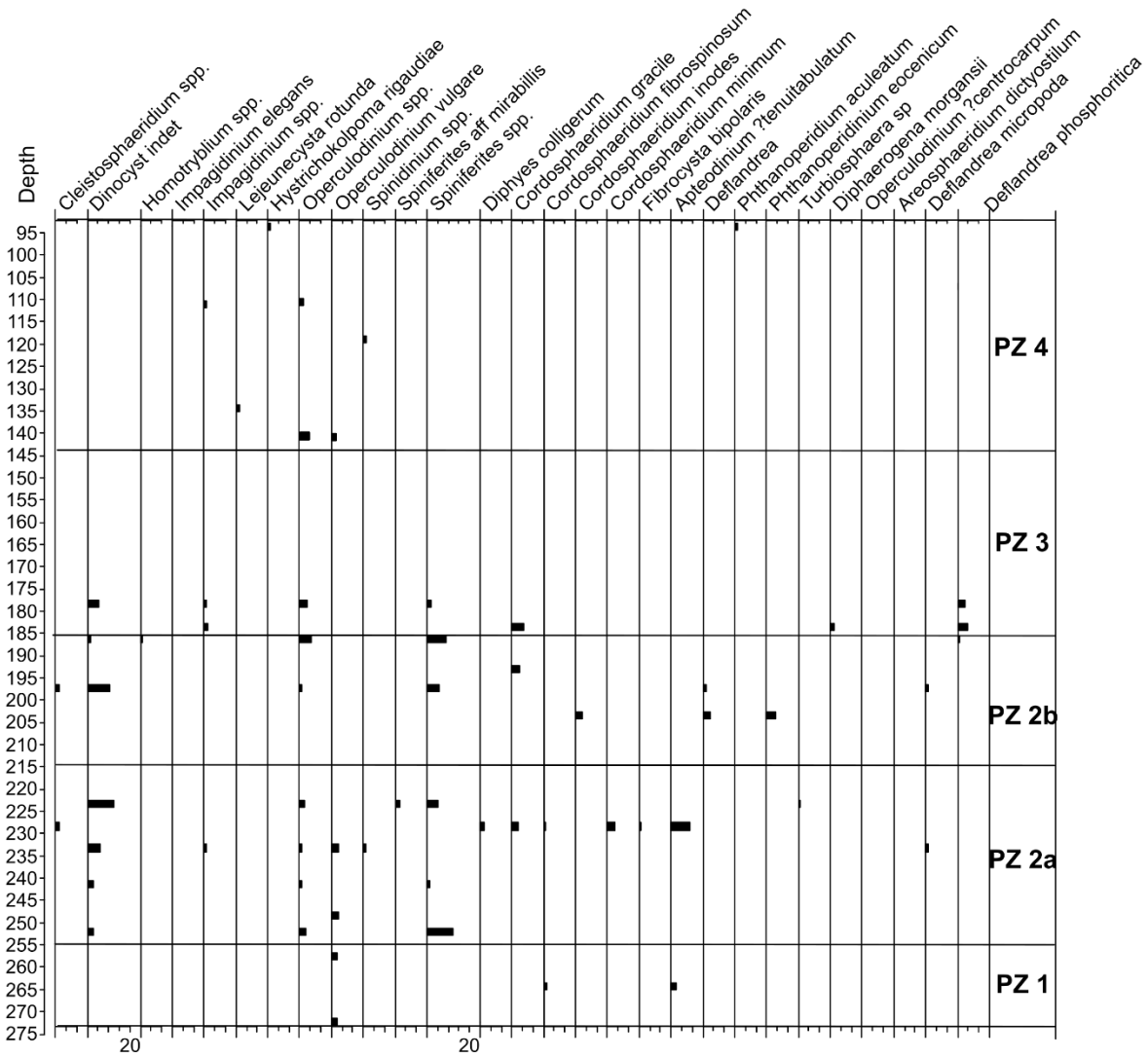

Figure 5.7. Dinoflagellate cysts relative abundance recovered from the middle Eocene to Oligocene. These dinocysts formed minor components of the sporomorph assemblage but do contain important stratigraphic markers discussed below. The TNW-1 core depths is reported in metres. PZ 1-4 are primarily based on sporomorphs.

5.3.1 Pollen Zone 1 (272.27-257.43 m; 4 samples)

Pollen Zone 1 (PZ 1) is characterised by a relative high abundance of *Myricipites harrisii* (Casuarinaceae/*Gymnostoma*; ~48%; Fig. 5.5) making them the dominant taxa in Other angiosperms (averagely accounting for ~65% of total sporomorphs). Other significant components of this group though they occur in minor amounts are *Proteacidites* spp. (Proteaceae), *Malvacipollis subtilis*, *Liliacidites* spp., *Bluffopollis scaboratus*, and *Arecipites waitakiensis* (Arecaceae). Cryptogams (~27%) form the second most abundant components of the sporomorph record in this PZ. These are represented in order of decreasing abundance by, *Cyathidites* spp. (Cyatheaceae), *Laevigatosporites* spp.

(Blechnaceae), *Gleicheniidites senonicus* (Gleicheniaceae), and *Cibotiidites tuberculiformis* (Schizaeaceae). *Nothofagidites* (*Nothofagus*) averagely accounts for ~ 1% of all non-reworked sporomorphs and are solely made up of the *fusca*-type *Nothofagus*. The *Lophozonia* (*menzii*-type) and *brassii*-type *Nothofagus* are conspicuously missing in this interval. Gymnosperms (~5%) generally show relative abundance and are represented in order of decreasing abundance by *Podocarpidites* spp. (*Podocarpus*), *Dacrydiumites praecupressinoides* (*Dacrydium*), *Phyllocladidites mawsonii* (*Lagarostrobos*), and *Trichotomosulcites subgranulatus* (extinct *Microcachrys*). Dinoflagellate cysts for this zone are represented by *Operculodinium vulgare*, *Cordosphaeridium fibrospinosum*, and *Apteodinium* ?*tenuitabulatum* (Fig. 5.6)

Quantitatively, PZ 1 is marked by relatively low number of sporomorph taxa diversity. The average number of sporomorph taxa based on rarefaction is 12.21 ± 3.42 (mean ± SD) species per sample at 75 individuals (Table 5.1). Shannon diversity (H) and equitability (J) on average are 1.67 ± 0.31 and 0.67 ± 0.08, respectively.

5.3.2 Pollen Zone 2 (252.93-186.37 m; 10 samples)

The relative abundance of *Nothofagidites* spp. increases substantially in this zone and on average, accounts for ~16% (Fig. 5.5) of all non-reworked sporomorph taxa. Within the *Nothofagus* group, the *fusca*-type *Nothofagus* still dominates, followed by the *brassii*-type and the *menzii*/*Lophozonia*-types. Other angiosperms (non-*Nothofagus*) are still dominated by *Myricipites harrisii* (Casuarinaceae/*Gymnostoma*), however, there is a marked decline in abundance from PZ 1 (~48%) to PZ 2 (13%). *Proteacidites* spp., *Myrtaceidites* spp., *Liliacidites* spp., *Bluffopollis scabratus*, *Rhoipites* spp., and *Ericipites* spp., occur sporadically across the interval. Cryptogams represent the most abundant sporomorph group and accounts for ~40% of all non-reworked miospores. This group shows an increase of ~12% from PZ 1. As in PZ 1, these cryptogams are dominated by *Cyathidites* spp. (Cyatheaceae). Other important elements of this group in order of decreasing abundance are, *Laevigatosporites* spp. (Blechnaceae), *Gleicheniidites senonicus* (Gleicheniaceae), *Polypodiisporites* spp. (Polypodiaceae), and *Clavifera* (Gleicheniaceae). Gymnosperms also see a substantial increase

relative abundance from 4% in PZ 1 to ~20% in PZ 2. These gymnosperms, in order of decreasing abundance, are represented by *Podocarpidites* spp. (*Podocarpus*), *Dacrydiumites praecupressinoides* (*Dacrydium*), *Araucariacites australis* (Araucariaceae), *Phyllocladidites mawsonii* (*Lagarostrobos*), and *Microcachryidites antarcticus* (*Microcachrys*).

Table 5.1. Summary of quantitative species diversity from the middle Eocene (Porangan) to Whaingaroan (Oligocene) of TNW-1 drillcore, Southland New Zealand.

Analysis	Pollen Zone 1		Pollen Zone 2		Pollen Zone 3		Pollen Zone 4	
	Mean	*(SD)*	*Mean*	*(SD)*	*Mean*	*(SD)*	*Mean*	*(SD)*
Rarefaction (75 individuals)	12.21	3.42	17.38	3.41	19.61	2.15	15.29	2.87
Shannon index (H)	1.67	0.31	2.36	0.30	2.55	0.14	2.17	0.29
Equitability (J)	0.67	0.08	0.83	0.06	0.85	0.02	0.79	0.07

Subzone 2a (251.93-223.44 m) is unique and can be distinguished from subzone 2b (203.3-186.37 m) by the presence of minor components such as *Myrtaceidites* spp., *Myrtaceidites parvus*, *Bluffopollis scrabratus*, *Bysmapollis pergranulatus*, and *Proteacidites parvus*, which are all absent in subzone 2b. *Nothofagus asperus*, *Nothofagidites falcatus*, *Proteacidites pseudomoides*, *Clavifera* sp., and *Proteacidites adenanthoides* first appear in subzone 2b. PZ 2 dinocysts are the most diverse and are represented by *Homotryblium* spp., *Impagidinium elegans*, *Impagidinium* spp., *Operculodinium* spp., *Operculodinium vulgare*, *Spinidinium* spp., *Spiniferites* spp., *Cordosphaeridium gracile*, *Cordosphaeridium fibrospinosum*, *Cordosphaeridium inodes*, *Cordosphaeridium minimum*, *Apteodinium* ?*tenuitabulatum*, *Phthanoperidium aculeatum*, *Deflandrea phosphoritica* and *Deflandrea micropoda* (Fig. 5.6)

Based on results from rarefaction, sporomorph species for this zone on average is 17.38 ± 3.41 species per sample at 75 individuals and higher than in PZ 1. Shannon diversity (H) and equitability (J) on average are 2.36 ± 0.30 and 0.83 ± 0.06 (Table 5.1), respectively.

5.3.3 Pollen Zone 3 (183.4-147.37 m; 7 samples)

PZ 3 shows a notable increase in *Nothofagus*, gymnosperms, and with a concomitant rise in sporomorph taxa diversity. Quantitatively, based on results from rarefaction analysis, the number of sporomorph taxa on average is 19.61 ± 2.15 species per sample at 75 individuals and are relatively higher than the first two PZs. Shannon diversity (H) and equitability (J) are on average 2.55 ± 0.14 and 0.85 ±0.02 (Table 1), respectively.

The palynoflora record of PZ 3 show a significant increase in *Nothofagidites* spp. from ~16% in PZ 2 to ~25%. This zone also sees a switch in the abundance of *Nothofagus* groups. The *brassii*-type *Nothofagus represented* by *N. matauraensis*, *N. cranwelliae*, *N. emarcidus*, and *N. falcatus* dominates and accounts for ~20% of all non-reworked sporomorphs. This is then followed the menzii- and *fusca*-types, respectively. Other angiosperms (non-*Nothofagus*) accounts for ~19% of all non-reworked sporomorphs and are still dominated by *Myricipites harrisii* (*Gymnostoma*), however, they show a slight decline in relative abundance from ~13% in PZ 2 to ~11% in PZ 3. Additional non-*Nothofagus* angiosperms form minor components of this group. These are represented, in order of decreasing abundance by, *Rhoipites* spp., *Malvacipollis subtilis*, *Liliacidites* spp., *Bluffopollis scabratus*, *Ericipites* spp., *Myrtaceidites* spp., *Myrtaceidites verrucosus*, *Myrtaceidites mesonesus*, *Proteacidites* spp., *Proteacidites pseudomoides*, and *Proteacidites pachypolus*. Gymnosperms, in this zone show some increase in relative abundance from ~20% in PZ 2 to ~24% in PZ 3. *Podocarpidites* spp. and *Dacrydiumites praecupressinoides* together co-dominates and accounts for 8% and 7%, respectively of all non-reworked sporomorphs. These are the followed by common occurrence of *Araucariaceae australis* (~5%) and *Phyllocladidites mawsonii*. Minor components of the gymnosperm group include *Microcachryidites antarcticus* and *Dilwynites granulatus*. Cryptogams on the other hand remains the dominant sporomorph group although they see a slight decline in comparison to PZ 2, and accounts for ~31% of all non-reworked sporomorphs. These are dominated by *Cyathidites* spp. (Cyatheaceae), with *Polypodiisporites* spp. (Polypodiaceae), *Laevigatosporites* spp. (Blechnaceae), *Gleicheniidites senonicus* (Gleicheniaceae), *Cibotiidites tuberculiformis* (Schizaeaceae), *Baculatisporites* sp. (Hymenophyllaceae), and *Clavifera* sp. (Gleicheniaceae) appearing as common to minor elements

within this group. PZ 3 dinoflagellate cyst taxa are represented by *Impagidinium* spp., *Operculodinium* spp., *Operculodinium vulgare*, *Spiniferites* spp., *Cordosphaeridium gracile* and *Deflandrea phosphoritica*.

5.3.4 Pollen zone 4 (138.75-93.49 m; 5 samples)

Nothofagidites spp. decline from ~25% in PZ 3 to ~19%. The dominance of the *brassii*-type *Nothofagus* continues and are represented by *N. cranwelliae*, *N. falcatus*, and *N. matauraensis* (Fig. 5.3). This is then followed by minor components of *fusca*- and *menzii*-types *Nothofagus*. *Myricipites harrisii* (*Gymnostoma*/Casuarinaceae) make up the dominant group of non-*Nothofagus* angiosperms and accounts for ~16% of all non-reworked sporomorphs. Other components of this group, though minor include *Bluffopollis scabratus* (Strasburgeriaceae), *Cupanieidites insularis* (Sapindaceae), *Ericipites longisulcatus* (Ericaceae), *Liliacidites variegatus* (Liliaceae), *Proteacidites* spp. (Proteaceae), and *Proteacidites pseudomoides* (*Carnarvonia*). Gymnosperms also see a substantial decline in relative abundance from a high of ~24% in PZ 3 to ~16% in PZ 4. These gymnosperms are represented by taxa (in order of decreasing abundance) such as *Podocarpidites* spp. (*Podocarpus*), *Dacrydiumites praecupressinoides* (*Dacrydium*), *Araucariacites australis* (Araucariaceae), *Phyllocladidites mawsonii* (*Lagarostrobos*), and *Dacrycarpites australiensis* (Podocarpaceae). Cryptogams see an increase in relative abundance in comparison to PZ 3 and account for ~45% of all non- reworked miospores. These are represented mainly by *Cyathidites* spp. (Cyatheaceae), *Polypodiisporites* spp. (Polypodiaceae), *Gleicheniidites senonicus* (Gleicheniaceae), and *Laevigatosporites* spp. (Blechnaceae). By PZ 4 there is a marked decline in dinoflagellate cysts, and these are represented by *Impagidinium* spp., *Lejeunecysta rotunda*, *Operculodinium* spp., *Hystrichokolpoma rigaudiae*, *Spiniferites* spp., and *Operculodinium vulgare*.

Based on results from rarefaction, sporomorph species for this zone on average is 15.29 ± 2.87 species per samples at 75 individuals. Shannon diversity (H) and equitability (J) on average are 2.17 ± 0.0.29 and 0.79 ± 0.07 (Table 5.1), respectively.

5.4. Discussion

5.4.1 Biostratigraphy

The preliminary magnetostratigraphy-based age-model for the Oligocene (after the formation of the Marshall Paraconformity; Fig. 5.2; Tinto, 2010) could be established with a higher degree of confidence for the TNW-1 drillcore. However, this model is poorly resolved in the interval before the formation of the unconformity (i.e., prior to the Oligocene). Using the miospore and dinocyst biozonation after (Cooper, 2004) in Fig. 5.7, along with updated ages after (Raine et al., 2015), this study provides a new age determination for the TNW-1 drillcore. Identification and description of abundant biozones that are determined by the acme events of miospores allows for the ages to be more precisely calibrated. The first appearance (FA), the last occurrence (LO), the common occurrence (CO), and the first common occurrence (FCO) of taxa are coupled with these (abundant and assemblage zones). The palynological results from the TNW-1 Well, Southland, New Zealand, reveal the existence of two primary assemblage zones (i.e., *Myricipites harrisii* and *Nothofagidites matauraensis* assemblage zones; Fig.5.8; 5.9).

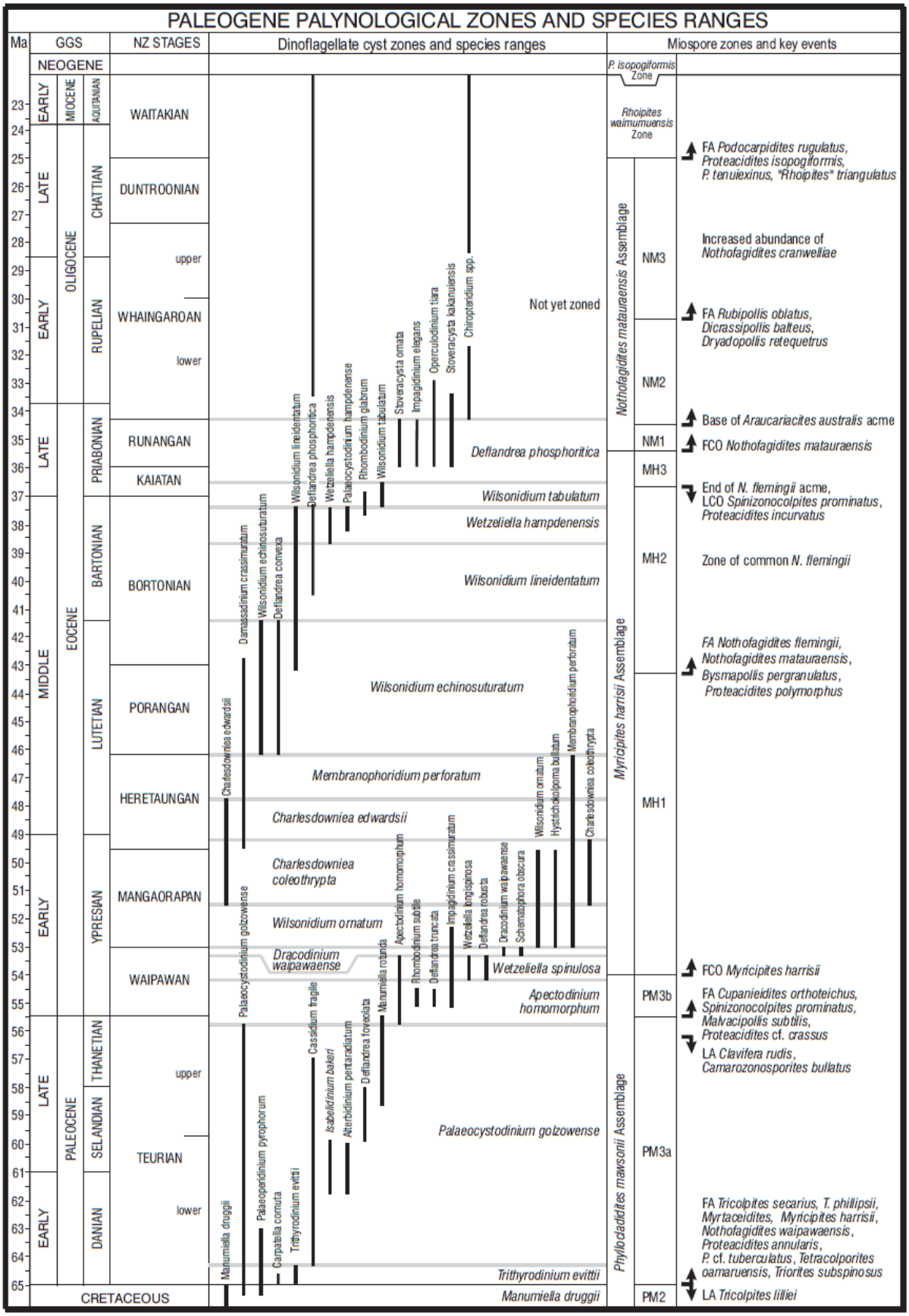

Figure 5.7. Miospores and dinoflagellate cyst zonation and stratigraphic ranges in the Palaeogene of New Zealand after Cooper (2004).

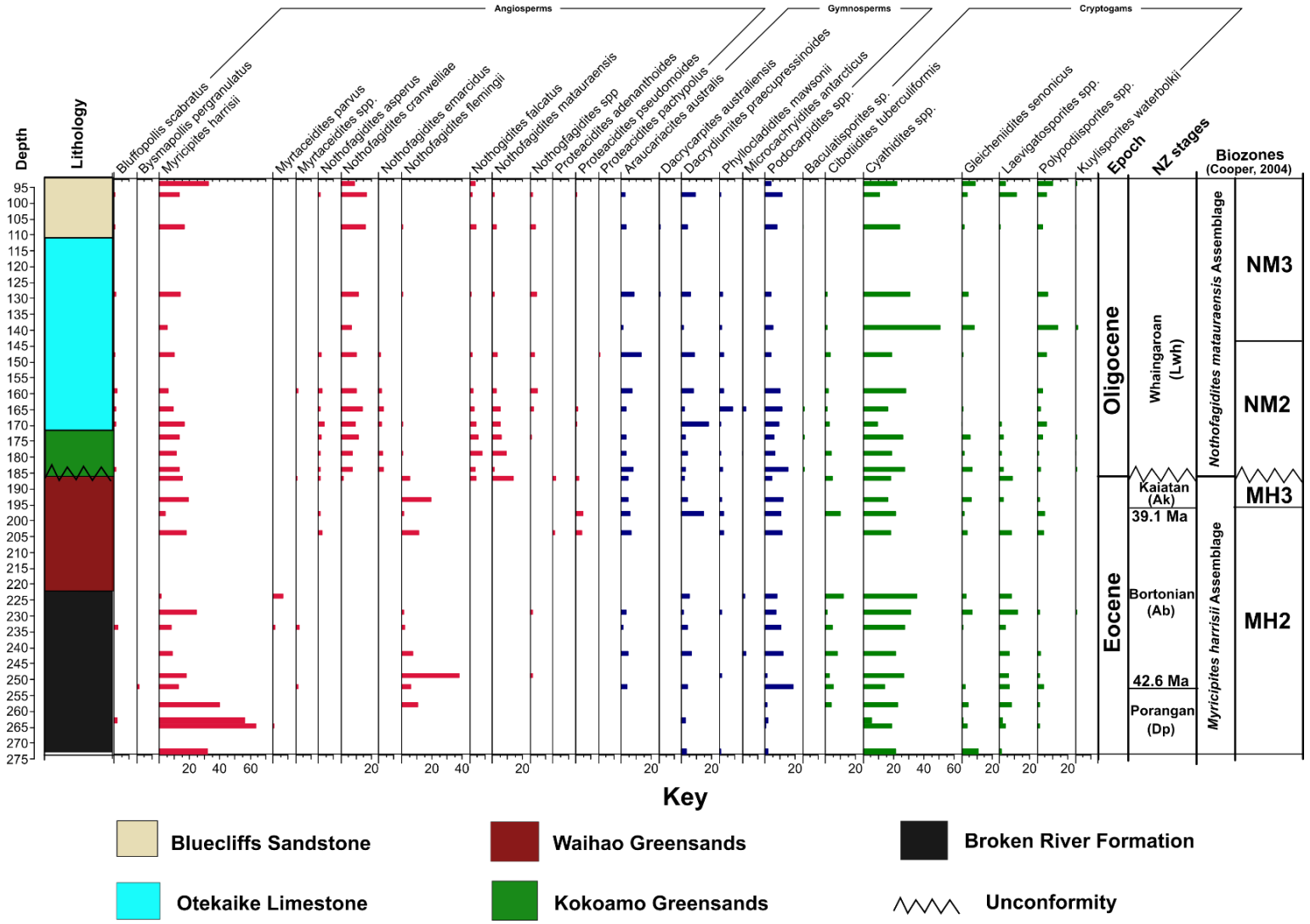

Figure 5.8. Sporomorph assemblages and relative abundance of important taxa and groups (angiosperms, gymnosperms, and cryptogams) combined with middle Eocene-Oligocene biozonation of New Zealand. The relative abundances of angiosperms, gymnosperms, and cryptogams are indicated by red, blue, and green bars, respectively. The TNW-1 core depths is reported in metres.

5.4.1.1 *Myricipites harrisii* Assemblage Zone (Porangan-Kaiatan; Mid-Eocene to Late Eocene)

Two subzones (Raine, 1984; Cooper., 2004) are identified: MH 2 and MH 3 (Fig. 5.8; 5.9). The lower part of the section (~272-~252 m) is correlated with the middle Eocene (late Porangan) MH 2 Zone, based on the FA of taxa such as *Nothofagidites flemingii* and *Bysmapollis pergranulatus*. The assigned age is further supported by the dominance of *Myricipites harrisii* (~50% of the total palynomorph assemblage). Additional support is given by previous studies which assign a Porangan to Bortonian age to the marginal marine Broken River Formation (Pocknall, 1984, Browne and Field, 1986; Cooper et al., 2001; Cooper, 2004) dominated by *Myricipites harrisii*.

The start of the Bortonian (middle Eocene) is marked by a sharp decline in *Myricipites harrisii*, though they remain common (Fig. 5.8; Fig. 5.9). The Bortonian (~252-195 m) is further characterised by the first common occurrence of *N. flemingii*. This is comparable to the Bortonian end member of MH2 subzone in the Taranaki Basin and South Canterbury Basin of Southland, New Zealand (Cooper, 2004). The age assignment for this interval (~252-195 m) is further supported by the MH2 subzone of common *N. flemingii* (Cooper, 2004; Fig. 5.7).

The Kaiatan (195-183 m) is characterised by the end of the *N. flemingii* acme event (Fig. 5.7; 5.8) and correlated with the MH3 subzone of Cooper (2004). The Runangan in the TNW-1 section cannot be clearly delineated due to periods of non-deposition/erosion which places the Kaiatan in direct contact with the Whaingaroan. This is further complicated by the Marshall Paraconformity reported to have formed in the Oligocene (Fulthorpe et al., 1996) and is located at ~183 m (Fig. 5.8; Fig. 5.9) of the TNW-1 section.

The Runangan, according to Cooper (2004) is marked by the FCO of *N. matauraensis* and base of *Araucariacites australis* acme events which cannot be identified in this section. The interval between 186-170 m, apart from containing the ~5 cm burrows (reported to be the Marshall Paraconformity; Tinto, 2010; Fig. 5.4) on top of the Waihao Greensands, also sees the CO of *N. cranwelliae* and FA of *N. falcatus*. These events most likely suggest the deposition of Oligocene (Whaingaroan) sediments

based on the assertion that *N. falcatus* does not appear until the Oligocene (Whaingaroan) of New Zealand (Pocknall, 1989).

Based on dinoflagellate cyst biostratigraphy, *Impagidinium elegans* Zone (Clowes, 2009) marks the FA of *Impagidinium elegans* (~217 m) and correlated with the middle Eocene Hampden Beach section (early Bortonian-late Bortonian; Fig. 5.9; Fig.5.10). Characteristic associated taxa include *Cordosphaeridium* spp., *C. fibrospinosum*, *C. gracile* and *C. inodes*. The FA of *Deflandrea* sp. and presence of *Phthanoperidium eocenicum* between 206 m and 196 m marks the end of the Bortonian (Clowes, 2009).

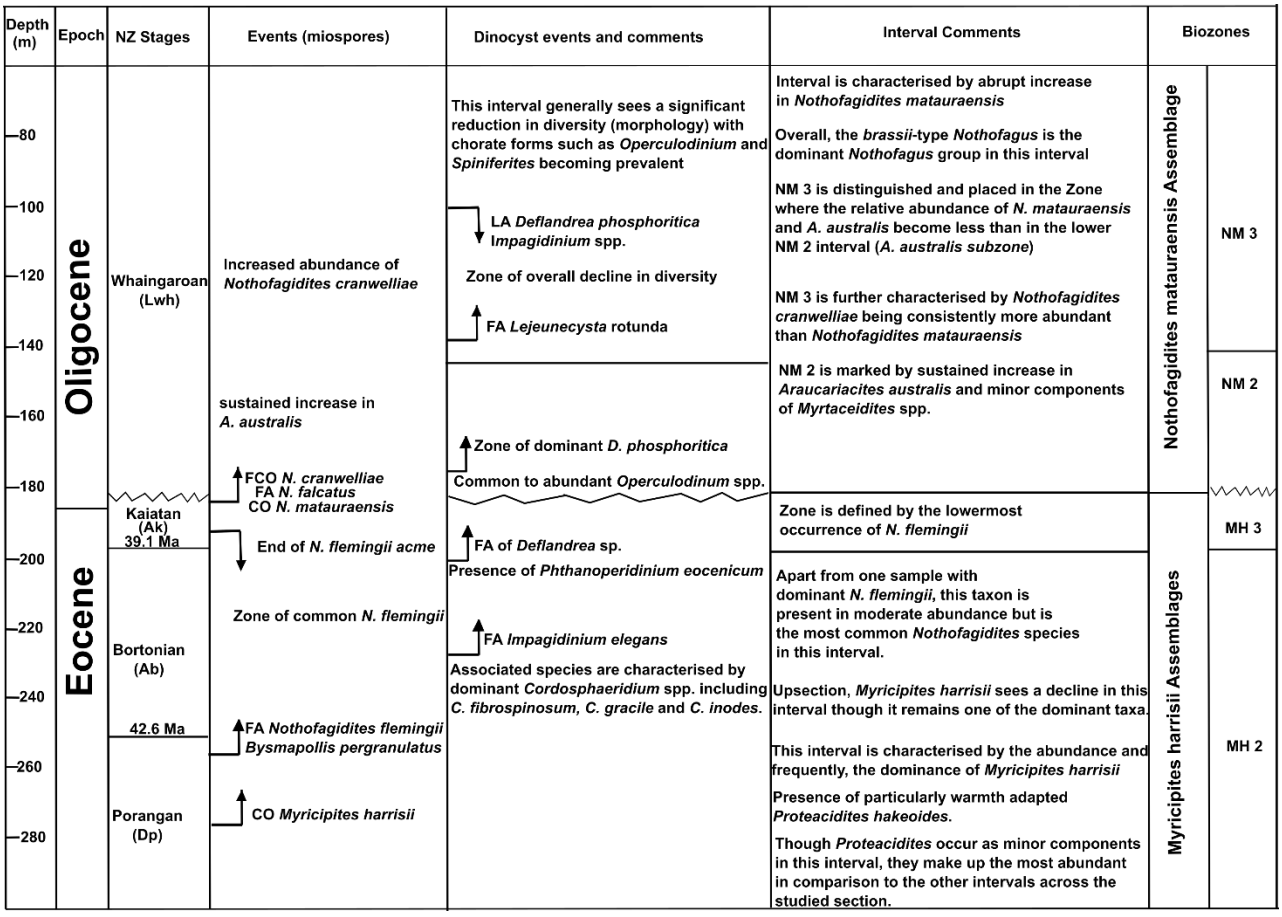

Figure 5.9: Miospores and dinoflagellate biozones of the Porangan to Whaingaroan of TNW-1, Southland, New Zealand. Wiggle line ~183 m (base of the Whaingaroan) represents the Marshall Paraconformity. New Zealand biozonation is based on Cooper (2004)

5.4.1.2 *Nothofagidites mataurаensis* Assemblage (Whaingaroan; Latest Eocene to Oligocene)

The base of this zone, as reported by Cooper (2004) is defined by the first common occurrence (FCO) of *Nothofagidites mataurаensis* of the mid-Runangan (late Eocene). The *Nothofagus mataurаensis* Assemblage Zone was originally described from strata off the west Coast to Taranaki Basin region by Raine (1984), where it is restricted to the late Eocene to Oligocene. The *N. mataurаensis* Assemblage zone (after Cooper, 2004; Fig. 5.7) is divided into three subunits which are NM 1, NM 2, and NM 3, respectively. However, the common occurrence of *N. cranwelliae* and FA of *N. mataurаensis* coupled with the hiatus associated with the Marshall Paraconformity suggest deposition in the Whaingaroan, and the Runangan in this section (TNW-1; Fig. 5.8; Fig. 5.9) is missing. There is likelihood that the FCO of *N. mataurаensis* may have been earlier and has subsequently been eroded. Hence, the NM 1 subzone (corresponding to the Runangan; latest Eocene), as described by Cooper (2004) cannot be found in TNW-1. This assemblage zone from TNW-1 drillcore/section spans ~186-93 m.

NM zone of TNW-1 is further characterised by a reduced frequency of *M. harrisii*, coinciding with the first common occurrence of *N. mataurаensis* at ~ 186 m. This occurs in association with other *brassii*-type *Nothofagus* such as *Nothofagidites falcatus*, *Nothofagidites emarcidus*, and *Nothofagidites cranwelliae*. *N. falcatus* did not appear until the Oligocene (Pocknall, 1989). Hence, their appearance, coupled with common occurrence of *N. cranwelliae* means the assemblage belongs to NM2 subzone (Fig. 5.8; Fig. 5.9), whereas NM1 is missing. Lower *N. mataurаensis* Zone of Pocknall and Mildenhall (1984) and Pocknall (1991) is the interval where *N. mataurаensis* exceeds *M. harrisii* (*Haloragacidites harrisii*) in abundance. Though *Myricipites harrisii* may have declined substantially, they are relatively more abundant than *N. mataurаensis* in the TNW-1 section, lending further support for the absence of the NM1 subzone corresponding to the Runangan. *N. cranwelliae*, however, becomes the dominant *Nothofagus* group, together with common *Araucariacites australis* and minor components of *Myrtaceidites* spp. in this zone leading to the assignment of this subzone to NM2 (spanning the early Oligocene; Fig. 5.8 and 5.9). Pocknall (1991) however describes this subzone (NM2) as the *Araucariacites australis* subzone defined by marked/sustained increase in *A. australis* whose base lies

within the upper Waikato Coal Measures spanning the upper Runangan (latest Eocene) into the Whaingaroan stage (early Oligocene).

By NM3 (~145 m), *N. cranwelliae* has overtaken *N. mataurаensis* in relative abundance in TNW-1 (Fig. 5.9 and Fig. 5.10) . In the Waikato Coal Measures, the base of this zone is placed at the level where *A. australis* and *N. mataurаensis* relative abundance become less abundant than the underlying Zone NM2 (Pocknall, 1991). The arbitrary positioning of the base of this zone places considerable limitation on the correlative potential of the NM3 subzone, hence the lowest occurrence of *Rubipollis oblatus* is used to define the base of this Zone in the North Island Waikato Coal Measures (Raine, 1984; Pocknall, 1991; Cooper, 2004). However, this taxon (*Rubipollis oblatus*) is not recovered from the TNW-1 samples of Southland, New Zealand. Pocknall and Mildenhall (1984) in their study of the Southland lignite sequences reported a marked increase in *N. cranwelliae* towards the top of the Upper *N. mataurаensis* zone. The marked increased in *N. cranwelliae* (from 140m to ~100m) toward the top is clearly identified in the top NM3 (early to late Oligocene) subzone of the TNW-1 section (Fig. 5.8; Fig. 5.9; 5.11).

This interval also sees the first and only occurrence of *Lejeunecysta rotunda* (Fig. 5.10), with a general overall reduction in dinoflagellate cyst diversity. This subzone is further characterised by the LA of *Deflandrea phosphoritica* and *Impagidinium* spp. In a regional Oligocene-Miocene dinoflagellate cyst calibration from offshore Wilkes land, East Antarctica, *Lejeunecysta rotunda* is assigned to early Oligocene (preferably between the top of C12n and top of C11n.1n; 30-29.5 Ma; (Bijl et al., 2018).

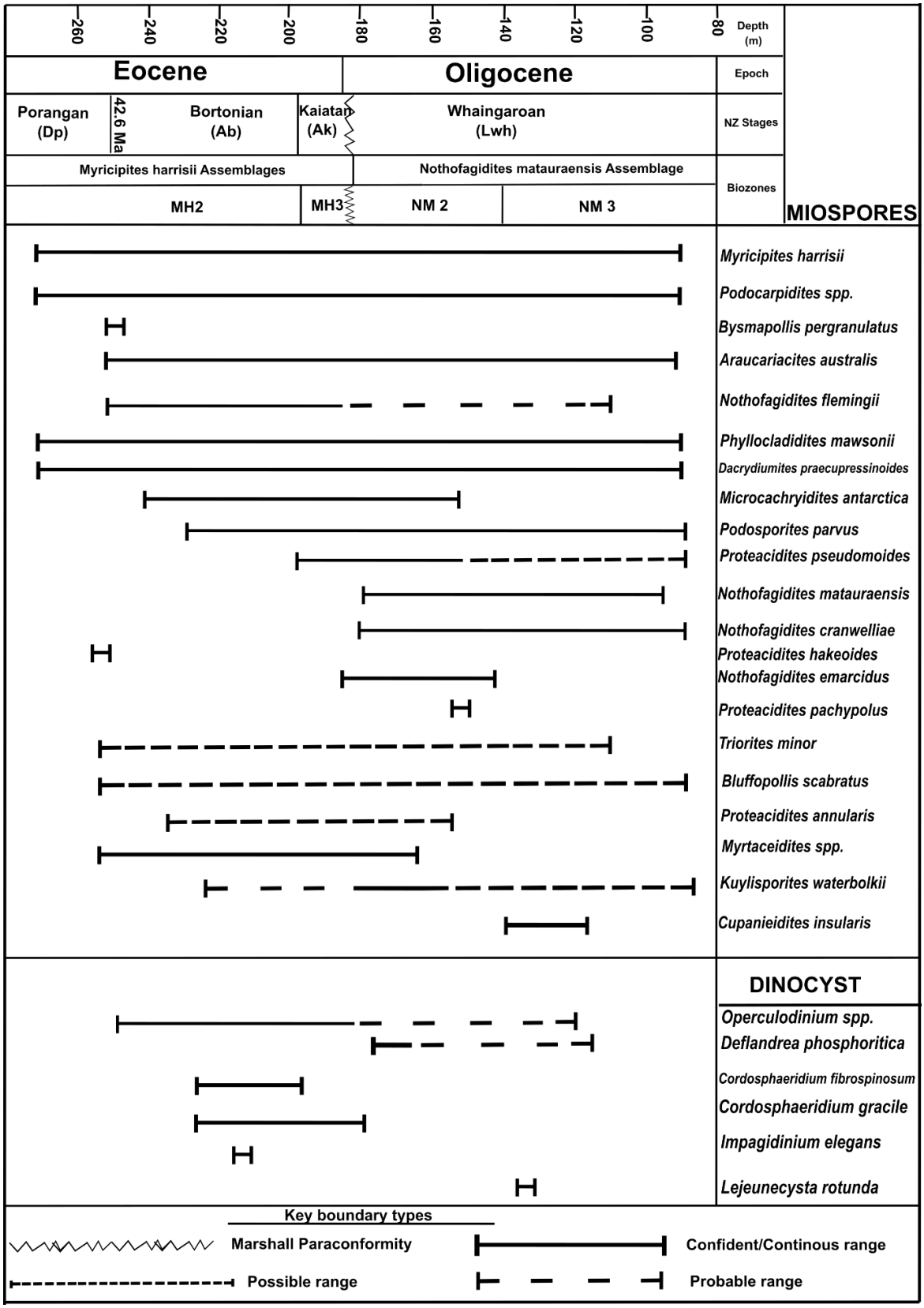

Figure 5.10. Stratigraphic range chart of selected sporomorph and dinoflagellate cyst taxa recovered from the TNW-1 well in the Canterbury Basin, Southland, New Zealand. The palynozonations are after Cooper (2004). TNW core depths are reported in metres and Marshall Paraconformity is indicated by the wiggle at ~183 m.

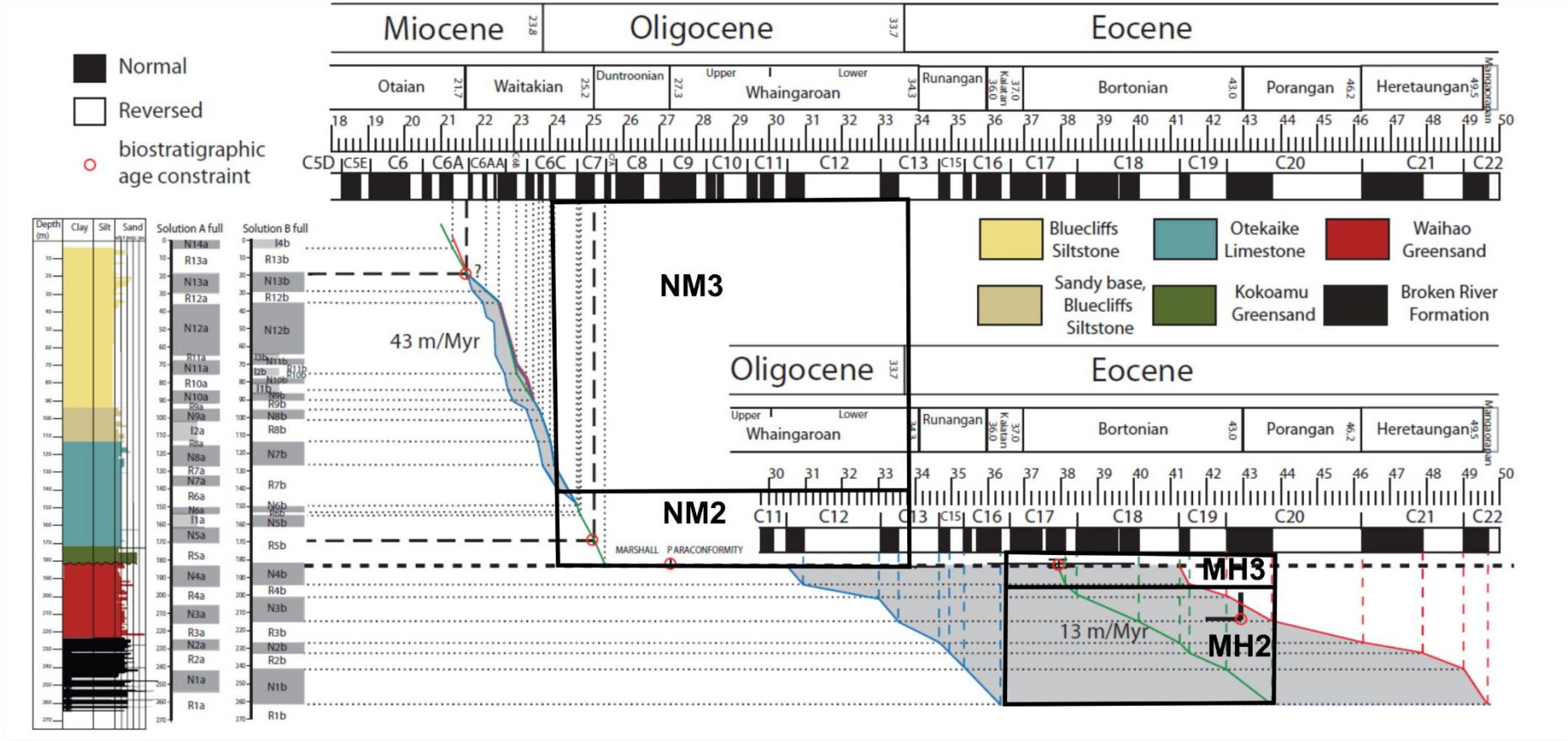

Figure 5.11 Miospore zonation in the TNW-1 section laid over the foram-constrained palaeomagnetostratigraphy data after Tinto (2010). The palynozonations are after Cooper (2004). MH2 and MH3 represent *Myricipites harrisii* Assemblage Zones 2 and 3, respectively. NM2 and NM3 represent *Nothofagidites mataurаensis* Assemblage Zones 2 and 3, respectively.

5.4.2 Before the development of the Marshall Paraconformity:- Middle Eocene (Porangan-Bortonian) to late Eocene (?Kaiatan) climate and vegetation

Abundant Casuarinaceae (*Myricipites harrisii*), along with frequent Proteaceae, Liliaceae, and minor elements of *Nothofagidites lachlaniae*, indicate coastal/lowland shrubs with small trees and minor components of hinterland rainforest during the Porangan (middle Eocene; 272.27-257.43 m; Fig. 5.5). The vegetation indicate past MATs between 14.9 and 16.75 °C, with an average of 15.5 °C, and MAPs of 1062-2460 mm/yr (Fig.5.12). Except for the absence of Araucariaceae and Sapindaceae, this vegetation association is comparable to late Porangan-Bortonian dated strata of the Broken River Formation (deposited in a marginal maritime environment) in South Canterbury (Pocknall, 1984; Pocknall, 1989). The hinterland taxa (i.e., *Podocarpus*, *Dacrydium*, *Nothofagus*) formed the rainforest elements, and are deemed to thrive at considerable distance from the shore and/or in terrain that are presumably elevated above the coastal plain. A previous study suggests that the hinterland vegetation is a relict of the late Cretaceous and Paleocene, when gymnosperm rainforest dominated New Zealand's forests (Pocknall, 1990). Additionally, the reduced abundances of *Nothofagus* in this interval is interpreted as the early establishment of the *brassii*, *Lophozonia*/menzii, and fusca-type *Nothofagus* groups in the hinterland association. Early to middle Eocene palynoflora record from Southland, New Zealand indicate that the coastal lowland vegetation primarily consisted of sclerophyll shrubland association dominated by Casuarinaceae with common Proteaceae (Pocknall, 1989), lending further support to the interpretation of this interval of the TNW-1 section.

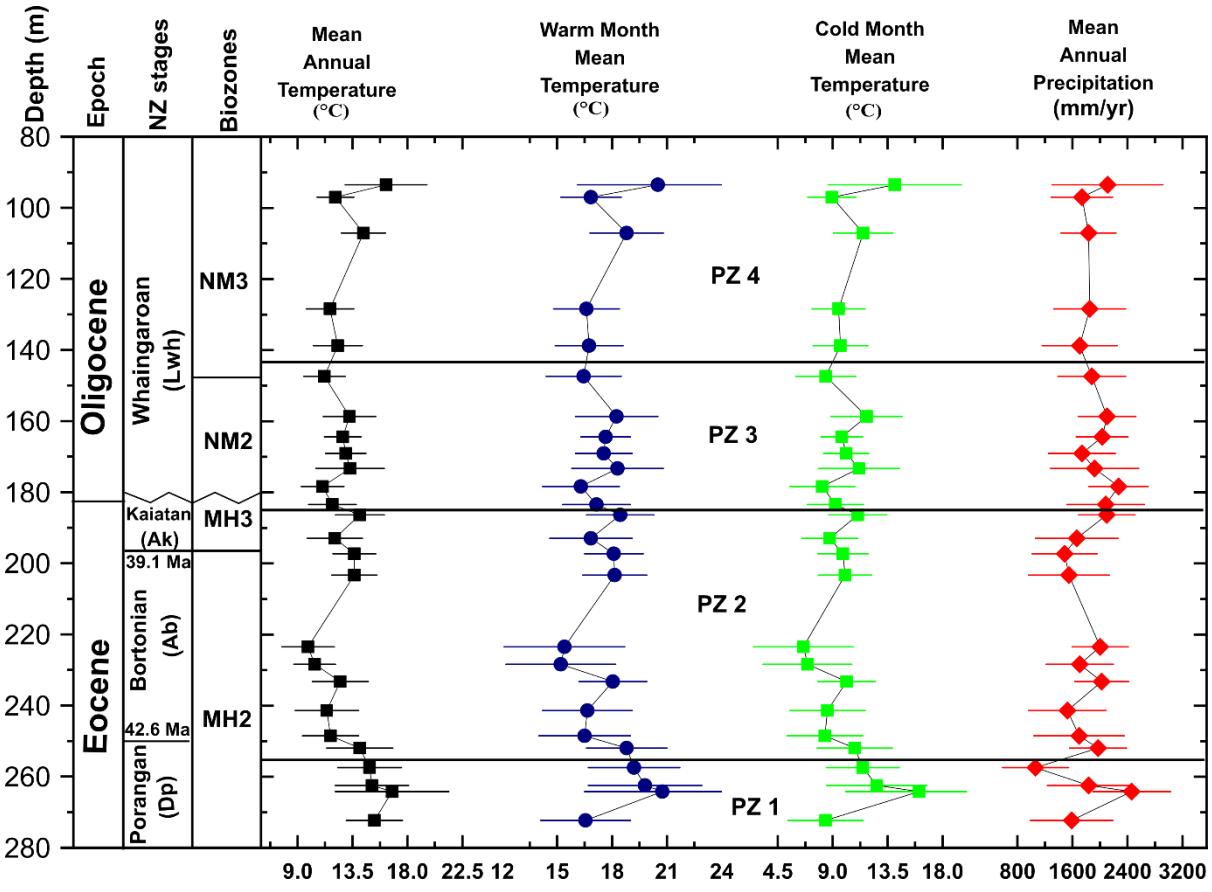

Figure 5.12 Sporomorph-based climate estimates using the probability density function (PDF) approach. From left to right: mean annual temperature (MAT), warm mean month temperature (WMMT), cold mean month temperature (CMMT), and mean annual precipitation (MAP). The quantitative temperature estimates are reported in °C, and MAP in mm/yr. The wiggle line separating the Kaiatan and Whaingaroan represents the Marshall Paraconformity.

The rise of cryptogams such as Cyatheaceae, Gleicheniaceae, and Blechnaceae from the middle to late Eocene (Bortonian to ?Kaiatan; ~257-~183 m; Fig. 5.5) most likely indicate the expansion of local wetland or marsh environment. However, abundance of Casuarinaceae, and occurrence of diverse Proteaceae point to the persistence of lowland coastal vegetation throughout the Bortonian of Southland, New Zealand. Increasing *Podocarpus* and *Nothofagus fusca*-type indicate an expansion of the hinterland rainforest vegetation. The emergence of new *Nothofagus*, cryptogams, and non-*Nothofagus* angiosperm (Fig. 5.5) taxa during transition translates into the increase in diversity (Table 5.1). Sporomorph-based MATs show a decline from 14.1 to 9.9 °C between ~251 to 223 m and a rebound to 14.1 °C by ~186 m in the late Eocene (Fig. 5.12). The presence of warmth-loving taxa such as Myrtaceae, *Strasburgeria robusta*, Epacridaceae in the bottom half of this interval (Fig. 5.7) and their

absence in the top section of this subzone may have accounted for the drop in MATs across this zone. The rebound, on the other hand, is aided by the presence of warmer taxa such *Carnarvonia* (NLR of *Proteacidites pseudomoides*). The palynoflora record within the top section of this interval (latest Bortonian to Kaiatan) resembles to the late Kaiatan vegetation recovered from the shallow marine Iron Creek Greensands in Canterbury (Pocknall, 1989).

5.4.3 After the development of the Marshall Paraconformity: - Early to late Oligocene (Whaingaroan) vegetation and climate

By the early Whaingaroan (PZ 3), *Nothofagus brassii*-type (*N. matauraensis*, *N. cranwelliae*, and *N. falcatus*) becomes the dominant *Nothofagus* group, with increases in Araucariaceae, *Dacrydium*, *Lagarostrobos*, and *Podocarpus*. These together constitute the hinterland vegetation association, and their dominance (especially the *Nothofagus*) in early Oligocene (Whaingaroan; 183.4-147.4 m) gives an indication of a forest or vegetation community thriving at some considerable distance from the coast, in Southland, New Zealand under MATs between 11.2 to 13.3 °C and MAPs between 1738-2270 mm/yr (Fig. 5.12). The marine transgression coupled with extensive peneplanation that started in the Cretaceous culminated in the Oligocene (McGlone et al., 1996). The landmass of New Zealand at this time was submerged and had been reduced to an archipelago with low lying, leached/infertile landscape, and everywhere close to the coast/shoreline (McGlone et al., 1996). Increases in cryptogams providing evidence for wetlands/boggy or marshy grounds, coupled with the dominance of rainforest taxa, suggest increased precipitation of 1738-2270 mm MAP (Fig. 5.12). This interval however captures the Marshall Paraconformity at its base (~183 m) in the Whaingaroan (early Oligocene). The formation of the Marshall unconformity is attributed to changes in ocean currents resulting from the tectonic deepening and widening of the Tasmanian Gateway (between 35.50-30.2 Ma; Stickley et al., 2004) and onward throughflow of the PLC into the Southwest Pacific. This throughflow deflects the Proto-Ross Gyre and cool water associated with the Tasman current across New Zealand resulting in the intensification of shallow water currents (Carter and Landis, 1972; Lyle et al, 2007). The non-deposition and/or erosion of sediments of the Runangan stage (inferred from the lack of marker sporomorph taxa) makes it

challenging to identify the boundary between the Whaingaroan and the Runangan corresponding to the start of the EOT. The decline, and to some extent, the near absence of the early coastal lowland vegetation association, such as the shrubby and small trees (e.g., *Casuarinaceae*, *Xylomelum*, and other Proteaceae), may have been due to the changes in coastal water temperatures (deflection of the Proto-Ross gyre and cold water associated with the Tasman current) that is unfavourable to the growth of these taxa. This interpretation is supported by Pocknall (1989) reporting that, the further spreading between Australia and Antarctica pushed cool water northward which ultimately brought predominantly cool temperate conditions to New Zealand from the late Eocene to the early Oligocene. However, aside from the first two samples at the base of this interval (183-178 m; Fig. 5.12) showing MATs within the cool temperate (< 12 °C) regime, the upper sections indicate warm temperate conditions (> 12 °C). Hence, sporomorph-based quantitative climate estimates show no sign of significant cooling in this interval.

The vegetation and climate regime of early Oligocene are very similar to that of late Oligocene (~141-93 m) with comparable quantitative sporomorph-based MATs (11.7 to 16.2 °C) and MAPs (1704-2109 mm/yr; Fig. 5.12). The *brassii*-type *Nothofagus* still dominated and most likely formed the main components of the inland rainforest vegetation, in conjunction with gymnosperms such as *Dacrydium* and *Podocarpus*. New Zealand at this time is reported to have been emerging from the extensive marine transgression (McGlone et al., 1996) that lead to the recorded increase in coastal lowland shrubs and small trees such as Casuarinaceae at the TNW-1 wellsite.

5.4.4 TNW-1 palynoflora and climate comparison with Site 1172 and the role of the deepening Tasmanian Gateway

The Kaiatan (late Eocene; 39.1-36.7 Ma; Raine et al., 2015) of TNW-1 (PZ 2; this study) bear striking similarity with the Priabonian (PZ 2; Chapter 4) palynoflora record of ODP Site 1172. Both sections show a dominance of *Nothofagus* (especially, the *brassii*-type), common Casuarinaceae, *Podocarpus*, Araucariaceae, *Dacrydium*, ferns (Gleicheniaceae and Cyatheaceae) and minor but diverse Proteaceae. Sporomorph-based MATs between both sites are comparable as well, with Site 1172 reporting MATs between 10-13 °C and TNW-1, 12-14 °C. Further palynoflora comparison in the late Eocene was not

possible due to the non-deposition and/or erosion of Runangan of TNW-1 and the early Whaingaroan, the formation of the Marshall Paraconformity. Coincidentally, the initial tectonic deepening and widening of the Tasmanian Gateway started at this time (~ 35.5 Ma; Stickley et al., 2004; Huber et al., 2004), with full deepening most likely to have occurred by the early Oligocene (30.2 Ma). During this time, Site 1172 (i.e., ~35.5-33 Ma) saw a widespread deposition of glauconite interpreted to mark the deepening of the Tasmanian Gateway. Similar glauconitic formations (i.e., Waihao and Kokoamu Greensands) are encountered in the TNW-1 section at this time of the Eocene-early Oligocene. The sequence of events in the Tasmanian Gateway region, seems to corroborate the assertion that, the formation of the Marshall Paraconformity is linked to changes in ocean currents resulting from the tectonic deepening and widening of the Tasmanian Gateway (between 35.50-30.2 Ma; Stickley et al., 2004) and onward throughflow of the PLC into the southwest Pacific. This then deflects the Proto-Ross Gyre and cool water associated with the Tasman current across New Zealand resulting in the intensification of shallow water currents.

5.5 Conclusion

The ~180 m long and almost continuous TNW-1 drillcore, processed and analysed for their palynomorph content, revealed a middle Eocene (Porangan) to Oligocene (Whaingaroan) age for Southland, New Zealand. The biozonation for the TNW-1 drillcore was based on Cooper (2004) miospore and dinocyst biozonation scheme of New Zealand, revealing the existence of two main Assemblage Zones (i.e., *Myricipites harrisii* and *Nothofagus mataurаensis* Assemblage Zones, respectively). The Marshall paraconformity (~183 m), based on biostratigraphic analysis, is assigned an early Whaingaroan (early Oligocene; probably developed between 33 to 30 Ma) age, which agrees with previous studies in New Zealand.

The Porangan (middle Eocene; 272 - ~257 m) palynological record reveals a warm temperate (MATs 14-17 °C) Casuarinaceae dominated shrubby or small trees coastal/lowland vegetation association with pockets of wetlands/bogs due to associated Cyatheaceae, Liliaceae and Gleicheniaceae families. This is then followed by a period of transition (257-183 m) reflected in drop in the decline in lowland/coastal

shrub or small trees vegetation and the increase in hinterland rainforest vegetation taxa (such as *Nothofagus*, *Podocarpus*, *Dacrydium* and Araucariaceae) throughout the Bortonian (middle Eocene) and Kaiatan (late Eocene). By the Whaingaroan (early Oligocene), the hinterland rainforest vegetation association had taken over becoming the dominant vegetation community thriving at a considerable distance from the coast under MATs between 11.2 to 13.3 °C.

The Kaiatan palynoflora of TNW-1 (PZ 2b; this Chapter) bear striking similarity with the Priabonian (PZ 2; Chapter 3) ODP Site 1172 palynoflora record. This is based on the dominance of *Nothofagus* (especially, the *brassii*-type), common Casuarinaceae, *Podocarpus*, Araucariaceae, *Dacrydium*, ferns (Gleicheniaceae and Cyatheaceae) and minor but diverse Proteaceae. Sporomorph-based MATs between both sites are similar as well, with Site 1172 reporting MATs between 10-13 °C and TNW-1, 12-14 °C. Further palynoflora comparison in the late Eocene was not made possible due to the non-deposition and/or erosion of Runangan of TNW-1 and by the early Whaingaroan, the formation of the Marshall Paraconformity. Coincidentally, the initial tectonic deepening and widening of the Tasmanian Gateway started around this time (~ 35.5 Ma; Stickley et al., 2004; Huber et al., 2004), with full deepening most likely to have occurred by the early Oligocene (30.2 Ma).

The sequence of events in the Tasmanian Gateway region around this time, seem to corroborate the assertion that, the formation of the Marshall Paraconformity is due to changes in ocean currents resulting from the tectonic deepening and widening of the Tasmanian Gateway (between 35.50-30.2 Ma; Stickley et al., 2004) and onward throughflow of the PLC into the southwest pacific. This throughflow then deflects the Proto-Ross Gyre and cool water associated with the Tasman current across New Zealand resulting in the intensification of shallow water currents.

6. Conclusions and Outlook

6.1 Introduction

Given that conclusions have already been provided at the end of each of the three results chapters (chapters three to five) in this thesis, the following section only provides a summary of those conclusions but also present some thoughts on the significance, limitations, and outlook. This study investigated Eocene to Oligocene past climate and vegetation dynamics of the southern high-latitude with focus on three main sites. These are ODP Site 1168 (chapter 3) on the east Tasman Plateau, ODP Site 1168 (chapter 4) on the western Tasmania margin, the TNW-1 site (chapter 5) in Southland, New Zealand. This study presents new quantitative sporomorph-based climate estimates of well-dated marine sediments on Tasmania (i.e., Site 1172 and 1168) and TNW-1 on Southland, New Zealand during the middle to late Palaeogene in the context of the tectonic deepening and widening of the Tasmanian Gateway, thereby establishing the relationship between the marine and terrestrial realm.

6.1.1 Eastern Tasmania climate and vegetation and role of deepening Tasmanian Gateway

Sporomorph-based climate and vegetation reconstruction of 66 samples across eastern Tasmania (Site 1172) were used to reconstruct climate and vegetation changes during the late Eocene to early Oligocene period. These findings not only provide valuable insights into the local evolution of this region but also shed light on the broader context of global change, particularly in relation to the Eocene-Oligocene Transition (EOT) and the role played by the deepening Tasmanian Gateway. The key events have been summarised in below:

- Late Eocene terrestrial cooling (37.30 Ma): At ~ 37.30 Ma, the sporomorph-based climate estimates reveal a noteworthy terrestrial cooling of ~ 2–3°C. This climatic shift was accompanied by a transition from a warm-temperate rainforest, characterized by dominant *Nothofagus* and Podocarpaceae with minor paratropical elements, to a cool-temperate rainforest

with secondary Podocarpaceae representation. This cooling event at 37.30 Ma aligns with a longer-term decline in SST from 23 to 19 °C at ODP Site 1172. Moreover, it coincides with a regional transient cooling event (PrOM) at ODP Site 738 on the Kerguelen Plateau and a sustained cooling trend in the Southern Ocean due to carbon being sequestered from the ocean surface.

- Late Eocene to early Oligocene Transition (35.5 to 34.30 Ma): Progressing into the latest Eocene (35.5 to 34.49 Ma), a dynamic interplay of cool- and warm-temperate forests is observed, followed by the pronounced cooling associated with the EOT (34.30–33.3 Ma). Recent geochemical, sedimentological, and palynological investigations corroborate these climate shifts. These include evidence of rising SST, a resurgence in MAAT of the soil-based MBT'5me biomarker thermometry, widespread deposition of glauconite, and the prevalence of low-latitude cosmopolitan and protoperidinioid dinocysts.
- The role of the deepening Tasmanian Gateway: A pivotal factor in this climatic and environmental transformation or transition appears to be the early deepening of the Tasmanian Gateway. This geological phenomenon facilitated the intrusion of warm waters associated with the PLC into the southwest Pacific, exerting a profound influence on both terrestrial and marine climates in the region. The significance of regional and local factors, including shifts in ocean circulation due to the tectonic deepening of the Tasmanian Gateway, emerges as a key driver of vegetation and terrestrial climate changes across eastern Tasmania.
- Post-EOT climate recovery (Early Oligocene, 33.55 to 33.06 Ma): The earliest Oligocene period witnesses a recovery in Tasmanian terrestrial temperatures, accompanied by the establishment of a warm-temperate rainforest association from 33.55 to 33.06 Ma. This climatic rebound coincides with an increase in atmospheric pCO_2 at the EOGM, concurrent with the expansion of the Antarctic ice sheet and the sustained deepening of the Tasmanian Gateway.

In summary, these results, as presented in Chapter 3, underscores the complex relationship between local and global climate drivers during the late Eocene to early Oligocene period. It illuminates how the deepening of the Tasmanian Gateway acted as a catalyst for profound climate and vegetation changes

across eastern Tasmania. These findings promote the understanding of the EOT and its implications for terrestrial ecosystems and climate systems within the context of global environmental change.

6.1.2 Western Tasmania climate and vegetation controls in the Oligocene

The findings presented in this chapter, drawn from ODP Site 1168, provide compelling evidence of shifting vegetation communities in western Tasmania during the late Eocene to the late Oligocene. These changes occurred under different climatic regimes, and in the process, shedding light on the intricate interplay between climate, tectonics, and ecological response in this region.

- PZ 1 (35.50-34.81 Ma): In the early phase of this site (35.50-34.81 Ma), the presence of a warm-temperate *Nothofagus* rainforest with paratropical elements in western Tasmania was uncovered. Sporomorph-derived MATs approximate around 13 °C during this period. Remarkably, this sporomorph assemblage resembles that of the latest Eocene PZ 3 of Site 1172, marking the initial deepening of the Tasmanian Gateway.
- PZ 2 (34.4-30.5 Ma): A notable transition unfolds in this PZ, characterized by a 2°C decline in terrestrial MATs coinciding with the EOT at 34.40-33.65 Ma. Following the EOT, a warm-temperate period ensues. However, it is crucial to note that the extended post-EOT warming creates a disconnect between atmospheric pCO_2 levels and terrestrial temperatures post-33 Ma. This observation suggests that factors beyond greenhouse forcing, such as the prolonged deepening of the Tasmanian Gateway and the resulting equatorward shift of the Australian landmass, may play a significant role in shaping climate patterns during this period.
- PZ 3 (30.5 Ma): A critical juncture in western Tasmania's climatic and ecological history occurs at in this PZ. During this phase, the emergence of new vegetation dynamics was witnessed. Gymnosperms (particularly Araucariaceae), cryptogams, and angiosperms, increase in abundance, accompanied by a modest rise in taxonomic diversity. This expansion of cool-temperate forests aligns with a concurrent decline in atmospheric pCO_2 levels during the early Oligocene.

- Ocean-atmosphere interactions and pCO_2: The synchronicity observed in the early Oligocene between declining temperatures (including sea surface temperatures and MATs) and falling atmospheric pCO_2 levels highlights the role of ocean-atmosphere interactions in southern Australia. This underscores the importance of pCO_2 as a driver of terrestrial climate and vegetation changes onshore Tasmania during this transformative period.
- Decoupling and synchroneity of vegetation and pCO_2: The overarching message from this study of the western Tasmania margin is the intriguing decoupling and synchroneity of vegetation and terrestrial temperature from atmospheric pCO_2 levels from the late Eocene to the early-late Oligocene. This decoupling offers compelling evidence for the varied influences of tectonic and pCO_2 forcing mechanisms, emphasizing the complex interplay of factors driving climate and ecological change in Tasmania during this era, as detailed in Chapter 4.

In summary, the study of western Tasmania's Oligocene climate and vegetation history not only unveils the intricate nuances of ecological response but also underscores the multifaceted nature of environmental change. Similar to eastern Tasmania (ODP Site 1172), the findings presented here contribute significantly to our understanding of how local and global forces, including tectonics and atmospheric pCO_2, shaped the terrestrial landscapes of Tasmania during this transformative period in Earth's history.

6.1.3 Southland, New Zealand: Pre- and post-Marshall Paraconformity climate and vegetation

In the study of Southland, New Zealand, before and after the development of the Marshall Paraconformity, a peculiar challenge in age assessment and determination, particularly in the TNW-1 drillcore was encountered. The limitations in age resolution, especially preceding the Marshall Paraconformity, necessitated the utilization of palynomorphs (including sporomorphs and dinocysts) for biostratigraphic purposes. These efforts unveiled the presence of *Myricipites harrisii* and *Nothofagus matauraensis* Assemblage Zones spanning the mid-Eocene (Porangan) to the Oligocene (Whaingaroan).

- The Porangan (Middle Eocene, 272-257 m): In the palynological record of the Porangan (middle Eocene), located at depths of 272-257 m, a dominant Casuarinaceae presence in coastal and lowland vegetation was recorded. Additionally, pockets of wetlands and bogs emerge, characterized by taxa from Cyatheaceae, Liliaceae, and Gleicheniaceae.
- Transitional Phase (Between 257-183 m): During the transitional phase between 257-183 meters, there is a notable decline in lowland and coastal shrub or small tree vegetation. This decline is accompanied by a surge in hinterland rainforest taxa, including *Nothofagus*, *Podocarpus*, *Dacrydium*, and Araucariaceae, during the Bortonian (middle Eocene) and Kaiatan (late Eocene) epochs.
- Whaingaroan (Early Oligocene): By this stage (early Oligocene), the hinterland rainforest vegetation association has firmly established itself, thriving under mean annual temperatures (MATs) ranging from 11.2 to 13.3°C.
- Comparative insights and the role of tectonics: Notably, the late Eocene palynoflora and MATs of TNW-1 exhibit remarkable similarities to the Priabonian (PZ 2) as observed at Site 1172. However, a comprehensive comparison is hindered by non-deposition and/or erosion during the latest Eocene (Runangan) to the earliest Oligocene, which coincides with the development of the Marshall Paraconformity. The sequence of events observed in New Zealand aligns seamlessly with the tectonic deepening and widening of the Tasmanian Gateway. This alignment lends strong support to the assertion that the development of the Marshall Paraconformity is intricately linked to the throughflow of the PLC. This flow effectively deflects the cool water associated with the proto-Ross Gyre across New Zealand, intensifying shallow water currents, hence the hiatus/non-deposition.

6.2 Summary of conclusions and significance of the study (EOT, pCO_2 vs Tectonics)

This PhD research investigated Eocene and Oligocene past climate and vegetation dynamics from three different sites in the southern high-latitude. The section synthesises the main findings as follows:

- Eastern Tasmania (Site 1172) experienced three main climate transition events. A 2-3 °C terrestrial cooling at ~37.30 Ma coinciding with declining SSTs and regional Southern Ocean cooling due to carbon sequestration. This is followed by a fluctuation between warm and cool temperate conditions between 35.5-34.49 Ma coinciding with widespread deposition of glauconite and the tectonic deepening of the Tasmanian Gateway. Cooling across the EOT and a significant rebound post-EOT linked to declining pCO_2, and their rebound in the phase of continued deepening of the Tasmanian Gateway.

- In western Tasmania three pollen zones are identified: PZ 1 (35.50-34.81 Ma) with warm-temperate *Nothofagus*- dominated rainforest, PZ 2 (34.4-30.5 Ma) showing a terrestrial MAT decline and warm-temperate conditions post-EOT, and PZ 3 (after 30.5 Ma) with an increase in gymnosperms and cool-temperate forest expansion. The early Oligocene (30.40–27.46 Ma) synchroneity between temperature (SST gradual decline and MATs) and atmospheric *p*CO2 most likely indicate the coupling of the ocean-atmosphere system in the southern Australian region, and the role of *p*CO2 in driving terrestrial climate and vegetation change onshore Tasmania.

- Sporomorph-based climate and vegetation reconstruction of both Site 1168 and 1172 records provide evidence for the importance of both tectonic and *p*CO2 forcing on vegetation and climate in the Tasmanian region during the late Eocene to Oligocene.

- Southland, New Zealand, experienced changes in vegetation and climate from the mid-Eocene to the early Oligocene. The palynological record indicates a transition from a Casuarinaceae-dominated coastal/lowland vegetation association to a hinterland rainforest dominated by taxa such as *Nothofagus*, *Podocarpus*, *Dacrydium*, and Araucariaceae. The formation of the Marshall Paraconformity is closely connected to the tectonic processes resulting from the deepening and widening of the Tasmanian Gateway. These changes in the gateway configuration influenced the flow of the Proto-Antarctic Circumpolar Current, which in turn affected the strength of shallow water currents in New Zealand. Interestingly, the geological and palynological record in eastern Tasmania reveals a series of events that indicate the

deepening of the Tasmanian Gateway, occurring around the same time as periods of non-deposition or hiatus in New Zealand. This correlation provides compelling evidence for a significant relationship between the formation of the Marshall Paraconformity and the accelerated deepening of the Tasmanian Gateway.

Across the three study sites in the southern high-latitude, the complex interplay between climate and tectonics emerged as a central theme from the late Eocene to the Oligocene. This stems from the fact that in ET, WT, and Southland New Zealand, the combined effects of the deepening Tasmanian Gateway and changes in pCO_2 concentrations at different phases (e.g., before and after the EOT), exert significant influence, driving climatic shifts and impacting vegetation. For example, with respect to the effects of tectonics on vegetation and climate, it has been demonstrated in this study that the initial tectonic deepening of the Tasmanian Gateway resulted in the throughflow of the warm PLC to access eastern Tasmania, thereby affecting climate and causing the introduction of warm-temperate elements in a rainforest that was predominantly cool-temperate. In the same vein, the impact of the deepening Tasmanian Gateway was recorded regionally in Southland, New Zealand, thereby supporting the hypothesis that this event led to the formation of the Marshall Paraconformity. Evidence of this is seen in the late Eocene palynoflora and MATs of TNW-1 which bear a striking resemblance to the Priabonian (PZ 2) of Site 1172 (eastern Tasmania). However, the lack of deposition and/or erosion from the latest Eocene (Runangan) to the earliest Oligocene hinders further comparison. The sequence of events in the Tasmanian Gateway region around this time seems to corroborate the assertion that, the formation of the Marshall Paraconformity is due to changes in ocean currents resulting from the tectonic deepening and widening of the Tasmanian Gateway and the onward throughflow of the PLC into the southwest Pacific. This throughflow then deflects the Proto-Ross Gyre and cool water associated with the Tasman current across New Zealand, resulting in the intensification of shallow water currents.

Further to the above, changes in pCO_2 concentrations are shown to have impacted terrestrial climate and vegetation. For example, though ODP Sites 1172 and 1168 were both under the influence of the warm PLC around 34.6-33.6 Ma, an overall decline in MATs (2 °C) were recorded. This cooling trend is comparable to that observed in the marine realm and linked to the global decline of atmospheric pCO_2

at the EOT. This shows the intricate dance and phased interplay between a local event such as the tectonic deepening of the Tasmanian Gateway and a global one such as pCO_2 changes in driving terrestrial climate and vegetation in southern Australia and New Zealand.

Regarding the main driver(s) of the EOT and post-EOT cooling and warming, respectively, this study draws a strong linkage and synchroneity between the marine and terrestrial realms (SSTs and terrestrial MAT trends). However, these trends and changes observed across the late Eocene and Oligocene are not simply due to declining global pCO_2 concentrations alone. Rather, the palynological, palaeoecological, and palaeoclimatological insights provided by this study, due to the proximity of the three sites to the Tasmanian Gateway and Antarctica, illustrate how localized geological events (e.g., deepening Tasmanian Gateway) can have far-reaching implications for terrestrial ecosystems and climate patterns, highlighting the intricate ways in which local/regional factors intersect with global climatic shifts.

Also, the terrestrial palynological findings discussed in this study may be useful for defining terrestrial climate boundary conditions, and validate future Cenozoic climate models, and subsequently improve the understanding of southern high-latitude terrestrial ecosystem responses to the tectonic deepening of the Tasmanian Gateway and changes in carbon dioxide forcing.

In summary, this study bridges the gap between regional geological events and global climate change, emphasizing the role of tectonics in shaping terrestrial landscapes. This study serves as a testament to the intricate web of connections between climate, tectonics, and ecology, offering valuable lessons for interpreting past, present, and future environmental changes on a global scale. As the world confronts contemporary climate challenges, the insights gained from these investigations will continue to inform strategies for a sustainable future.

6.3 Limitations and Outlook

The high resolution ETP and WT pollen records reveal the crucial role played by local/regional events, including changes in ocean circulation due to the tectonic deepening of the Tasmanian Gateway as well as global events such as pCO_2 concentration changes in vegetation and terrestrial climate across eastern Tasmania. Future studies, preferably, palynomorph records on mainland southeastern Australia, preferably peatlands, but still under the influence of the PLC and TC, would allow a better comparison with Site 1172 and 1168 records and pick up on whether the ETP and WT vegetation dynamics are responding to local or regional events. The advantage of sampling such records will remove the effects of taphonomic bias and over-and-underrepresentation of plant taxa due to their mode of transportation.

Also, the integration of terrestrial and marine past environmental proxies from the same site (i.e., Site 1172) underpins the value of combining these proxies to better understand the interaction between the terrestrial and marine realms. Further studies should focus on a similar multiproxy approach for the Oligocene at Site 1168 (western Tasmania) and (TNW-1) Southland, New Zealand.

Finally, for a more robust inter-regional vegetation and climate comparison between the Eocene and Oligocene of eastern Tasmania (Site 1172) and Southland, New Zealand (TNW-1), sampling resolution of future studies in Southland, New Zealand, should be increased to give a detailed picture of events, especially the period just before the tectonic deepening of the Tasmanian Gateway and the EOT.

Bibliography

Abele, C., Gloe, C. S., Hocking, J. B., Holdgate, G., Kenley, P. R., Lawrence, C. R., Ripper, D., & Threlfall, W. F. (1976). Teriary. In D. J. Douglas & J. A. Ferguson (Eds.), *Geology of Victoria* (Vol. 5, pp. 177–273). Geological Society of Australia.

Amoo, M., Salzmann, U., Pound, M. J., Thompson, N., & Bijl, P. K. (2022). Eocene to Oligocene vegetation and climate in the Tasmanian Gateway region were controlled by changes in ocean currents and pCO2. *Climate of the Past*, *18*(3), 525–546. https://doi.org/10.5194/cp-18-525-2022

Anagnostou, E., John, E. H., Edgar, K. M., Foster, G. L., Ridgwell, A., Inglis, G. N., Pancost, R. D., Lunt, D. J., & Pearson, P. N. (2016). Changing atmospheric CO2 concentration was the primary driver of early Cenozoic climate. *Nature*, *533*(7603), 380–384. https://doi.org/10.1038/nature17423

Anderson, J. B., Warny, S., Askin, R. A., Wellner, J. S., Bohaty, S. M., Kirshner, A. E., Livsey, D. N., Simms, A. R., Smith, T. R., Ehrmann, W., Lawver, L. A., Barbeau, D., Wise, S. W., Kulhanek, D. K., Weaver, F. M., & Majewski, W. (2011). Progressive Cenozoic cooling and the demise of Antarctica's last refugium. *Proceedings of the National Academy of Sciences*, *108*(28), 11356–11360. https://doi.org/10.1073/pnas.1014885108

Anker, S. A., Colhoun, E. A., Barton, C. E., Peterson, M., & Barbetti, M. (2001). Holocene Vegetation and Paleoclimatic and Paleomagnetic History from Lake Johnston, Tasmania. *Quaternary Research*, *56*(2), 264–274. https://doi.org/10.1006/qres.2001.2233

Askin, R. A. (2000). Spores and pollen from the McMurdo Sound Erratics, Antarctica. In J. D. Stillwell & R. M. Feldmann (Eds.), *Paleobiology and Paleoenvironments of Eocene Rocks, McMurdo Sound, East Antarctica* (Vol. 76, pp. 161–181). American Geophysical Union Antarctic Research Series.

Askin, R. A., & Raine, J. I. (2000). Oligocene and Early Miocene Terrestrial Palynology of the Cape Roberts Drillhole CRP-2/2A, Victoria Land Basin, Antarctica. *Terra Antarctica*, *7*(4), 493–501.

Baatsen, M., Van Hinsbergen, D. J. J., Von Der Heydt, A. S., Dijkstra, H. A., Sluijs, A., Abels, H. A., & Bijl, P. K. (2016). Reconstructing geographical boundary conditions for palaeoclimate modelling during the Cenozoic. *Climate of the Past*, *12*(8), 1635–1644. https://doi.org/10.5194/cp-12-1635-2016

Barrier, A. (2019). *Tectonics, sedimentation and magmatism of the Canterbury Basin, New Zealand*. University of Canterbury.

Barron, E. J. (1987). Eocene equator-to-pole surface ocean temperatures: A significant climate problem? *Paleoceanography*, *2*(6), 729–739. https://doi.org/10.1029/PA002i006p00729

Beerling, D. J., & Royer, D. L. (2011). Convergent Cenozoic CO2 history. *Nature Geoscience*, *4*(7), 418–420. https://doi.org/10.1038/ngeo1186

Benbow, M. C., Alley, N. F., Callan, R. A., & Greenwood, D. R. (1995). *Geological history and palaeoclimate* (J. F. Dexel & W. V. Preiss (eds.); 2nd ed., pp. 208–217).

Biffin, E., Brodribb, T. J., Hill, R. S., Thomas, P., & Lowe, A. J. (2012). Leaf evolution in Southern Hemisphere conifers tracks the angiosperm ecological radiation. *Proceedings of the Royal Society B: Biological Sciences*, *279*(1727), 341–348. https://doi.org/10.1098/rspb.2011.0559

Bijl, P. K., Bendle, J. A. P., Bohaty, S. M., Pross, J., Schouten, S., Tauxe, L., Stickley, C. E., McKay, R. M., Roḧl, U., Olney, M., Sluijs, A., Escutia, C., & Brinkhuis, H. (2013). Eocene cooling linked to early flow across the Tasmanian Gateway. *Proceedings of the National Academy of Sciences of the United States of America*, *110*(24), 9645–9650. https://doi.org/10.1073/pnas.1220872110

Bijl, P. K., Frieling, J., Cramwinckel, M. J., Boschman, C., Sluijs, A., & Peterse, F. (2021). Maastrichtian–Rupelian paleoclimates in the southwest Pacific – a critical re-evaluation of biomarker paleothermometry and dinoflagellate cyst paleoecology at Ocean Drilling Program Site 1172. *Climate of the Past*, *17*(6), 2393–2425. https://doi.org/10.5194/cp-17-2393-2021

Bijl, P. K., Houben, A. J. P., Bruls, A., Pross, J., & Sangiorgi, F. (2018). Stratigraphic calibration of

Oligocene–Miocene organic-walled dinoflagellate cysts from offshore Wilkes Land, East Antarctica, and a zonation proposal. *Journal of Micropalaeontology*, *37*(1), 105–138. https://doi.org/10.5194/jm-37-105-2018

Bijl, P. K., Houben, A. J. P., Hartman, J. D., Pross, J., Salabarnada, A., Escutia, C., & Sangiorgi, F. (2018). Paleoceanography and ice sheet variability offshore Wilkes Land, Antarctica – Part 2: Insights from Oligocene–Miocene dinoflagellate cyst assemblages. *Climate of the Past*, *14*(7), 1015–1033. https://doi.org/10.5194/cp-14-1015-2018

Birkenmajer, K., & Zastawniak, E. (1989). Late Cretaceous-early Tertiary floras of King George Island, West Antarctica: their stratigraphic distribution and palaeoclimatic significance. *Geological Society, London, Special Publications*, *47*(1), 227–240. https://doi.org/10.1144/GSL.SP.1989.047.01.17

Birks, H. J.B., & Line, J. M. (1992). The use of rarefaction analysis for estimating palynological richness from Quaternary pollen-analytical data. *The Holocene*, *2*(1), 1–10. https://doi.org/10.1177/095968369200200101

Birks, H. John B., Felde, V. A., Bjune, A. E., Grytnes, J. A., Seppä, H., & Giesecke, T. (2016). Does pollen-assemblage richness reflect floristic richness? A review of recent developments and future challenges. *Review of Palaeobotany and Palynology*, *228*, 1–25. https://doi.org/10.1016/j.revpalbo.2015.12.011

Boland, D., Brooker, M., Chippendale, G., Hall, N., Hyland, B., Johnston, R., Kleinig, D., McDonald, M., & Turner, J. (2006). *Forest trees of Australia* (5th ed.). CSIRO.

Brinkhuis, H., Sengers, S., Sluijs, A., Warnaar, J., & Williams, G. L. (2003). Latest Cretaceous–Earliest Oligocene and Quaternary Dinoflagellate Cysts, ODP Site 1172, East Tasman Plateau. In *Proceedings of the Ocean Drilling Program, 189 Scientific Results*. https://doi.org/10.2973/odp.proc.sr.189.106.2003

Browne, G. H., Kennedy, E. M., Constable, R. M., Raine, J. I., Crouch, E. M., & Sykes, R. (2008). An

outcrop-based study of the economically significant Late Cretaceous Rakopi Formation, northwest Nelson, Taranaki Basin, New Zealand. *New Zealand Journal of Geology and Geophysics*, *51*(4), 295–315. https://doi.org/10.1080/00288300809509867

Cande, S. C., & Stock, J. M. (2004). Cenozoic reconstruction of the Australia-New Zealand-south Pacific sector of Antarctica. In N. F. Exon, J. P. Kennett, & M. J. Malone (Eds.), *The Cenozoic Southern Ocean: Tectonics, sedimentation and climate change between Australia and Antarctica* (pp. 5–18). Geophysical Monograph Series, American Geophysical Union.

Cantrill, D.J. (2001). Early Oligocene Nothofagus from CRP-3, Antarctica: implications for the vegetation history. *Terra Antartica*, *8*(4), 401–406.

Cantrill, David J., & Poole, I. (2012). After the heat: late Eocene to Pliocene climatic cooling and modification of the Antarctic vegetation. In David J. Cantrill & I. Poole (Eds.), *The Vegetation of Antarctica through Geological Time*. Cambridge University Press. https://doi.org/10.1017/CBO9781139024990.009

Carpenter, R. J., Jordan, G. J., Mildenhall, D. C., & Lee, D. E. (2011). Leaf fossils of the ancient Tasmanian relict Microcachrys (Podocarpaceae) from New Zealand. *American Journal of Botany*, *98*(7), 1164–1172. https://doi.org/10.3732/ajb.1000506

Carter, R. M. (1985). The Mid-Oligocene Marshall Paraconformity, New Zealand: Coincidence with Global Eustatic Sea-Level Fall or Rise? In *Source: The Journal of Geology* (Vol. 93, Issue 3).

Carter, R. M., & Landis, C. A. (1972). Correlative Oligocene Unconformities in Southern Australasia. *Nature Physical Science*, *237*(70), 12–13. https://doi.org/10.1038/physci237012a0

Carter, R. M., McCave, I. N., & Carter, L. (2004). Leg 181 Synthesis: Fronts, Flows, Drifts, Vocanoes, and the Evolution of the Southwestern Gateway to the Pacific Ocean, Eastern New Zealand. In *Proceedings of the Ocean Drilling Program, 181 Scientific Results*. Ocean Drilling Program. https://doi.org/10.2973/odp.proc.sr.181.210.2004

Cavalli-Sforza, L. L., & Edwards, A. W. (1967). Phylogentic analysis. *American Journal of Human*

Genetics, *19*, 233–257.

Christophel, D.C., Harris, W. K., & Syber, A. K. (1987). The Eocene flora of the Anglesea Locality, Victoria. *Alcheringa: An Australasian Journal of Palaeontology*, *11*(4). https://doi.org/10.1080/03115518708619139

Christophel, David C., & Greenwood, D. R. (1989). Changes in climate and vegetation in Australia during the tertiary. *Review of Palaeobotany and Palynology*, *58*(2–4). https://doi.org/10.1016/0034-6667(89)90079-1

Clowes, C. D. (2009). *Dinoflagellate Taxonomy and Biostratigraphy of the Mid- to Late Eocene and Early Oligocene of New Zealand*. Victoria University of Wellington.

Colwyn, D. A., & Hren, M. T. (2019). An abrupt decrease in Southern Hemisphere terrestrial temperature during the Eocene–Oligocene transition. *Earth and Planetary Science Letters*, *512*, 227–235. https://doi.org/10.1016/j.epsl.2019.01.052

Contreras, L., Pross, J., Bijl, P. K., O'Hara, R. B., Raine, J. I., Sluijs, A., & Brinkhuis, H. (2014). Southern high-latitude terrestrial climate change during the Palaeocene–Eocene derived from a marine pollen record (ODP Site 1172, East Tasman Plateau). *Climate of the Past*, *10*(4). https://doi.org/10.5194/cp-10-1401-2014

Contreras, Lineth, Pross, J., Bijl, P. K., Koutsodendris, A., Raine, J. I., van de Schootbrugge, B., & Brinkhuis, H. (2013). Early to Middle Eocene vegetation dynamics at the Wilkes Land Margin (Antarctica). *Review of Palaeobotany and Palynology*, *197*, 119–142. https://doi.org/10.1016/j.revpalbo.2013.05.009

Cooper, R. (2004). *The New Zealand Geological Timescale*. Institute of Geological and Nuclear Sciences.

Cooper, W., & Cooper, W. (2004). *Fruits of the Australian tropical rainforest*. Nokomis Publications.

Coxall K., H., Wilson A., P., Palike, H., Lear H., C., & Backman, J. (2005). Rapid stepwise onset of Antarctic glaciation and deeper calcite compensation in the Pacific Ocean. *Nature*, *433*(7021),

53–57. https://doi.org/10.1038/nature03135

Cramwinckel, M. J., Huber, M., Kocken, I. J., Agnini, C., Bijl, P. K., Bohaty, S. M., Frieling, J., Goldner, A., Hilgen, F. J., Kip, E. L., Peterse, F., van der Ploeg, R., Röhl, U., Schouten, S., & Sluijs, A. (2018). Synchronous tropical and polar temperature evolution in the Eocene. *Nature*, *559*(7714). https://doi.org/10.1038/s41586-018-0272-2

Daly, R. J., Jolley, D. W., Spicer, R. A., & Ahlberg, A. (2011). A palynological study of an extinct arctic ecosystem from the Palaeocene of Northern Alaska. *Review of Palaeobotany and Palynology*, *166*(1–2), 107–116. https://doi.org/10.1016/j.revpalbo.2011.05.008

Davy, B. (2014). Rotation and offset of the Gondwana convergent margin in the New Zealand region following Cretaceous jamming of Hikurangi Plateau large igneous province subduction. *Tectonics*, *33*(8), 1577–1595. https://doi.org/10.1002/2014TC003629

De Vleeschouwer, D., Vahlenkamp, M., Crucifix, M., & Pälike, H. (2017). Alternating Southern and Northern Hemisphere climate response to astronomical forcing during the past 35 m.y. *Geology*, *45*(4), 375–378. https://doi.org/10.1130/G38663.1

Deconto, R. M., & Pollard, D. (2003). Rapid Cenozoic glaciation of Antarctica induced by declining atmospheric CO2. *Nature*, *1317*(2001), 245–249. https://doi.org/https://doi.org/10.1038/nature01290

Dettmann, M. E., Pocknall, D. T., Romero, E. J., & Zamaloa, M. del C. (1990). Nothofagidites Erdtman ex Potonie, 1960; a catalogue of species with notes on the paleogeographic distribution of Nothofagus Bl. (southern beech). *New Zealand Geological Survey Paleontological Bulletin*, *60*, 1–77.

Dowe, J. L. (2010). *Australian Palms*. CSIRO Publishing. https://doi.org/10.1071/9780643098022

Elsworth, G., Galbraith, E., Halverson, G., & Yang, S. (2017). Enhanced weathering and CO2 drawdown caused by latest Eocene strengthening of the Atlantic meridional overturning circulation. *Nature Geoscience*, *10*(3), 213–216. https://doi.org/10.1038/ngeo2888

Emanuel, W. R., Shugart, H. H., & Stevenson, M. P. (1985). Climatic change and the broad-scale distribution of terrestrial ecosystem complexes. *Climatic Change*, *7*(1), 29–43. https://doi.org/10.1007/BF00139439

Evi, E., Hill, R. S., & Scriven, L. J. (1995). The angiosperm-dominated woody vegetation of Antarctica: a review. *Review of Palaeobotany and Palynology*, *86*, 175–198.

Exon, N. F., Berry, R. F., Crawford, A. J., & Hill, P. J. (1997). Geological evolution of the East Tasman Plateau, a continental fragment southeast of Tasmania. *Australian Journal of Earth Sciences*, *44*(5). https://doi.org/10.1080/08120099708728339

Exon, N. F., Kennett, J. P., & Malone, M. J. (2004a). *The Cenozoic Southern Ocean: Tectonics, sedimentation and climate change between Australia and Antarctica*. Geophysical Monograph Series, 151, American Geophysical Union.

Exon, N. F., Kennett, J. P., & Malone, M. J. (2004b). Leg 189 Synthesis: Cretaceous–Holocene History of the Tasmanian Gateway. In N. F. Exon, J. P. Kennett, & M. J. Malone (Eds.), *Proceedings of the Ocean Drilling Program, 189 Scientific Results*. Ocean Drilling Program. https://doi.org/10.2973/odp.proc.sr.189.101.2004

Farjon, A. (2010). *A handbook of the World's Conifers* (Vol. 1). Koninklijke Brill.

Fick, S. E., & Hijmans, R. J. (2017). WorldClim 2: new 1-km spatial resolution climate surfaces for global land areas. *International Journal of Climatology*, *37*(12), 4302–4315. https://doi.org/10.1002/joc.5086

Field, B. D., & Browne, G. H. (1989). *Cretaceous and Cenozoic Sedimentary Basins and Geological Evolution of the Canterbury Region, South Island, New Zealand* (Vol. 2). New Zealand Geological Survey.

Findlay, R. H. (1980). The Marshall Paraconformity (Note). *New Zealand Journal of Geology and Geophysics*, *23*(1), 125–133. https://doi.org/10.1080/00288306.1980.10424198

Foster, G. L., & Rohling, E. J. (2013). Relationship between sea level and climate forcing by CO_2 on

geological timescales. *Proceedings of the National Academy of Sciences*, *110*(4), 1209–1214. https://doi.org/10.1073/pnas.1216073110

Francis, J. E., Marenssi, S., Levy, R., Hambrey, M., Thorn, V. C., Mohr, B., Brinkhuis, H., Warnaar, J., Zachos, J., Bohaty, S., & DeConto, R. (2008). From Greenhouse to Icehouse - The Eocene/Oligocene in Antarctica. In *Developments in Earth and Environmental Sciences* (Vol. 8, pp. 309–368). https://doi.org/10.1016/S1571-9197(08)00008-6

Francis, Jane E, & Poole, I. (2002). Cretaceous and early Tertiary climates of Antarctica: evidence from fossil wood. *Palaeogeography, Palaeoclimatology, Palaeoecology*, *182*(1–2), 47–64. https://doi.org/10.1016/S0031-0182(01)00452-7

Fuller, M., & Touchard, Y. (2004). On the magnetostratigraphy of the East Tasman Plateau, timing of the opening of the Tasmanian Gateway and paleoenvironmental changes. In N. Exon, J. P. Kennett, & M. Malone (Eds.), *The Cenozoic Southern Ocean: tectonics, sedimentation and climate change between Australia and Antarctica* (pp. 127–151). American Geophysical Union, Geophysical Monograph series. https://doi.org/10.1029/151GM05

Fulthorpe, C. S., Carter, R. M., Miller, K. G., & Wilson, J. (1996). Marshall Paraconformity: a mid-Oligocene record of inception of the Antarctic circumpolar current and coeval glacio-eustatic lowstand? *Marine and Petroleum Geology*, *13*(1), 61–77. https://doi.org/10.1016/0264-8172(95)00033-X

Gaina, C., Müller, R. D., Royer, J.-Y., & Symonds, P. (1999). Evolution of the Louisiade triple junction. *Journal of Geophysical Research: Solid Earth*, *104*(B6). https://doi.org/10.1029/1999JB900038

Galeotti, S., DeConto, R., Naish, T., Stocchi, P., Florindo, F., Pagani, M., Barrett, P., Bohaty, S. M., Lanci, L., Pollard, D., Sandroni, S., Talarico, F. M., & Zachos, J. C. (2016). Antarctic Ice Sheet variability across the Eocene-Oligocene boundary climate transition. *Science*, *352*(6281), 76–80. https://doi.org/10.1126/science.aab0669

Gasson, E., Lunt, D. J., DeConto, R., Goldner, A., Heinemann, M., Huber, M., LeGrande, A. N., Pollard, D., Sagoo, N., Siddall, M., Winguth, A., & Valdes, P. J. (2014). Uncertainties in the modelled CO₂ threshold for Antarctic glaciation. *Climate of the Past*, *10*(2), 451–466. https://doi.org/10.5194/cp-10-451-2014

Gauch, H. G. (1982). Ordination. In *Multivariate Analysis in Community Ecology* (pp. 109–172). Cambridge University Press. https://doi.org/10.1017/CBO9780511623332

Goldner, A., Herold, N., & Huber, M. (2014). Antarctic glaciation caused ocean circulation changes at the Eocene-Oligocene transition. *Nature*, *511*(7511), 574–577. https://doi.org/10.1038/nature13597

Goldner, A., Huber, M., & Caballero, R. (2013). Does Antarctic glaciation cool the world? *Climate of the Past*, *9*(1), 173–189. https://doi.org/10.5194/cp-9-173-2013

Goodall, D. W. (1954). Objective methods for the classification of vegetation. III. An essay in the use of factor analysis. *Australian Journal of Botany*, *2*, 304–324.

Gradstein, F. M., Ogg, J. G., Schmitz, M. D., & Ogg, G. M. (2012). The Geologic Time Scale 2012. *The Geologic Time Scale*, *2*, 437–1144.

Greenwood, D. R., Keefe, R. L., Reichgelt, T., & Webb, J. A. (2017). Eocene paleobotanical altimetry of Victoria's Eastern Uplands. *Australian Journal of Earth Sciences*, *64*(5), 625–637. https://doi.org/10.1080/08120099.2017.1318793

Greenwood, David R., Archibald, S. B., Mathewes, R. W., & Moss, P. T. (2005). Fossil biotas from the Okanagan Highlands, southern British Columbia and northeastern Washington State: Climates and ecosystems across an Eocene landscape. *Canadian Journal of Earth Sciences*, *42*(2), 167–185. https://doi.org/10.1139/e04-100

Greenwood, David R., & Wing, S. L. (1995). Eocene continental climates and latitudinal temperature gradients. *Geology*, *23*(11), 1044–1048. https://doi.org/10.1130/0091-7613(1995)023<1044:ECCALT>2.3.CO;2

Griener, K. W., & Warny, S. (2015). Nothofagus pollen grain size as a proxy for long-term climate change: An applied study on Eocene, Oligocene, and Miocene sediments from Antarctica. *Review of Palaeobotany and Palynology*, *221*, 138–143. https://doi.org/10.1016/j.revpalbo.2015.06.003

Grimm, E. C. (1987). CONISS: a FORTRAN 77 program for stratigraphically constrained cluster analysis by the method of incremental sum of squares. *Computers and Geosciences*, *13*(1), 13–35. https://doi.org/10.1016/0098-3004(87)90022-7

Grimm, E. C. (1990). Tilia and Tiliagraph. PC spreadsheet and graphics software for pollen data. *INQUA Working Group on Data Handling Methods, Newsletter*, *4*, 5–7.

Hammer, Ø., Harper, D. A. T., & Ryan, P. D. (2001). Past: Paleontological statistics software package for education and data analysis. *Palaeontologia Electronica*, *4*(1), 178.

Harbert, R. S., & Nixon, K. C. (2015). Climate reconstruction analysis using coexistence likelihood estimation (CRACLE): A method for the estimation of climate using vegetation. *American Journal of Botany*, *102*(8), 1277–1289. https://doi.org/10.3732/ajb.1400500

Harrington, G. J. (2001). Impact of Paleocene/Eocene Greenhouse Warming on North American Paratropical Forests. *PALAIOS*, *16*(3), 266–278. https://doi.org/10.1669/0883-1351(2001)016<0266:IOPEGW>2.0.CO;2

Hayek, L. C., & Buzas, M. A. (2010). *Surveying Natural Populations*. Columbia University Press.

Heureux, A. M. C., & Rickaby, R. E. M. (2015). Refining our estimate of atmospheric CO2 across the Eocene–Oligocene climatic transition. *Earth and Planetary Science Letters*, *409*, 329–338. https://doi.org/10.1016/j.epsl.2014.10.036

Hijmans, R. J., Phillips, S., Leathwick, J., & Elith, J. (2017). dismo: Species distribution modelling. *R Package Version*, *1*(4), 1.

Hill, M. O., & Gauch, H. G. (1980). Detrended correspondence analysis: An improved ordination technique. *Vegetatio*, *43*, 47–58.

Hill, P. J., & Exon, N. F. (2004). Tectonics and basin development of the offshore Tasmanian area; incorporating results from deep ocean drilling. In N. F. Exon, J. P. Kennett, & M. Malone (Eds.), *The Cenozoic Southern Ocean; tectonics, sedimentation and climate between Australia and Antarctica* (pp. 19–19). Geophysical Monograph Series, 151, American Geophysical Union.

Hill, Roberst S. (1994). *History of the Australian Vegetation: Cretaceous to Recent* (Robert S Hill (ed.)). University of Adelaide Press.

Hill, Robert S., & Macphail, M. K. (1983). Reconstruction of the oligocene vegetation at pioneer, northeast tasmania. *Alcheringa*, *7*(4), 281–299. https://doi.org/10.1080/03115518308619613

Hill, Robert S., & Scriven, L. J. (1995). The angiosperm-dominated woody vegetation of Antarctica: a review. *Review of Palaeobotany and Palynology*, *86*(3–4), 175–198. https://doi.org/10.1016/0034-6667(94)00149-E

Hill, Robert S., Whang, S. S., Korasidis, V., Bianco, B., Hill, K. E., Paull, R., & Guerin, G. R. (2020). Fossil evidence for the evolution of the Casuarinaceae in response to low soil nutrients and a drying climate in Cenozoic Australia. *Australian Journal of Botany*, *68*(3), 179–194. https://doi.org/10.1071/BT19126

Hill, Robert S. (2017). *History of the Australian Vegetation: Cretaceous to Recent* (R. S. Hill (ed.)). University of Adelaide Press. https://doi.org/10.20851/australian-vegetation

Hill, S. R., & Dettmann, E. M. (1996). Origin and diversification of the Genus Nothofagus. In T. Thomas Veblen, S. R. Hill, & J. Read (Eds.), *The Ecology and Biogeography of Nothofagus forests* (pp. 11–24). Yale University Press.

Hoem, F. S., Sauermilch, I., Hou, S., Brinkhuis, H., Sangiorgi, F., & Bijl, P. K. (2021). Late Eocene–early Miocene evolution of the southern Australian subtropical front: a marine palynological approach. *Journal of Micropalaeontology*, *40*(2), 175–193. https://doi.org/10.5194/jm-40-175-2021

Hoem, F., Sauermilch, I., Aleksinski, A., Huber, M., Peterse, F., & Bijl, P. (2022). Strength and

variability of the Oligocene Southern Ocean surface temperature gradient. *Research Square [Preprint]*, 1–23.

Holdgate, G. R., Sluiter, I. R. K., & Taglieri, J. (2017). Eocene-Oligocene coals of the Gippsland and Australo-Antarctic basins – Paleoclimatic and paleogeographic context and implications for the earliest Cenozoic glaciations. In *Palaeogeography, Palaeoclimatology, Palaeoecology* (Vol. 472, pp. 236–255). Elsevier B.V. https://doi.org/10.1016/j.palaeo.2017.01.035

Hollis, C. J., Hines, B. R., Littler, K., Villasante-Marcos, V., Kulhanek, D. K., Strong, C. P., Zachos, J. C., Eggins, S. M., Northcote, L., & Phillips, A. (2015). The Paleocene–Eocene Thermal Maximum at DSDP Site 277, Campbell Plateau, southern Pacific Ocean. *Climate of the Past*, *11*(7), 1009–1025. https://doi.org/10.5194/cp-11-1009-2015

Hollis, Christopher J., Dunkley Jones, T., Anagnostou, E., Bijl, P. K., Cramwinckel, M. J., Cui, Y., Dickens, G. R., Edgar, K. M., Eley, Y., Evans, D., Foster, G. L., Frieling, J., Inglis, G. N., Kennedy, E. M., Kozdon, R., Lauretano, V., Lear, C. H., Littler, K., Lourens, L., … Lunt, D. J. (2019). The DeepMIP contribution to PMIP4: Methodologies for selection, compilation and analysis of latest Paleocene and early Eocene climate proxy data, incorporating version 0.1 of the DeepMIP database. *Geoscientific Model Development*, *12*(7), 3149–3206. https://doi.org/10.5194/gmd-12-3149-2019

Hollis, Christopher J., Tayler, M. J. S., Andrew, B., Taylor, K. W., Lurcock, P., Bijl, P. K., Kulhanek, D. K., Crouch, E. M., Nelson, C. S., Pancost, R. D., Huber, M., Wilson, G. S., Ventura, G. T., Crampton, J. S., Schiøler, P., & Phillips, A. (2014). Organic-rich sedimentation in the South Pacific Ocean associated with Late Paleocene climatic cooling. *Earth-Science Reviews*, *134*, 81–97. https://doi.org/10.1016/j.earscirev.2014.03.006

Homes, A. M., Cieraad, E., Lee, D. E., Lindqvist, J. K., Raine, J. I., Kennedy, E. M., & Conran, J. G. (2015). A diverse fern flora including macrofossils with in situ spores from the late Eocene of southern New Zealand. *Review of Palaeobotany and Palynology*, *220*, 16–28. https://doi.org/10.1016/j.revpalbo.2015.04.007

Hope, G. S. (1996). History of Nothofagus in New Guinea and New Caledonia. In Thomas. T Veblen, R. S. Hill, & J. Read (Eds.), *The Ecology and Biogeography of Nothofagus Forests* (pp. 257–270). Yale University Press.

Houben, A. J. P., Bijl, P. K., Sluijs, A., Schouten, S., & Brinkhuis, H. (2019). Late Eocene Southern Ocean cooling and invigoration of circulation preconditioned Antarctica for full-scale glaciation. *Geochemistry, Geophysics, Geosystems*, *20*(5), 2214–2234. https://doi.org/10.1029/2019GC008182

Houben, A. J. P., van Mourik, C. A., Montanari, A., Coccioni, R., & Brinkhuis, H. (2012). The Eocene–Oligocene transition: Changes in sea level, temperature or both? *Palaeogeography, Palaeoclimatology, Palaeoecology*, *335–336*. https://doi.org/10.1016/j.palaeo.2011.04.008

Huber, M., & Caballero, R. (2011). The early Eocene equable climate problem revisited. *Climate of the Past*, *7*(2), 603–633. https://doi.org/10.5194/cp-7-603-2011

Huber, Matthew, Brinkhuis, H., Stickley, C. E., Döös, K., Sluijs, A., Warnaar, J., Schellenberg, S. A., & Williams, G. L. (2004). Eocene circulation of the Southern Ocean: Was Antarctica kept warm by subtropical waters? *Paleoceanography*, *19*(4), 1–12. https://doi.org/10.1029/2004PA001014

Hunt, R. J., & Poole, I. (2003). Paleogene West Antarctic climate and vegetation history in light of new data from King George Island. In *Causes and consequences of globally warm climates in the early Paleogene*. Geological Society of America. https://doi.org/10.1130/0-8137-2369-8.395

Hutchinson, D. K., Coxall, H. K., Lunt, D. J., Steinthorsdottir, M., De Boer, A. M., Baatsen, M., Von Der Heydt, A., Huber, M., Kennedy-Asser, A. T., Kunzmann, L., Ladant, J. B., Lear, C. H., Moraweck, K., Pearson, P. N., Piga, E., Pound, M. J., Salzmann, U., Scher, H. D., Sijp, W. P., … Zhang, Z. (2021). The Eocene-Oligocene transition: A review of marine and terrestrial proxy data, models and model-data comparisons. In *Climate of the Past* (Vol. 17, Issue 1, pp. 269–315). Copernicus GmbH. https://doi.org/10.5194/cp-17-269-2021

Huurdeman, E. P., Frieling, J., Reichgelt, T., Bijl, P. K., Bohaty, S. M., Holdgate, G. R., Gallagher, S.

J., Peterse, F., Greenwood, D. R., & Pross, J. (2021). Rapid expansion of meso-megathermal rain forests into the southern high latitudes at the onset of the Paleocene-Eocene Thermal Maximum. *Geology*, *49*(1), 40–44. https://doi.org/10.1130/G47343.1

Hyland, B. P. M. (1995). Carnarvonia. In P. McCarthy (Ed.), *Flora of Australia, Volume 16, Elaeagnaceae, Proteaceae 1* (Vol. 16, pp. 343–345). CSIRO Publishing/Australian Biological Resources Study.

Jaramillo, C. A. (2002). Response of Tropical Vegetation to Paleogene Warming. In *Source: Paleobiology* (Vol. 28, Issue 2).

Katz, M. E., Miller, K. G., Wright, J. D., Wade, B. S., Browning, J. V., Cramer, B. S., & Rosenthal, Y. (2008). Stepwise transition from the Eocene greenhouse to the Oligocene icehouse. *Nature Geoscience*, *1*(5), 329–334. https://doi.org/10.1038/ngeo179

Kemp, E. M. (1978). Tertiary climatic evolution and vegetation history in the Southeast Indian Ocean region. *Palaeogeography, Palaeoclimatology, Palaeoecology*, *24*(3), 169–208. https://doi.org/10.1016/0031-0182(78)90042-1

Kennedy, E. M. (2003). Late Cretaceous and Paleocene terrestrial climates of New Zealand: Leaf fossil evidence from South Island assemblages. *New Zealand Journal of Geology and Geophysics*, *46*(2), 295–306. https://doi.org/10.1080/00288306.2003.9515010

Kennedy, E. M., Arens, N. C., Reichgelt, T., Spicer, R. A., Spicer, T. E. V., Stranks, L., & Yang, J. (2014). Deriving temperature estimates from Southern Hemisphere leaves. *Palaeogeography, Palaeoclimatology, Palaeoecology*, *412*, 80–90. https://doi.org/10.1016/j.palaeo.2014.07.015

Kennett, J. P. (1977). Cenozoic evolution of Antarctic glaciation, the circum-Antarctic Ocean, and their impact on global paleoceanography. *Journal of Geophysical Research*, *82*(27), 3843–3860. https://doi.org/10.1029/jc082i027p03843

Kershaw, A. . (1988). *Vegetation history* (B. Huntley & T. Webb (eds.); pp. 237–306). Springer Netherlands. https://doi.org/10.1007/978-94-009-3081-0

Kershaw, P., & Wagstaff, B. (2001). The southern conifer family Araucariaceae: History, status, and value for paleoenvironmental reconstruction. In *Annual Review of Ecology and Systematics* (Vol. 32, Issue 1, pp. 397–414). https://doi.org/10.1146/annurev.ecolsys.32.081501.114059

Klages, J. P., Salzmann, U., Bickert, T., Hillenbrand, C. D., Gohl, K., Kuhn, G., Bohaty, S. M., Titschack, J., Müller, J., Frederichs, T., Bauersachs, T., Ehrmann, W., van de Flierdt, T., Pereira, P. S., Larter, R. D., Lohmann, G., Niezgodzki, I., Uenzelmann-Neben, G., Zundel, M., … Scheinert, M. (2020). Temperate rainforests near the South Pole during peak Cretaceous warmth. *Nature*, *580*(7801), 81–86. https://doi.org/10.1038/s41586-020-2148-5

Korasidis, V. A., Wallace, M. W., Wagstaff, B. E., & Hill, R. S. (2019). Terrestrial cooling record through the Eocene-Oligocene transition of Australia. *Global and Planetary Change*, *173*, 61–72. https://doi.org/10.1016/j.gloplacha.2018.12.007

Korasidis, V. A., Wallace, M. W., Chang, T.-J., & Phillips, D. (2023). Eocene paleoclimate and young mountain-building in the Australian Eastern Highlands. *Review of Palaeobotany and Palynology*, *312*, 104875. https://doi.org/10.1016/j.revpalbo.2023.104875

Kühl, N., Gebhardt, C., Litt, T., & Hense, A. (2002a). Probability density functions as botanical-climatological transfer functions for climate reconstruction. *Quaternary Research*, *58*(3), 381–392. https://doi.org/10.1006/qres.2002.2380

Kühl, N., Gebhardt, C., Litt, T., & Hense, A. (2002b). Probability density functions as botanical-climatological transfer functions for climate reconstruction. *Quaternary Research*, *58*(3), 381–392. https://doi.org/10.1006/qres.2002.2380

Kumaran, N., Punekar, S., & Limaye, R. (2011). Palaeoclimate and phytogeographical appraisal of Neogene pollen record from India. *Journal of Palynology*, *46*, 315–330.

Ladant, J. B., Donnadieu, Y., & Dumas, C. (2014). Links between CO2, glaciation and water flow: Reconciling the cenozoic history of the antarctic circumpolar current. *Climate of the Past*, *10*(6), 1957–1966. https://doi.org/10.5194/cp-10-1957-2014

Laird, M. G., & Bradshaw, J. D. (2004). The Break-up of a Long-term Relationship: the Cretaceous Separation of New Zealand from Gondwana. *Gondwana Research*, *7*(1), 273–286. https://doi.org/10.1016/S1342-937X(05)70325-7

Lanyon, R., Varne, R., & Crawford, A. J. (1993). Tasmanian Tertiary basalts, the Balleny plume, and opening of the Tasman Sea (southwest Pacific Ocean). *Geology*, *21*(6), 555–558. https://doi.org/10.1130/0091-7613(1993)021<0555:TTBTBP>2.3.CO;2

Larcher, W., & Winter, A. (1981). Frost susceptibility of palms: experimental data and their interpretation. *Principes*, *25*(4), 143–155.

Lauretano, V., Kennedy-Asser, A. T., Korasidis, V. A., Wallace, M. W., Valdes, P. J., Lunt, D. J., Pancost, R. D., & Naafs, B. D. A. (2021). Eocene to Oligocene terrestrial Southern Hemisphere cooling caused by declining pCO 2. *Nature Geoscience*. https://doi.org/10.1038/s41561-021-00788-z

Lear, C. H., Bailey, T. R., Pearson, P. N., Coxall, H. K., & Rosenthal, Y. (2008). Cooling and ice growth across the Eocene-Oligocene transition. *Geology*, *36*(3), 251–254. https://doi.org/10.1130/G24584A.1

Lee, D. E., Lee, W. G., Jordan, G. J., & Barreda, V. D. (2016). The Cenozoic history of New Zealand temperate rainforests: comparisons with southern Australia and South America. *New Zealand Journal of Botany*, *54*(2), 100–127. https://doi.org/10.1080/0028825X.2016.1144623

Legendre, P., & Legendre, F. (2012). *Numerical Ecology* (3rd ed.). Elsevier.

Lever, J., Krzywinski, M., & Altman, N. (2017). Principal component analysis. *Nature Methods*, *14*(7), 641–642. https://doi.org/10.1038/nmeth.4346

Lewis, D. W. (1992). Anatomy of an unconformity on mid-Oligocene Amuri Limestone, Canterbury, New Zealand. *New Zealand Journal of Geology and Geophysics*, *35*(4), 463–475. https://doi.org/10.1080/00288306.1992.9514541

Lewis, D. W., & Belliss, S. E. (1984). Mid Tertiary Unconformities in the Waitaki Subdivision, North

Otago. *Journal of the Royal Society of New Zealand*, *14*(3), 251–276. https://doi.org/10.1080/03036758.1984.10426303

Liebrand, D., de Bakker, A. T. M., Beddow, H. M., Wilson, P. A., Bohaty, S. M., Ruessink, G., Pälike, H., Batenburg, S. J., Hilgen, F. J., Hodell, D. A., Huck, C. E., Kroon, D., Raffi, I., Saes, M. J. M., van Dijk, A. E., & Lourens, L. J. (2017). Evolution of the early Antarctic ice ages. *Proceedings of the National Academy of Sciences*, *114*(15), 3867–3872. https://doi.org/10.1073/pnas.1615440114

Liu, Z., Pagani, M., Zinniker, D., DeConto, R., Huber, M., Brinkhuis, H., Shah, S. R., Leckie, R. M., & Pearson, A. (2009). Global cooling during the Eocene-Oligocene climate transition. *Science*, *323*(5918), 1187–1190. https://doi.org/10.1126/science.1166368

Liu, Zhonghui, He, Y., Jiang, Y., Wang, H., Liu, W., Bohaty, S. M., & Wilson, P. A. (2018). Transient temperature asymmetry between hemispheres in the Palaeogene Atlantic Ocean. *Nature Geoscience*, *11*(9), 656–660. https://doi.org/10.1038/s41561-018-0182-9

Lyle, M., Gibbs, S., Moore, T. C., & Rea, D. K. (2007). Late Oligocene initiation of the Antarctic Circumpolar Current: Evidence from the South Pacific. *Geology*, *35*(8), 691–694. https://doi.org/10.1130/G23806A.1

Mabberley, D. J. (1997). *The Plant-Book* (Second). Cambridge University Press.

Macphail, M., Alley, F., Truswell, E., & Sluiter, I. R. K. (1994). Early Tertiary vegetation: Evidence from spores and pollen. In R.S. Hill (Ed.), *History of the Australian Vegetation: Cretaceous to Recent* (pp. 189–261). Cambridge University Press.

Macphail, M.K. (1999). Palynostratigraphy of the murray basin, inland Southeastern Australia. *Palynology*, *23*(1), 197–240. https://doi.org/10.1080/01916122.1999.9989528

Macphail, M.K., & Truswell, E. M. (2004). Palynology of Site 1166, Prydz Bay, East Antarctica. In A. K. Cooper, P. E. O'Brien, & C. Richter (Eds.), *Proceedings of the Ocean Drilling Program, Scientific Results* (Vol. 188, pp. 1–43). Ocean Drilling Program.

https://doi.org/10.2973/odp.proc.sr.188.013.2004

Macphail, M K. (2007). Australian Palaeoclimates: Cretaceous to Tertiary - A review of palaeobotanical and related evidence to the year 2000. *CRC LEME Special Volume Open File Report 151*, *November*, 266pp.

Macphail, Michael K., & Hill, R. S. (2018). What was the vegetation in northwest Australia during the Paleogene, 66–23 million years ago? *Australian Journal of Botany*, *66*(7), 556–574. https://doi.org/10.1071/BT18143

Macphail, Mike, & Cantrill, D. J. (2006). Age and implications of the Forest Bed, Falkland Islands, southwest Atlantic Ocean: Evidence from fossil pollen and spores. *Palaeogeography, Palaeoclimatology, Palaeoecology*, *240*(3–4), 602–629. https://doi.org/10.1016/j.palaeo.2006.03.010

Martin, H. (1994). Australian Tertiary phytogeography: Evidence for palynology. In R.S. Hill (Ed.), *History of the Australian vegetation: Cretaceous to Holocene* (pp. 104–142). Cambridge University Press.

Martin, H. A. (2006). Cenozoic climatic change and the development of the arid vegetation in Australia. *Journal of Arid Environments*, *66*(3 SPEC. ISS.), 533–563. https://doi.org/10.1016/j.jaridenv.2006.01.009

McGlone, M. S., Mildenhall, D. C., & Pole, M. S. (1996). History and palaeoecology of New Zealand Nothofagus forests. In T.T. Veblen, R. S. Hill, & J. Read (Eds.), *The ecology and biogeography of Nothofagus forest* (pp. 83–130). Yale University Press.

Miller, K. G., Janecek, T. R., Katz, M. E., & Keil, D. J. (1987). Abyssal circulation and benthic foraminiferal changes near the Paleocene/Eocene boundary. *Paleoceanography*, *2*(6), 741–761. https://doi.org/10.1029/PA002i006p00741

Miller, K., Wright, J. D., Katz, M. E., Wade, B. S., Browning, J. V., Cramer, B. S., & Rosenthal, Y. (2009). Climate threshold at the Eocene-Oligocene transition: Antarctic ice sheet influence on

ocean circulation. In C. Koeberl & A. Montanari (Eds.), *The Late Eocene Earth-Hothouse, Icehouse, and Impacts* (Vol. 452, pp. 169–178). Geological Society of America Special Papers.

Mortimer, N., & Campbell, H. (2014). *Zealandia: Our Continent Revealed*. Penguin.

Mortimer, Nick, Campbell, H. J., Tulloch, A. J., King, P. R., Stagpoole, V. M., Wood, R. A., Rattenbury, M. S., Sutherland, R., Adams, C. J., Collot, J., & Seton, M. (2017). Zealandia: Earth's Hidden Continent. *GSA Today*, 27–35. https://doi.org/10.1130/GSATG321A.1

Mosbrugger, V. (2009). Nearest-Living-Relative Method. In V. Gornitz (Ed.), *Encyclopedia of Paleoclimatology and Ancient Environments* (pp. 607–609). Springer Netherlands. https://doi.org/10.1007/978-1-4020-4411-3_149

Mosbrugger, V., & Utescher, T. (1997). The coexistence approach - A method for quantitative reconstructions of Tertiary terrestrial palaeoclimate data using plant fossils. *Palaeogeography, Palaeoclimatology, Palaeoecology*, *134*(1–4), 61–86. https://doi.org/10.1016/S0031-0182(96)00154-X

Myerscough, P., Whelan, R., & Bradstock, R. (2007). Ecology of Proteaceae with special reference to the Sydney region. *Cunninghamia*, *6*(4), 951–1015.

Naafs, B. D. A., Inglis, G. N., Zheng, Y., Amesbury, M. J., Biester, H., Bindler, R., Blewett, J., Burrows, M. A., del Castillo Torres, D., Chambers, F. M., Cohen, A. D., Evershed, R. P., Feakins, S. J., Gałka, M., Gallego-Sala, A., Gandois, L., Gray, D. M., Hatcher, P. G., Honorio Coronado, E. N., … Pancost, R. D. (2017). Introducing global peat-specific temperature and pH calibrations based on brGDGT bacterial lipids. *Geochimica et Cosmochimica Acta*, *208*, 285–301. https://doi.org/10.1016/j.gca.2017.01.038

Ogden, J., Stewart, G. H., & Allen, R. B. (1996). Ecology of New Zealand Nothofagus Forest. In Thomas T. Veblen, R. S. Hill, & J. Read (Eds.), *The Ecology and Biogeography of Nothofagus Forests* (pp. 25–82). Yale University Press.

Oksanen, J., Blanchet, F. G., Friendly, M., Kindt, R., Legendre, P., McGlinn, D., Minchin, P. R.,

O'Hara, R. B., Simpson, G. L., Solymos, P., Stevens, M. H. H., Szoecs, E., & Wagner, H. (2019). *Vegan: community ecology package*. R Package Version 2.5-6. https://cran.r-project.org/package=vegan

Pagani, M., Huber, M., Liu, Z., Bohaty, S. M., Henderiks, J., Sijp, W., Krishnan, S., & DeConto, R. M. (2011). The role of Carbon dioxide during the onset of Antarctic glaciation. *Science*, *334*(6060), 1261–1264. https://doi.org/10.1126/science.1203909

Pagani, Mark, Zachos, J. C., Freeman, K. H., Tipple, B., & Bohaty, S. (2005). Marked Decline in Atmospheric Carbon Dioxide Concentrations During the Paleogene. *Science*, *309*(5734), 600–603. https://doi.org/10.1126/science.1110063

Pälike, H., Norris, R. D., Herrle, J. O., Wilson, P. A., Coxall, H. K., Lear, C. H., Shackleton, N. J., Tripati, A. K., & Wade, B. S. (2006). The heartbeat of the Oligocene climate system. *Science*, *314*(5807), 1894–1898. https://doi.org/10.1126/science.1133822

Partridge, A., & Dettmann, M. (2003). Plant microfossils. In W. D. Birch (Ed.), *Geology of Victoria* (pp. 639–652). Geological Society of Australia Special Publication.

Passchier, S., Ciarletta, D. J., Miriagos, T. E., Bijl, P. K., & Bohaty, S. M. (2017). An Antarctic stratigraphic record of stepwise ice growth through the Eocene-Oligocene transition. *Bulletin of the Geological Society of America*, *129*(3–4), 318–330. https://doi.org/10.1130/B31482.1

Pearson, P. N., Foster, G. L., & Wade, B. S. (2009). Atmospheric carbon dioxide through the Eocene–Oligocene climate transition. *Nature*, *461*(7267), 1110–1113. https://doi.org/10.1038/nature08447

Pearson, P. N., & Palmer, M. R. (1999). Middle Eocene Seawater pH and Atmospheric Carbon Dioxide Concentrations. *Science*, *284*(5421), 1824–1826. https://doi.org/10.1126/science.284.5421.1824

Peet, R. K., Knox, R. G., Case, J. S., & Allen, R. B. (1988). Putting Things in Order: The Advantages of Detrended Correspondence Analysis. In *Source: The American Naturalist* (Vol. 131, Issue 6).

Pfuhl, H. A., & McCave, I. N. (2003). Integrated Age Models for the Early Oligocene–Early Miocene, Sites 1168 and 1170-1172. *Proceedings of the Ocean Drilling Program, 189 Scientific Results*, 1–21. https://doi.org/10.2973/odp.proc.sr.189.108.2003

Pocknall, D. T. (1985). Palynology of Waikato Coal Measures (Late Eocene-late Oligocene) from the Raglan area, North Island, New Zealand. *New Zealand Journal of Geology and Geophysics*, *28*(2), 329–349. https://doi.org/10.1080/00288306.1985.10422231

Pocknall, D.T. (1984). *Summary of palynological investigations in the Ohai Coalfield*.

Pocknall, David T. (1989). Late Eocene to early Miocene vegetation and climate history of New Zealand. *Journal of the Royal Society of New Zealand*, *19*(1), 1–18. https://doi.org/10.1080/03036758.1989.10426451

Pocknall, David T. (1990). Palynological evidence for the early to middle Eocene vegetation and climate history of New Zealand. *Review of Palaeobotany and Palynology*, *65*(1–4), 57–69. https://doi.org/10.1016/0034-6667(90)90056-O

Pocknall, David T. (1991). Palynostratigraphy of the Te Kuiti Group (late Eocene-Oligocene), Waikato Basin, New Zealand. *New Zealand Journal of Geology and Geophysics*, *34*(4), 407–417. https://doi.org/10.1080/00288306.1991.9514479

Pole, M. S., & Macphail, M. K. (1996). Eocene Nypa from Regatta Point, Tasmania. *Review of Palaeobotany and Palynology*, *92*, 55–67.

Prebble, J. G., Raine, J. I., Barrett, P. J., & Hannah, M. J. (2006). Vegetation and climate from two Oligocene glacioeustatic sedimentary cycles (31 and 24 Ma) cored by the Cape Roberts Project, Victoria Land Basin, Antarctica. *Palaeogeography, Palaeoclimatology, Palaeoecology*, *231*(1–2), 41–57. https://doi.org/10.1016/j.palaeo.2005.07.025

Prebble, Joseph G., Kennedy, E. M., Reichgelt, T., Clowes, C., Womack, T., Mildenhall, D. C., Raine, J. I., & Crouch, E. M. (2021). A 100 million year composite pollen record from New Zealand shows maximum angiosperm abundance delayed until Eocene. *Palaeogeography,*

Palaeoclimatology, Palaeoecology, 566. https://doi.org/10.1016/j.palaeo.2020.110207

Prider, J. N., & Christophel, D. C. (2000). Distributional ecology of Gymnostoma australianum (Casuarinaceae), a putative palaeoendemic of Australian wet tropic forests. *Australian Journal of Botany*, *48*(4), 427–434. https://doi.org/10.1071/BT99006

Pross, J. (2001). Paleo-oxygenation in Tertiary epeiric seas: evidence from dinoflagellate cysts. *Palaeogeography, Palaeoclimatology, Palaeoecology*, *166*, 369–381. https://doi.org/10.1016/S0031-0182(00)00219-4

Pross, Jörg, Contreras, L., Bijl, P. K., Greenwood, D. R., Bohaty, S. M., Schouten, S., Bendle, J. A., Röhl, U., Tauxe, L., Raine, J. I., Huck, C. E., Van De Flierdt, T., Jamieson, S. S. R., Stickley, C. E., Van De Schootbrugge, B., Escutia, C., Brinkhuis, H., Escutia Dotti, C., Klaus, A., … Yamane, M. (2012). Persistent near–tropical warmth on the antarctic continent during the early eocene epoch. *Nature*, *488*(7409), 73–77. https://doi.org/10.1038/nature11300

Quilty, P. G. (2001). Late Eocene foraminifers and palaeoenvironment, Cascade Seamount, southwest Pacific Ocean: Implications for seamount subsidence and Australia Antarctica Eocene correlation. *Australian Journal of Earth Sciences*, *48*(5), 633–641. https://doi.org/10.1046/j.1440-0952.2001.485886.x

R Core Team. (2019). *R: A language and environment for statistical computing*. R Foundation for Statistical Computing. https://www.r-project.org/

Raine, J., Beu, A., Boyes, A., Campbell, H., Cooper, R., Crampton, J., Crundwell, M., Hollis, C., Morgans, H., & Mortimer, N. (2015). New Zealand Geological Timescale NZGT 2015/1. *New Zealand Journal of Geology and Geophysics*, *58*(4), 398–403. https://doi.org/10.1080/00288306.2015.1086391

Raine, J. C., Mildenhall, D. C., & Kennedy, E. M. (2011). New Zealand fossil spores and pollen: an illustrated catalogue. *GNS Science Miscellaneous Series No. 4*, 1–25.

Raine, J. I. (1984). *Outline of a palynological zonation of Cretaceous to Paleogene terrestrial*

sediments in West Coast region, South Island, New Zealand.

Raine, J. I., & Askin, R. A. (2001). Terrestrial palynology of Cape Roberts Project drillhole CRP-3, Victoria Land Basin, Antarctica. *Terra Antartica*, *8*(4), 389–400.

Read, J., & Hill, R. S. (1985). Dynamics of Nothofagus-dominated rainforest on mainland Australia and lowland Tasmania. *Vegetatio*, *63*(2), 67–78. https://doi.org/10.1007/BF00032607

Read, J., Hope, G. S., & Hill, R. S. (2005). Phytogeography and climate analysis of Nothofagus subgenus Brassospora in New Guinea and New Caledonia. *Australian Journal of Botany*, *53*(4), 297–312. https://doi.org/10.1071/BT04155

Reichgelt, T., West, C. K., & Greenwood, D. R. (2018). The relation between global palm distribution and climate. *Scientific Reports*, 2–12. https://doi.org/10.1038/s41598-018-23147-2

Riding, J. B. (2021). A guide to preparation protocols in palynology. *Palynology*, *45*(sup1), 1–110. https://doi.org/10.1080/01916122.2021.1878305

Royer, J., & Rollet, N. (1997). Plate-tectonic setting of the Tasmanian region. *Australian Journal of Earth Sciences*, *44*(5), 543–560. https://doi.org/10.1080/08120099708728336

Sahoo, T., King, P., Bland, K., Strogen, D., Sykes, R., & Bache, F. (2014). Tectono-sedimentary evolution and source rock distribution of the mid to Late Cretaceous succession in the Great South Basin, New Zealand. *The APPEA Journal*, *54*(1), 259. https://doi.org/10.1071/AJ13026

Sanguinetti, J., & Kitzberger, T. (2008). Patterns and mechanisms of masting in the large-seeded southern hemisphere conifer Araucaria araucana. *Austral Ecology*, *33*(1), 78–87. https://doi.org/10.1111/j.1442-9993.2007.01792.x

Sauermilch, I., Whittaker, J. M., Bijl, P. K., Totterdell, J. M., & Jokat, W. (2019). Tectonic, Oceanographic, and Climatic Controls on the Cretaceous-Cenozoic Sedimentary Record of the Australian-Antarctic Basin. *Journal of Geophysical Research: Solid Earth*, *124*(8), 7699–7724. https://doi.org/10.1029/2018JB016683

Sauermilch, Isabel, Whittaker, J. M., Klocker, A., Munday, D. R., Hochmuth, K., Bijl, P. K., & LaCasce, J. H. (2021). Gateway-driven weakening of ocean gyres leads to Southern Ocean cooling. *Nature Communications*, *12*(1), 6465. https://doi.org/10.1038/s41467-021-26658-1

Scher, H. D., Bohaty, S. M., Smith, B. W., & Munn, G. H. (2014). Isotopic interrogation of a suspected late Eocene glaciation. *Paleoceanography*, *29*(6), 628–644. https://doi.org/10.1002/2014PA002648

Seppelt, R. D. (2006). Sphagnaceae. In *Flora of Australia Volume 51 (Mosses 1)* (Vol. 51, pp. 89–104). ABRS & CSIRO Publishing.

Shannon, C. E. (1948). A Mathematical Theory of Communication. *Bell System Technical Journal*, *27*(3), 379–423. https://doi.org/10.1002/j.1538-7305.1948.tb01338.x

Shipboard Scientific Party. (2001). Site 1172. In N. F. Exon, J. P. Kennett, & M. J. Malone (Eds.), *Proceedings of the Ocean Drilling Program, 189 Initial Reports* (pp. 1–149). Ocean Drilling Program. https://doi.org/10.2973/odp.proc.ir.189.107.2001

Silva, I. P., & Jenkins, D. G. (1993). Decision on the Eocene-Oligocene boundary stratotype. *Episodes*, *16*(3), 379–382. https://doi.org/10.18814/epiiugs/1993/v16i3/002

Sluijs, A., Brinkhuis, H., Stickley, C. E., Warnaar, J., Williams, G. L., & Fuller, M. (2003). Dinoflagellate Cysts from the Eocene–Oligocene Transition in the Southern Ocean: Results from ODP Leg 189. In *Proceedings of the Ocean Drilling Program, 189 Scientific Results* (Vol. 189, pp. 1–42). Ocean Drilling Program. https://doi.org/10.2973/odp.proc.sr.189.104.2003

Sluiter, I. R. K., Holdgate, G. R., Reichgelt, T., Greenwood, D. R., Kershaw, A. P., & Schultz, N. L. (2022). A new perspective on Late Eocene and Oligocene vegetation and paleoclimates of South-eastern Australia. *Palaeogeography, Palaeoclimatology, Palaeoecology*, *596*, 110985. https://doi.org/10.1016/j.palaeo.2022.110985

Steane, D. A., Wilson, K. L., & Hill, R. S. (2003). Using matK sequence data to unravel the phylogeny of Casuarinaceae. *Molecular Phylogenetics and Evolution*, *28*(1), 47–59.

https://doi.org/10.1016/S1055-7903(03)00028-9

Stickley, C. E., Brinkhuis, H., Schellenberg, S. A., Sluijs, A., Röhl, U., Fuller, M., Grauert, M., Huber, M., Warnaar, J., & Williams, G. L. (2004). Timing and nature of the deepening of the Tasmanian Gateway. *Paleoceanography*, *19*(4), 1–18. https://doi.org/10.1029/2004PA001022

Stuchlik, L. (1981). Tertiary pollen spectra from the Ezcurra Inlet Group of Admirality Bay, King George Island (South Shetlands, Antarctica). *Studia Geologica Polonica*, *72*, 109–132.

ter Braak, C. J. F., & Šmilauer, P. (2002). *CANOCO Reference Manual and CanoDraw for Windows User's Guide: Software for Canonical Community Ordination* (4.5).

Thompson, N., Salzmann, U., López-Quirós, A., Bijl, P. K., Hoem, F. S., Etourneau, J., Sicre, M.-A., Roignant, S., Hocking, E., Amoo, M., & Escutia, C. (2022). Vegetation change across the Drake Passage region linked to late Eocene cooling and glacial disturbance after the Eocene–Oligocene transition. *Climate of the Past*, *18*(2), 209–232. https://doi.org/10.5194/cp-18-209-2022

Thorn, V. C., & DeConto, R. (2006). Antarctic climate at the Eocene/Oligocene boundary - Climate model sensitivity to high latitude vegetation type and comparisons with the palaeobotanical record. *Palaeogeography, Palaeoclimatology, Palaeoecology*. https://doi.org/10.1016/j.palaeo.2005.07.032

Tibbett, E. J., Scher, H. D., Warny, S., Tierney, J. E., Passchier, S., & Feakins, S. J. (2021). Late Eocene record of hydrology and temperature from Prydz Bay, East Antarctica. *Paleoceanography and Paleoclimatology*, *36*(4). https://doi.org/10.1029/2020PA004204

Tinto, K. (2010). *The Marshall Paraconformity and its signi_ficance for global climate change in the Oligocene*. University of Otago.

Tomlinson, P. B. (2006). The uniqueness of palms. *Botanical Journal of the Linnean Society*, *151*(1), 5–14. https://doi.org/10.1111/j.1095-8339.2006.00520.x

Tripathi, S. K., & Srivastava, D. (2012). Palynology and palynofacies of the early Palaeogene lignite bearing succession of Vastan, Cambay Basin, Western India. *Acta Palaeobotanica*, *52*(1), 157–

175.

Troedson, A. L., & Smellie, J. L. (2002). The Polonez Cove Formation of King George Island, Antarctica: stratigraphy, facies and implications for mid-Cenozoic cryosphere development. *Sedimentology*, *49*(2), 277–301. https://doi.org/10.1046/j.1365-3091.2002.00441.x

Truswell, E. M., & MacPhail, M. K. (2009). Polar forests on the edge of extinction: What does the fossil spore and pollen evidence from East Antarctica say? *Australian Systematic Botany*, *22*(2), 57–106. https://doi.org/10.1071/SB08046

Truswell, Elizabeth M. (1993). Vegetation changes in the Australian tertiary in response to climatic and phytogeographic forcing factors. *Australian Systematic Botany*, *6*(6), 533–557. https://doi.org/10.1071/SB9930533

Vajda, V., Raine, J. I., & Hollis, C. J. (2001). Indication of global deforestation at the Cretaceous-Tertiary boundary by New Zealand fern spike. *Science*, *294*(5547), 1700–1702. https://doi.org/10.1126/science.1064706

Vajda, Vivi, & Raine, J. I. (2003). Pollen and spores in marine Cretaceous/Tertiary boundary sediments at mid-Waipara River, North Canterbury, New Zealand. *New Zealand Journal of Geology and Geophysics*, *46*(2), 255–273. https://doi.org/10.1080/00288306.2003.9515008

van Hinsbergen, D. J. J., de Groot, L. V., van Schaik, S. J., Spakman, W., Bijl, P. K., Sluijs, A., Langereis, C. G., & Brinkhuis, H. (2015). A Paleolatitude Calculator for Paleoclimate Studies. *PLOS ONE*, *10*(6), 1–21. https://doi.org/10.1371/journal.pone.0126946

Veblen, Thomas T., Hill, R. S., & Read, J. (1996). *The ecology and biogeography of Nothofagus forests* (Issue 2). Yale University Press.

Veblen, Thomas T. (1982). Regeneration Patterns in Araucaria araucana Forests in Chile. In *Journal of Biogeography* (Vol. 9, Issue 1).

Verma, P., Garg, R., Rao, M. R., & Bajpai, S. (2020). Palynofloral diversity and palaeoenvironments of early Eocene Akri lignite succession, Kutch Basin, western India. *Palaeobiodiversity and*

Palaeoenvironments, *100*(3), 605–627. https://doi.org/10.1007/s12549-019-00388-1

Villa, G., Fioroni, C., Pea, L., Bohaty, S., & Persico, D. (2008). Middle Eocene-late Oligocene climate variability: Calcareous nannofossil response at Kerguelen Plateau, Site 748. *Marine Micropaleontology*, *69*(2), 173–192. https://doi.org/10.1016/j.marmicro.2008.07.006

Villa, Giuliana, Fioroni, C., Persico, D., Roberts, A. P., & Florindo, F. (2014). Middle Eocene to Late Oligocene Antarctic glaciation/deglaciation and Southern Ocean productivity. *Paleoceanography*, *29*(3), 223–237. https://doi.org/10.1002/2013PA002518

Willard, D. A., Donders, T. H., Reichgelt, T., Greenwood, D. R., Sangiorgi, F., Peterse, F., Nierop, K. G. J., Frieling, J., Schouten, S., & Sluijs, A. (2019). Arctic vegetation, temperature, and hydrology during Early Eocene transient global warming events. *Global and Planetary Change*, *178*, 139–152. https://doi.org/10.1016/j.gloplacha.2019.04.012

Wing, S. L., & Currano, E. D. (2013). Plant response to a global greenhouse event 56 million years ago. *Source: American Journal of Botany*, *100*(7), 1234–1254. https://doi.org/10.3732/ajb

Wood, R. A., & Herzer, R. H. (1993). The Chatham Rise, New Zealand. In P. F. Ballance (Ed.), *South Pacific sedimentary basins* (Vol. 2, pp. 329–349). Elsevier Science Publishers.

Yapp, C. J. (2004). Fe(CO3)OH in goethite from a mid-latitude North American Oxisol: estimate of atmospheric CO2 concentration in the Early Eocene “climatic optimum.” *Geochimica et Cosmochimica Acta*, *68*(5), 935–947. https://doi.org/10.1016/j.gca.2003.09.002

Zachos, J. C., Breza, J. R., & Wise, S. W. (1992). Early Oligocene ice-sheet expansion on Antarctica: Stable isotope and sedimentological evidence from Kerguelen Plateau, southern Indian Ocean. *Geology*, *20*(6), 569. https://doi.org/10.1130/0091-7613(1992)020<0569:EOISEO>2.3.CO;2

Zachos, J. C., Dickens, G. R., & Zeebe, R. E. (2008). An early Cenozoic perspective on greenhouse warming and carbon-cycle dynamics. In *Nature* (Vol. 451, Issue 7176, pp. 279–283). Nature Publishing Group. https://doi.org/10.1038/nature06588

Zachos, J. C., Quinn, T. M., & Salamy, K. A. (1996). High-resolution (104 years) deep-sea

foraminiferal stable isotope records of the Eocene-Oligocene climate transition. *Paleoceanography*, *11*(3), 251–266. https://doi.org/10.1029/96PA00571

Zanazzi, A., Kohn, M. J., MacFadden, B. J., & Terry, D. O. (2007). Large temperature drop across the Eocene–Oligocene transition in central North America. *Nature*, *445*(7128), 639–642. https://doi.org/10.1038/nature05551

Zhang, Y. G., Henderiks, J., & Liu, X. (2020). Refining the alkenone-pCO2 method II: Towards resolving the physiological parameter ‘b.’ *Geochimica et Cosmochimica Acta*, *281*, 118–134. https://doi.org/10.1016/j.gca.2020.05.002

Appendix 1

Fossil taxon	Botanical Affinity	Source	Selected NLR for climate analysis	Inferred climate Range (Macphail, 2007)
Gymnosperms				
Araucariacites australis	Araucariaceae	Raine et al. (2011)	Araucariaceae	Lower to upper ?mesotherm
Dilwynites granulatus	Araucariaceae	Raine et al. (2011)	Araucariaceae	Lower to upper ?mesotherm
Dacrydiumites preacupressinoides	Podocarpaceae	Raine et al. (2011)	*Dacrydium cupressinum*	
Podocarpidites ellipticus	Podocarpaceae	Raine et al. (2011)	Podocarpaceae	Microtherm to? megatherm
Podocarpidites spp.	Podocarpaceae	Truswell & Macphail (2009)	Podocarpaceae	Microtherm to ?megatherm
Dacrycarpites australiensis	Podocarpaceae	Truswell & Macphail (2009)	Podocarpaceae	Upper microtherm to lower mesotherm
Podocarpidites marwickii	Podocarpaceae	Raine et al. (2011)	Podocarpaceae	Microtherm to ?megatherm
Phyllocladidites mawsonii	*Lagarostrobos*	Raine et al. (2011)	*Lagarostrobos*	Upper microtherm to lower mesotherm
Phyllocladidites reticulasaccatus	Podocarpaceae	Raine et al. (2011)	Podocarpaceae	
Microcachryidites antarcticus	Podocarpaceae	Raine et al. (2011)	*Microcachrys*	Upper microtherm to lower mesotherm
Taxodiaceaepollenites hiatus	Cupressaceae	Raine et al. (2011)	Cupressaceae	
Microalatidites sp.	Podocarpaceae	Raine et al. (2011)	Podocarpaceae	Upper microtherm to lower mesotherm
Microalatidites palaeogenicus	Podocapaceae	Raine et al. (2011)	Podocarpaceae	
Angiosperms				

Malvacipollis subtilis	Euphorbiaceae	Raine et al. (2011)	Euphorbiaceae	
Clavatipollenites ascarinoides	Chloranthaceae	Macphail and Partridge (2006); Raine et al. (2011)	*Ascarina, Hedyosmum*	
Bluffopollis scabratus	Strasburgeriaceae	Raine et al. (2011)	*Strasburgeria robusta*	
Bysmapollis pergranulatus	Epacridaceae	Raine et al. (2011)	Epacridaceae	
Arecipites waitakiensis	Arecaceae	Raine et al. (2011)	Arecaceae	
Myricipites harrisii	Casuarinaceae	Raine et al. (2011) Macphail (2007)	*Gymnostoma*, Casuarinaceae	Lower mesotherm to megatherm
Beaupreaidites elegansiformis	Proteaceae	Raine et al. (2011)	*Beauprea*	
Beaupreaidites diversiformis	Proteaceae	Raine et al. (2011)	*Beauprea*	
Cupanieidites insularis	Sapindaceae	Raine et al. (2011)	*Cupania*	
Liliacidites perforatus	Liliaceae	Raine et al. (2011)	Liliaceae	
Palaeocoprosmadites zelandiae	Rubiaceae	Raine et al. (2011); Macphail (1998)	*Coprosma, Opercularia*	
Nothofagidites flemingii	*Nothofagus* subg. *Fuscospora*	Raine et al. (2011)	*Nothofagus* subg. *Fuscospora*	Upper microtherm to lower mesotherm
Nothofagidites spp.	*Nothofagus*	Raine et al. (2011)	*Nothofagus*	Upper microtherm to lower mesotherm
Nothofagidites emarcidus complex	*Nothofagus* subg. *Brassospora*	Truswell & Macphail (2009)	*Nothofagus* subg. *Brassospora*	Upper microtherm to lower mesotherm
Nothofagidites falcatus	*Nothofagus* subg. *Brassospora*	Raine et al. (2011)	*Nothofagus* subg. *Brassospora*	Upper microtherm to lower mesotherm

Nothofagidites lachlaniae complex	*Nothofagus* subg. *Fuscospora*	Raine et al. (2011)	*Nothofagus* subg. *Fuscospora*	Upper microtherm to lower mesotherm
Nothofagidites waipawaensis	*Nothofagus* subg. *Fuscospora*	Raine et al. (2011)	*Nothofagus* subg. *Fuscospora*	Upper microtherm to lower mesotherm
Nothofagidites asperus	*Nothofagus* subg. *Lophozonia*	Truswell & Macphail (2009)	*Nothofagus* subg. *Lophozonia*	Upper microtherm to lower mesotherm
Nothofagidites senectus	*Nothofagus*	Raine et al. (2011)	*Nothofagus*	
Nothofagidites brachyspinulosus	*Nothofagus* subg. *Fuscospora*	Raine et al. (2011)	*Nothofagus* subg. *Fuscospora*	
Proteacidites crassus	Proteaceae	Raine et al. (2011)	Proteaceae	Lower to upper mesotherm
Proteacidites pachypolus	Proteaceae	Macphail & Hill (2018)	Proteaceae	Lower to upper mesotherm
Proteacidites pseudomoides	Proteaceae	Raine et al. (2011)	*Carnarvonia*	Lower to upper mesotherm
Proteacidites leightonii	Proteaceae	Truswell & Macphail (2009)	Proteaceae	Lower to upper mesotherm
Proteacidites reticulatus	Proteaceae	Truswell & Macphail (2009) Raine et al. (2011)	Proteaceae	Lower to upper mesotherm
Proteacidites annularis	Proteaceae	Macphail (1998); Raine et al. (2011)	Xylomelum occidentale	
Proteacidites scaboratus	Proteaceae	Raine et al. (2011)	Proteaceae	Lower to upper mesotherm
Proteacidites similis	Proteaceae	Raine et al. (2011)	Proteaceae	Lower to upper mesotherm
Proteacidites parvus	Proteaceae	Bowman et al. (2014) Raine et al. (2011)	*Bellendena*	Lower to upper mesotherm
Periporopollenites polyoratus	Caryophyllaceae Trimeniaceae	Raine et al. (2011)	Caryophyllaceae	

Parsonsidites psilatus	*Parsonsia*	Raine et al. (2011)	*Parsonsia*	
Spinizonocolpites sp.	Arecaceae	Raine et al. (2011) Kumaran et al. 2011	Arecaceae	Upper mesotherm to megatherm
Tricolpites trioblatus	Scrophulariaceae Convolvulaceae	Raine et al. (2011)	*Hebe*	Lower to upper mesotherm
Myrtaceidites cf. parvus	Myrtaceae	Raine et al., (2011)	Myrtaceae	
Malvacearumpollis mannanensis	Malvaceae	Raine et al. (2011)	Malvaceae	
Nupharipollis mortonensis	Araceae Nymphaeaceae	Raine et al. (2011)	*Nuphar*	Upper mesotherm to megatherm
Sapotaceoidaepollenites cf latizonatus	Sapotaceae	Raine et al. (2011)	Sapotaceae	
Cryptogams				
Cyathidites australis	Cyatheaceae	Raine et al. (2011) Macphail (1994)	Cyatheaceae	Upper microtherm to lower mesotherm
Cyathidites minor	Cyatheaceae	Raine et al. (2011)	Cyatheaceae	Upper microtherm to lower mesotherm
Cyathidites sp.	Cyatheaceae	Raine et al. (2011)	Cyatheaceae	Upper microtherm to lower mesotherm
Laevigatosporites ovatus	Blechnaceae	Raine et al. (2011) Truswell & Macphail (2009)	Blechnaceae	
Osmundacidites wellmanii	Osmundaceae	Raine et al. (2011)	*Todea*	
Osmundacidites sp.	Osmundaceae	Raine et al. (2011)	Osmundaceae	
Baculatisporites comaumensis	Osmundaceae, Hymenophyllaceae	Raine et al. (2011)	*Hymenophyllum*	

		Truswell & Macphail (2009)		
		Macphail and Cantrill (2006)		
Gleicheniidites senonicus	Gleicheniaceae	Truswell & Macphail (2009)	Gleicheniaceae	
		Raine et al. (2011)		
Gleicheniidites spp.	Gleicheniaceae	Truswell & Macphail (2009)	Gleicheniaceae	
Dictyophyllidites arcuatus	Gleicheniaceae	Raine et al. (2011)	Gleicheniaceae	
Kuylisporites waterbolkii	Cyatheaceae	Raine et al. (2011)	Cyatheaceae	Upper microtherm to lower mesotherm
Clavifera rudis	Gleicheniaceae	Raine et al. (2011)	Gleicheniaceae	
		Raine et al. (2011)		
Clavifera triplex	Gleicheniaceae	Truswell & Macphail (2009)	Gleicheniaceae	
		Truswell & Macphail (2009)		
Laevigatosporites major	Blechnaceae	Raine et al. (2011)	Blechnaceae	
		Macphail & Hill (2018)		
Stereisporites antiquasporites	Sphagnaceae	Truswell & Macphail (2009)	*Sphagnum*	± microtherm
Ceratosporites equalis	Selaginellaceae	Raine et al. (2011)	*Selaginella*	
		Raine et al. (2011)		
Cibotiidites tuberculiformis	Schizaeaceae	Daly et al. (2011)	Schizaeaceae	

Polypodiisporites radiatus	Polypodiaceae	Raine et al. (2011)	Polypodiaceae
Retriletes austroclavatidites	Lycopodiaceae	Raine et al. (2011)	*Lycopodium*

Appendix 2

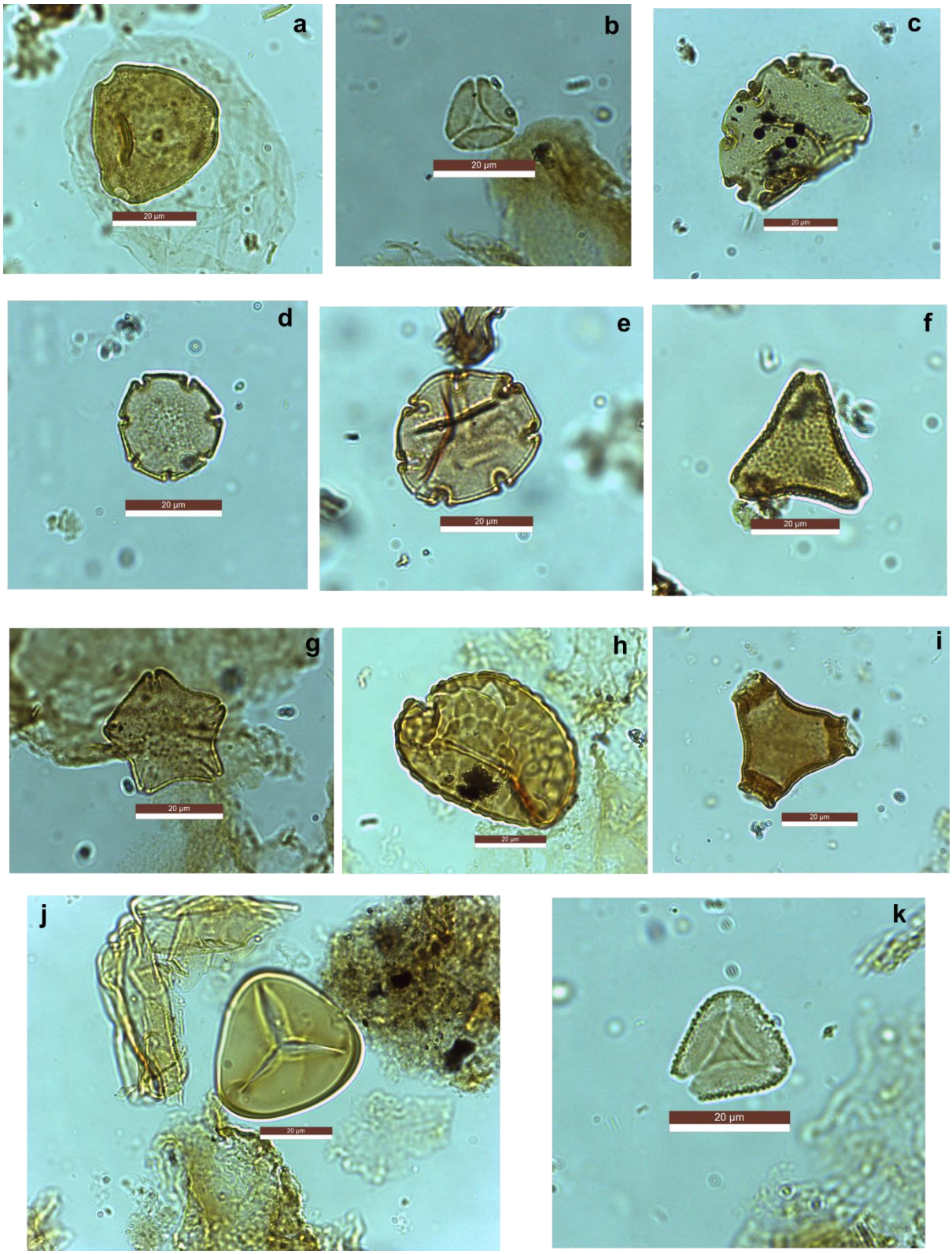

Appendix 3

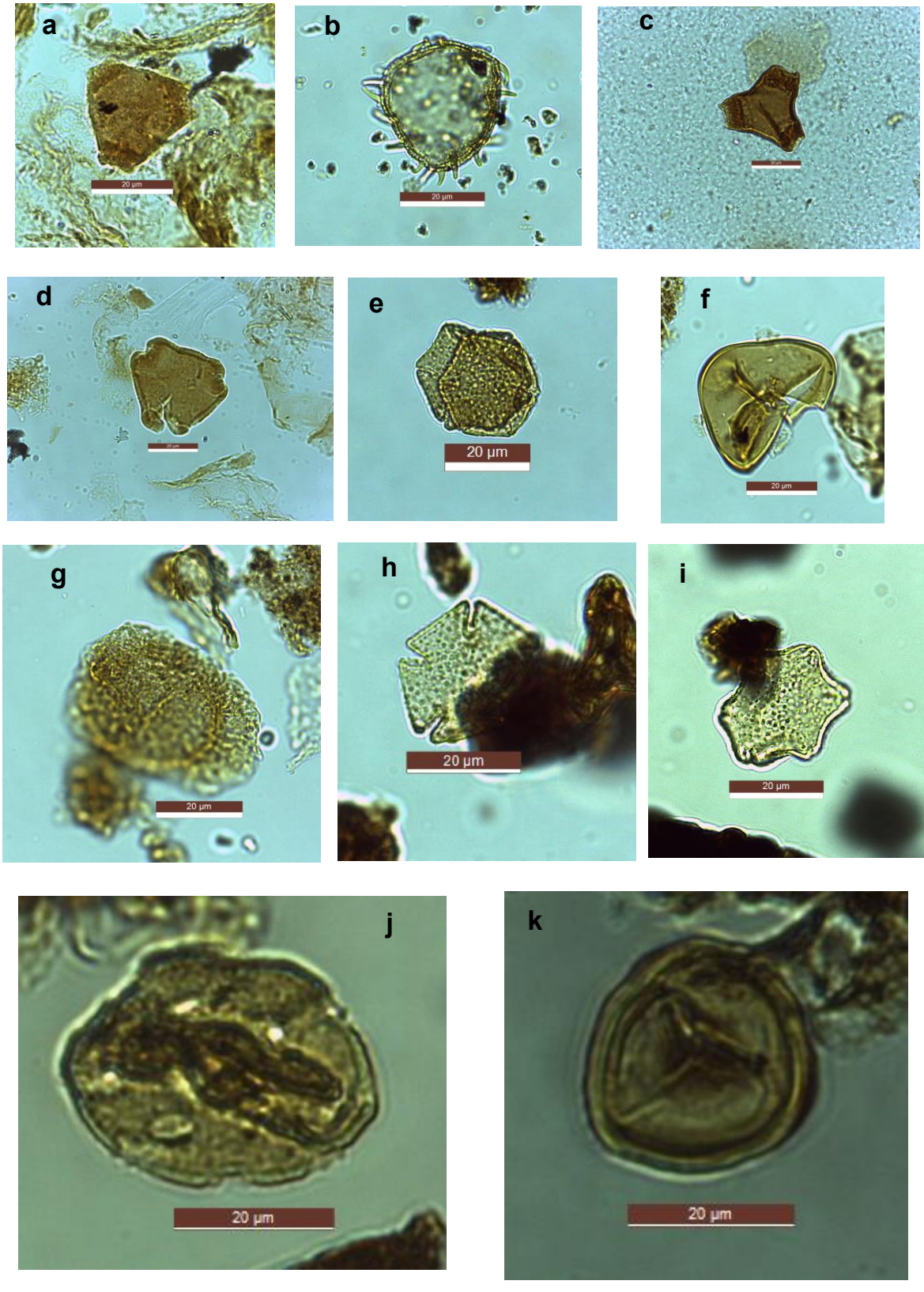

Appendix 4

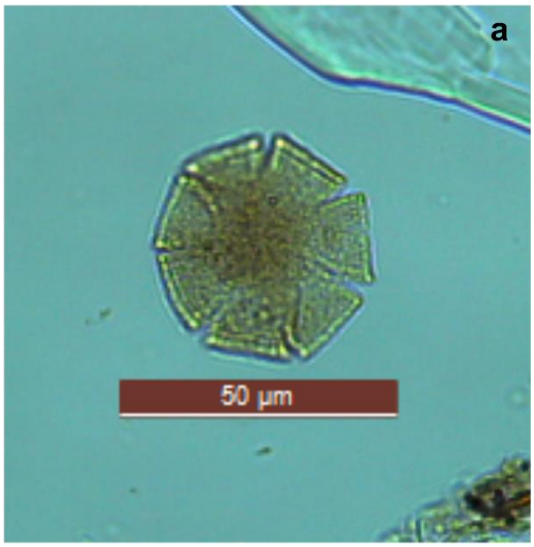

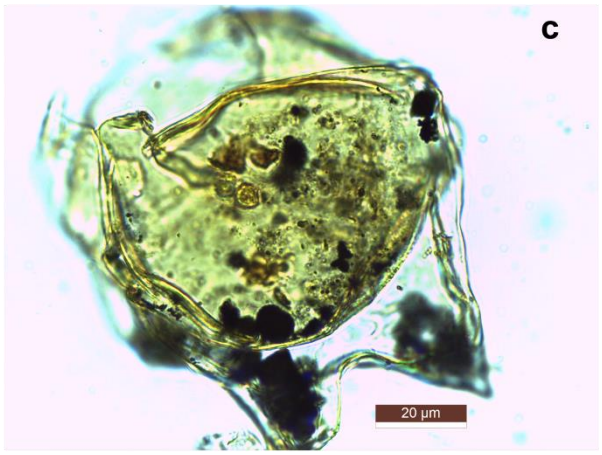

Appendix 2

a) *Myricipites harrisii* (Site 1168; sample 073x-02w slide 2, England finder coordinates R48/1)
b) *Myrtaceidites* sp. (TNW-1 site; sample 158.65 m)
c) *Nothofagidites flemingii* (Site 1168; sample 77x-1 slide 1, England finder coordinates P31/2
d) *Nothofagidites lachlaniae* (Site 1168; sample 78x-02w; England finder coordinates R39/1
e) *Nothofagidites flemingii* (Site 1168; sample 79x-01; England finder coordinates S34
f) *Proteacidites parvus* (Site 1168; sample 79x-04w; England finder coordinates R42/4)
g) *Nothofagidites mataurаensis* (Site 1168; sample 77x-01; England finder coordinates H36/4
h) *Polydiisporites* sp. (Site 1168; sample 067x-01w; England finder coordinates O47)
i) *Proteacidites annularis* (TNW-1; sample 186.37 m)
j) *Cyathidites australis* (TNW-1; Sample 272 m)
k) Cupanieidites insularis (Site 1168; sample 79x-06; England finder coordinates P36/3

Appendix 3

a) *Proteacidites pseudomoides* (Site 1168; sample 77x-06; England finder coordinates Q38/4)
b) *Spinizonocolpites* sp. (Site 1168; sample 03w-058; England finder coordinates H60)
c) *Proteacidites annularis* (TNW-1 site; Sample 169.07 m; England finder coordinates H45/3)
d) *Bluffopollis scabratus* (TNW-1 site; sample 107.07 m; England finder coordinates G33/2)
e) *Nothofagidites emarcidus* (Site 1168; sample 061x-04w; England finder coordinates O59/2)
f) *Cyathidites australis* (Site 1168; sample 061x-04w; England finder coordinates P56)
g) *Dacrydium praecupressinoides* (TNW-1 site; sample 128.4 m)
h) *Nothofagidites mataurаensis* (Site 1168; 067x-03w ; England finder coordinates U65/4)
i) *Nothofagidites falcatus* (Site 1168; 067x-03w ; England finder coordinates W51)
j) *Periporopollenites polyoratus* (TNW-1 site; sample 158.65 m)
k) *Stereisporites antiquasporites* (Site 1172; sample 039x-05w; England finder coordinates R51)

Appendix 4

a) *Nothofagidites asperus* (Site 1172; sample D/02R-05w; England finder coordinates T44/1)
b) *Apteodinium tenuitabulatum* (TNW-1 site; sample 228.35 m)
c) Deflandrea phosphoritica (TNW-1 site; sample 186.37 m)

d) Lejeunecysta rotunda (TNW-1 site; sample 134.71 m)
e) Deflandrea micropoda (TNW-1 site; sample 197.21 m)
f) Spiniferites mirabillis (TNW-1 site; sample 223.44 m)